

AD-A100 269

AIR FORCE GEOPHYSICS LAB HANSCOM AFB MA
CIRRUS PARTICLE DISTRIBUTION STUDY. PART 7. (U)
OCT 80 D J VARLEY, I D COHEN, A A BARNES

F/6 4/2

UNCLASSIFIED

AFGL-TR-80-0324

NL

1 of 1
AD-A100 269

END
DATE
FMTWBR
7-81
DTIC

AFGL-TR-80-0324
AIR FORCE SURVEYS IN GEOPHYSICS, NO. 433

LEVEL II

12



Cirrus Particle Distribution Study, Part 7

**DONALD J. VARLEY, Lt Col, USAF
IAN D. COHEN, Capt, USAF
ARNOLD A. BARNES, JR.**

DTIC
SELECTED
JUN 16 1981

16 October 1980

Approved for public release; distribution unlimited.

DTMC FILE COPY

METEOROLOGY DIVISION **PROJECT 2310**
AIR FORCE GEOPHYSICS LABORATORY
HANSOM AFB, MASSACHUSETTS 01731

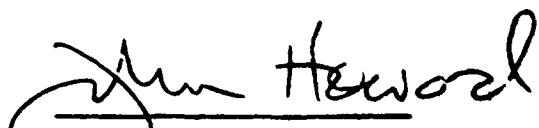


81 615 139

This report has been reviewed by the ESD Information Office (OI) and is
releasable to the National Technical Information Service (NTIS).

This technical report has been reviewed and
is approved for publication.

FOR THE COMMANDER


John Heward
Chief Scientist

Qualified requestors may obtain additional copies from the
Defense Technical Information Center. All others should apply to the
National Technical Information Service.

Unclassified

SECURITY CLASSIFICATION OF THIS PAGE (When Data Entered)

REPORT DOCUMENTATION PAGE		READ INSTRUCTIONS BEFORE COMPLETING FORM
1. REPORT NUMBER AFGL-TR-80-0324	2. GOVT ACCESSION NO A100269	3. RECIPIENT'S CATALOG NUMBER
4. TITLE (and Subtitle) CIRRUS PARTICLE DISTRIBUTION STUDY PART 7.	5. TYPE OF REPORT & PERIOD COVERED Scientific. Interim.	
7. AUTHOR/MA	6. PERFORMING ORG. REPORT NUMBER AFSG No. 433	
Donald J. Varley, Lt Col, USAF* Ian D. Cohen, Capt, USAF Arnold A. Barnes, Jr.	8. CONTRACT OR GRANT NUMBER/S	
9. PERFORMING ORGANIZATION NAME AND ADDRESS Air Force Geophysics Laboratory (LYC) Hanscom AFB Massachusetts 01731	10. PROGRAM ELEMENT PROJECT TASK AREA & WORK UNIT NUMBERS 61102F 2310G501 C3605F 317J0901	
11. CONTROLLING OFFICE NAME AND ADDRESS Air Force Geophysics Laboratory (LYC) Hanscom AFB Massachusetts 01731	12. REPORT DATE 16 October 1980	
14. MONITORING AGENCY NAME & ADDRESS (if different from Controlling Office)	13. NUMBER OF PAGES 82	
	15. SECURITY CLASS. (of this report) Unclassified	
	15a. DECLASSIFICATION DOWNGRADING SCHEDULE	
16. DISTRIBUTION STATEMENT (of this Report) Approved for public release; distribution unlimited.		
17. DISTRIBUTION STATEMENT (of the abstract entered in Block 20, if different from Report)		
18. SUPPLEMENTARY NOTES *Retired. Current affiliation: Lockheed Aerospace Corporation, San Jose, California.		
19. KEY WORDS (Continue on reverse side if necessary and identify by block number) Cirrus Subvisible cirrus Cloud particles Particle distribution Cloud spectra		
20. ABSTRACT (Continue on reverse side if necessary and identify by block number) Particle data obtained during C-130 cirrus sampling flights on 28 and 29 January and 2 February 1979 over the southwestern United States are described. The first flight sampled cirriform clouds ahead of a developing storm; the second flight obtained data in the tops of the cirriform clouds of a fully developed storm; and the third examined cirrus formed by a weak polar front and strong upper level winds. All flights sampled a variety of densities of cirrus; however, those sampled on 29 January, were the most complex		

DD FORM 1 JAN 73 1473 EDITION OF 1 NOV 65 IS OBSOLETE

Unclassified

SECURITY CLASSIFICATION OF THIS PAGE (When Data Entered)

Unclassified

SECURITY CLASSIFICATION OF THIS PAGE (When Data Entered)

20. Abstract (Continued)

and also at the lowest altitude. This flight provided numerous samples having as many as 350,000 particles per cubic meter in the 47 to 4700- μm size range. The largest particle sizes were generally less than 1100 μm , but some cirrus particles as large as 2.5 mm were detected at altitudes between 5.9 and 7.7 km. Generally, the calculated ice water content (IWC) values were 0.04 g m^{-3} or less, with a maximum of 0.10 g m^{-3} in the active storm situation. On the other two days, the cirrus was of varying density with most particles less than 1400 μm and IWCs of 0.03 g m^{-3} or less. Particles as large as 2.5 mm were detected in the cirrus on all three flights. The in-flight meteorologist's characterization of heavy or thin clouds is better correlated with total particle number than particle size. Several atmospheric and particle spectral properties are tabulated for consecutive 15-sec data samples for the 3 flights.

Cloud-free periods were examined; some showed the presence of the two types of subvisible cirrus. The first type consisted of a background of small particles less than a few tens of microns; the second type consisted of large subvisible cirrus particles of the order of 100 μm or larger. The density of subvisible particles larger than 100 μm during a cloud-free period on 2 February 1979 was 7 μm^{-3} .

Unclassified

SECURITY CLASSIFICATION OF THIS PAGE (When Data Entered)

Accession For	
NTIS GPA&I	<input checked="" type="checkbox"/>
DTIC TAB	<input type="checkbox"/>
Unclassified	<input type="checkbox"/>
Justification	
Re	
List No	
Additional Codes	
Dist	1
A	

Preface

The authors extend their appreciation to the many persons responsible for the successful acquisition and processing of the data presented in this report. The AFGL technicians who flew on the C-130 were SMSgt Thomas Moraski, MSgt James Bush, MSgt Stephen Crist, SrA Grant Matsuoka, SrA Lou Ames, Jr. and A1C Wayne Domeier. The 4950th Test Wing pilots, crew, and technicians did an outstanding job in flying and maintaining the airplane. Most of the computer processing of the large volume of data was expertly accomplished by Mr. Michael Francis and Mr. James Lally of Digital Programming Services, Inc. The authors also thank Mr. Morton Glass for his helpful suggestions, Ms Barbara Main for preparing the illustrations, and Mrs. Patricia Sheehy for her excellent typing support.

Contents

1. INTRODUCTION	9
2. INSTRUMENTATION AND DATA PROCESSING	11
3. SYNOPTIC DISCUSSION FOR THE PERIOD 28 JANUARY TO 2 FEBRUARY 1979	12
4. 28 JANUARY 1979 FLIGHT AND DATA	23
4.1 Data Variations During the Flight	23
4.2 Data for Particular Passes	27
5. 29 JANUARY 1979 FLIGHT AND DATA	33
5.1 Data Variations During the Flight	33
5.2 Data for Particular Passes	36
6. 2 FEBRUARY 1979 FLIGHT AND DATA	41
6.1 Data Variations During the Flight	41
6.2 Data for Particular Passes	44
7. SUBVISIBLE CIRRUS	49
8. CONCLUDING COMMENTS	50
REFERENCES	53
APPENDIX A: 28 January 1979 Data Tabulations	55
APPENDIX B: 29 January 1979 Data Tabulations	63
APPENDIX C: 2 February 1979 Data Tabulations	69
APPENDIX D: List of Abbreviations	77

Illustrations

1. Surface Synoptic Chart at 2100Z, 28 January 1979	13
2. 300-mb Analysis at 1200Z, 28 January 1979	13
3. GOES-West Visible Picture Showing New Mexico and West Texas Area at 1845Z, 28 January 1979	14
4. GOES-West Infrared Picture at 1815Z, 28 January 1979	14
5. El Paso, Texas 1200Z, 28 January 1979 Sounding	15
6. Midland, Texas 0000Z, 29 January 1979 Sounding	15
7. Surface Synoptic Chart at 2100Z, 29 January 1979	16
8. GOES-East Visible Photo of Cloud Conditions Over Southwest U.S. at 1901Z on 29 January 1979	17
9. GOES-East Infrared Photo of Southwest U.S. at 1930Z on 29 January 1979	17
10. 300-mb Analysis 1200Z, 29 January 1979	18
11. Albuquerque, N. M. Sounding 4 hr After 29 January 1979 Sampling	18
12. Denver, Colorado Sounding 4 hr After 29 January 1979 Sampling	19
13. Surface Synoptic Chart at 2100Z, 2 February 1979	19
14. GOES-West Visible Photo Centered on New Mexico at 2045Z, 2 February 1979	20
15. GOES Infrared Photo at 1445Z, 2 February 1979	20
16. 300-mb Analysis at 0000Z, 3 February 1979	21
17. El Paso, Texas Sounding at 1200Z on 2 February 1979 Sampling Flight	22
18. Albuquerque, N. M. Sounding at 1200Z on 2 February 1979 Sampling Flight	22
19. Path of C-130 Sampling Flight on 28 January 1979	23
20. Variation With Time During 28 January Flight of (a) Aircraft Altitude and Temperature, (b) Ice Water Content from ASSP, (c) Ice Water Content from 1-D PMS Cloud and Precipitation Probes, (d) Median Volume Diameter of "Melted" Particles, and (e) Total Number of Particles Over 47-4700 μ m Range	24
21. Typical Spectra and Representative Form Factor Values	27
22. Percentage Frequency by Class of Five Measured or Calculated Variables	28
23. Description of Data Format	30
24. Representative Ice Crystal Spectrum for a 15-sec Interval During Pass 1 on 28 January 1979	31
25. Representative Spectrum for a 15-sec Interval During Pass 2 on 28 January 1979	32

Illustrations

26. Representative Spectrum for a 15-sec Interval During Pass 3 Through Heavy Cs on 28 January 1979	32
27. Flight Track of Sampling Aircraft on 29 January 1979	34
28. Variation With Time During 29 January 1979 Flight of (a) Aircraft Altitude and Temperature, (b) Ice Water Content from ASSP, (c) Ice Water Content from 1-D PMS Cloud and Precipitation Probes, (d) Median Volume Diameter of "Melted" Particles, and (e) Total Number of Particles Over 47-4700 μm Range	35
29. Photo of Thin Cirrus Sampled Above Main Cs Cloud, 29 January at 1906Z	37
30. Photo of Main Cs Cloud, 29 January at 1951Z	37
31. Percentage Frequency by Class of Five Measured or Calculated Variables	39
32. Representative Spectrum for a 15-sec Interval During Pass 4 on 29 January 1979	40
33. Representative Spectrum for a 15-sec Interval During Pass 5 on 29 January 1979	40
34. Representative Spectrum for a 15-sec Interval During Pass 6 on 29 January 1979	41
35. Flight Track of Sampling Aircraft on 2 February 1979	42
36. Variation With Time During 2 February 1979 Flight of (a) Aircraft Altitude and Temperature, (b) Ice Water Content from ASSP, (c) Ice Water Content from PMS Cloud, 1-D and Precipitation Probes, (d) Median Volume Diameter of "Melted" Particles, and (e) Total Number of Particles Over 47-4700 μm Range	43
37. Percentage Frequency by Class of Five Measured or Calculated Variables	45
38. Representative Particle Spectrum for a 15-sec Interval During Pass 7 on 2 February 1979	47
39. Representative Particle Spectrum for a 15-sec Interval During Pass 8 on 2 February 1979	47
40. Representative Particle Spectrum for a 15-sec Interval During Pass 9 on 2 February 1979	48
41. Representative Particle Spectrum for a 15-sec Interval During Pass 10 on 2 February 1979	48
42. Representative Particle Spectrum for a 15-sec Interval During Pass 11 on 2 February 1979	49

Tables

1. Portions of 28 January 79 Flight Examined in Figure 22	27
2. Portions of 29 January 79 Flight Examined in Figure 31	36
3. Portions of 2 February 79 Flight Examined in Figure 37	44

Cirrus Particle Distribution Study, Part 7

I. INTRODUCTION

This report continues the presentation of data from a series of cirrus sampling flights made for the Air Force Weapons Laboratory (AFWL) under the Advanced Radiation Technology (ART) program. The flights in the series also provide information for a study of cirrus being conducted for the Air Force Office of Scientific Research (AFOSR). In this report, the data were gathered in the course of three flights, 28 and 29 January 1979, and 2 February 1979, from Kirtland Air Force Base, Albuquerque, New Mexico.

A summary of the series follows: The first report described some of the sampling instrumentation (Varley)¹ available on the specially equipped MC-130E (maintained and flown by personnel of the 4950th Test Wing) used in all the flights; this first report also considered data acquired at 7.6 km before an approaching upper level trough. The second report, by Varley and Brooks,² presented particle spectra for heavy cirrostratus and thin cirrus, whereas the third report (Varley)³ described a flight that acquired primarily very small crystals ($\sim 30 \mu\text{m}$) in a high haze-like cloud layer.

(Received for publication 16 October 1980)

Because of the number of references cited above, they will not be listed here. See References, page 53.

which has been reported in the middle part of this section by Varley and Barnes.⁴ The latter report on a multi-layered cloud that appeared related to a band of strong winds. In the upper part of the cloud, the altostratus and cirrostratus were found to be associated with strong winds. The winds along the generally less than 30 m/s streamers were relatively weak. The similarity of the CIRROSTRATUS Patterns to the CIRRUS patterns is associated with the same winds.

The present material is somewhat similar to that in this previous paper, in that it is from a single flight, but with a different set of conditions. The streamers were not as well developed, and the form factors were not as large as in that flight. The range of particle sizes was also somewhat different, ranging between 0.064 and 0.11 microns. The mean particle size was 0.085 microns, and the median size was 0.070 microns. The latter values are in the upper range of the sizes found in the CIRRUS patterns, and the former is in the lower range. The mean particle size in the CIRROSTRATUS patterns was 0.095 microns, and the median size was 0.080 microns.

It is of interest to note that the mean particle size in the CIRROSTRATUS patterns is larger than that in the CIRRUS patterns, and the mean particle size in the CIRRUS patterns is larger than that in the CIRROSTRATUS patterns. This is in agreement with previous work.

It is of interest to note that the mean particle size in the CIRROSTRATUS patterns is larger than that in the CIRRUS patterns, and the mean particle size in the CIRRUS patterns is larger than that in the CIRROSTRATUS patterns. This is in agreement with previous work. The mean particle size in the CIRROSTRATUS patterns is larger than that in the CIRRUS patterns, and the mean particle size in the CIRRUS patterns is larger than that in the CIRROSTRATUS patterns. This is in agreement with previous work. The mean particle size in the CIRROSTRATUS patterns is larger than that in the CIRRUS patterns, and the mean particle size in the CIRRUS patterns is larger than that in the CIRROSTRATUS patterns. This is in agreement with previous work.

This report has two main purposes: First, to add more particle data to the paucity of information that now exists on cirrus particle spectra and their

4. Varley, D.J., and Barnes, A.A., Jr. (1979) Cirrus Particle Distribution Study, Part 4, AFGI-TR-79-0134, Air Force Surveys in Geophysics 414, AD A074 763, 91 pp.
5. Cohen, I.D. (1979) Cirrus Particles Distribution Study, Part 5, AFGI-TR-79-0155, Air Force Surveys in Geophysics 414, AD 077 361, 81 pp.
6. Cohen, I.D., and Barnes, A.A., Jr. (1980) Cirrus Particle Distribution Study, Part 6, AFGI-TR-80-0261, Air Force Surveys in Geophysics 420, (in press).
7. Heymsfield, A. and Kleinenberg, R. (1972) Properties of cirrus generating cells, J. Atmos. Sci. 29:1568-1566.
8. Heymsfield, A. (1974) Ice crystal growth in deep cirrus systems. Proceedings of Conf. on Cloud Physics, 1973, 311-316.
9. Heymsfield, A. (1977) A cirrus cirrus generating cells in the vicinity of cirrostratus clouds. Proceedings of Conf. on Cloud Physics, 1976, 301-306.

verifying second, to provide information on subvisible cirrus. In our study, the former, more emphasis is placed on number concentration of冰的 samples, the correlating contributions of ice water content with particular particle sizes, and on the correlation of "form factors" with each spectrum.

2. INSTRUMENTATION AND DATA PROCESSING

The primary cloud physics instrumentation used during the three flights discussed in this report include: PMS (Particle Measuring Systems, Inc.) one-dimensional (1-D) and two dimensional (2-D) particle spectrometers, a PMS axial scattering spectrometer probe (ASSP), and a formvar replicating system. Other recorded data include outside air temperature and altitude, as well as aircraft heading and airspeed.

The PMS spectrometers are widely used instruments that have been described, for example, by Knollenberg^{10, 11} and Cunningham.¹² After the particle data were acquired and recorded on magnetic tape aboard the sampling aircraft, they were computer processed, as described by Cunningham.¹² Varley¹ and Varley and Barnes⁴ in previous parts of this study. Essentially, the equivalent melted diameter of all recorded ice crystals is determined using AFGL "melting" equations for standard particle types. Calculations of ice water content (IWC) are then made based on the number of particles recorded in each channel of the spectrometer probes.

The melting equations used for all data in this report are the same as those used for the AFGL type "bullet rosettes." This type was selected based on a review of the 2-D shadowgraph data from each flight. Studies by Heymsfield and Knollenberg⁷ and Heymsfield⁹ have shown that bullet rosettes and bullets are the most common crystal type in cirriform cloudiness. While the bullet rosette is most easily recognized, we strongly agree with the finding of Hobbs and Atkinson¹³

10. Knollenberg, R. (1975) The Response of Optical Array Spectrometers to Ice and Snow: A Study of Probe Size to Crystal Mass Relationships, AFGL-TR-75-0494, AD A020 276.
11. Knollenberg, R. (1976) Three new instruments for cloud physics measurements: the 2-D spectrometer, the forward scattering probe, and the active scattering spectrometer. Preprints of Intnl. Cld. Physics Conf., Boulder, Colorado, Amer. Meteor. Soc., 554-561.
12. Cunningham, R. (1978) Analysis of particle spectral data from optical array (PMS) 1-D and 2-D sensors. In Preprints of AMS Fourth Symposium on Meteorological Observations and Instrumentation, Denver, Colorado.
13. Hobbs, P. V., and Atkinson, D. G. (1976) The concentrations of ice particles in orographic clouds and cyclonic storms over the Cascade Mountains. J. Atmos. Sci., 33:1363-1374.

that most particle shapes in ice clouds are irregular, with reference to standard ice or snow particle classifications.

Values of microphysical variables in this report have been averaged over 15-sec periods, providing somewhat better resolution of cloud conditions than the 30-sec averaging employed in previous parts of this series. Brief descriptions of other types of data will be given as initially presented.

A discussion of the weather in the southwestern United States on 28 January to 2 February, the period covered by the three flights, follows. Flight and sample data will be discussed separately.

3. SYNOPTIC DISCUSSION FOR THE PERIOD 28 JANUARY TO 2 FEBRUARY 1979

During the morning of 28 January 1979, the weather in the southwestern United States was dominated by two low pressure areas. At 1200Z, one was located over southeastern California; the other was in Mexico, 120 miles south of El Paso, Texas. During the day, the first of those low pressure areas moved eastward into Arizona, while the other remained stationary. Southeast flow around the two lows brought moisture from the Gulf of Mexico into the system, causing both lows to intensify and a trough to form between them (see Figure 1). This development was aided by an upper air wave over the western United States. The position of this wave is seen in Figure 2. The Jet Stream followed the 9240-m contour, as can be seen by the 150-kt wind at El Paso, Texas. With the combination of southeast flow at low levels and west-south-west flow at high levels, the system continued to intensify. As the GOES-west satellite pictures show, (Figures 3 and 4) an extensive shield of clouds formed around the southern low pressure area. The flight of 28 January sampled the cirriform clouds on top of this cloud shield. The rawinsonde soundings shown in Figures 5 and 6 point out how the moisture in west Texas increased during the day on 28 January. During the next twelve hours, the two surface lows shown in Figure 1 merged and the two surface troughs developed into an occluded front.

During 29 January, this system deepened into an extensive storm. The position of this storm at 2100Z on 29 January 1979 is shown in Figure 7. The sampling flight of 29 January sampled cirriform clouds while the storm was at its greatest intensity. As the GOES-east satellite photos in Figures 8 and 9 show, an extensive cloud mass covered a large area ahead of the front extending from Texas through Oklahoma, Kansas, and Colorado to Wyoming. Rain and drizzle were observed in Texas and snow was reported throughout the rest of the area; most stations in the sampling area were reporting light, continuous snow. The upper air wave had

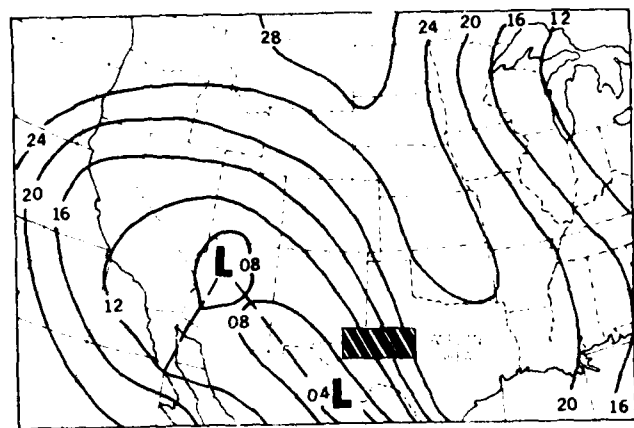


Figure 1. Surface Synoptic Chart at 2100Z,
28 January 1979. Add 1000 millibars to
isobar values.

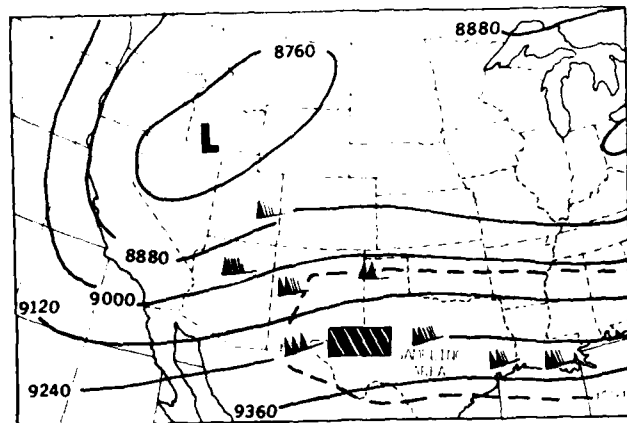


Figure 2. 300-mb Analysis at 1200Z,
28 January 1979. Contour values in
geopotential meters.

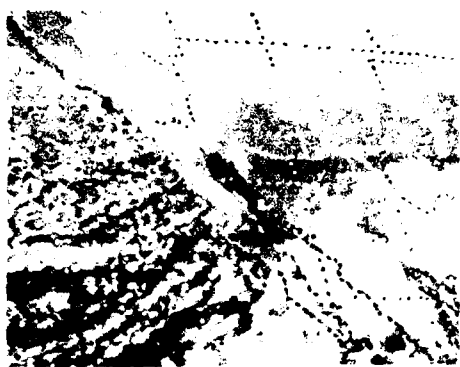


Figure 3. GOES-West Visible Picture
Showing New Mexico and West Texas
Area at 1845Z, 23 January 1979.
Resolution: 2 mi

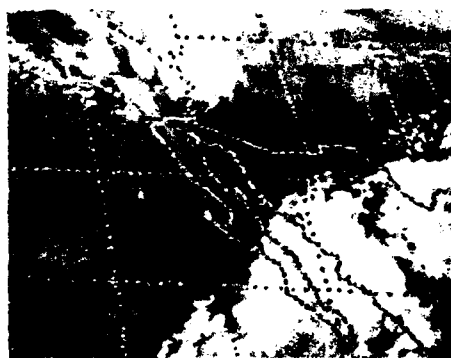
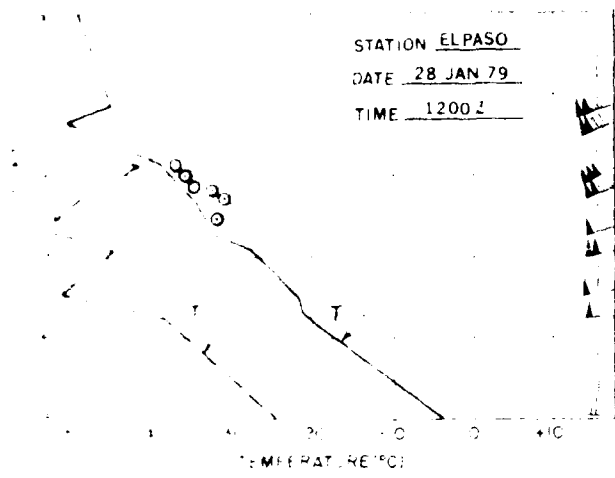


Figure 4. GOES-West Infrared Picture
at 1815Z, 28 January 1979

STATION EL PASO

DATE 28 JAN 79

TIME 1200 Z



STATION MIDLAND

DATE 29 JAN 79

TIME 0000 Z

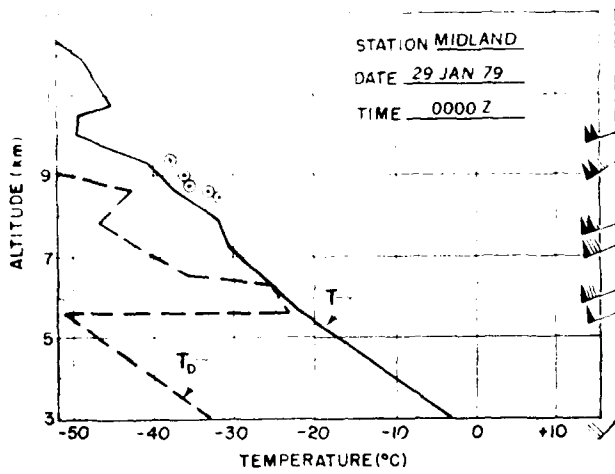


Figure 5. Midland, Texas - 0000Z, 29 January 1979 sounding. Circles are C-130 temperature measurements on E-Pase plot. Tropopause was at 10.0 km AGL.

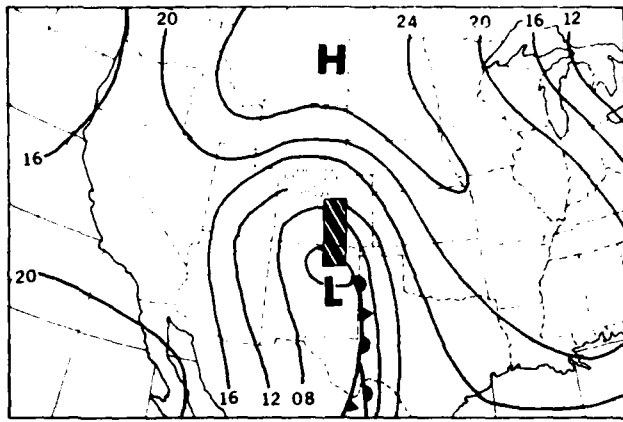


Figure 7. Surface Synoptic Chart at 2100Z, 29 January 1979. Add 1000 millibars to isobar values

deepened considerably, as can be seen in Figure 10. Figures 11 and 12 show the radiosonde soundings for Albuquerque, New Mexico, and Denver, Colorado. While Albuquerque was already well behind the front and thus clearing, the Denver radiosonde shows both a moist layer 6 km thick as well as the front that caused it (at 3 1/2 km), marked by a strong inversion and a wind shift. The westerly and northwesterly flow both aloft and at the surface brought rapid clearing to western New Mexico, and as the storm moved eastward, rapid clearing occurred in the sampling area. The upper air trough became stationary, and as the storm moved eastward, it weakened as dry air from a high pressure area, located in Montana (Figure 7) caused it to lose energy.

This continental high pressure area pushed southward and provided the New Mexico area with two days of clear weather until a complex system moved in from the Pacific Ocean. A weak Pacific cold front moved through southern California and Arizona on 31 January and passed through New Mexico on 1 February. Meanwhile, a second cold front formed over Nevada and Utah, as colder continental polar air pushed toward this area. By 1200Z on 2 February, the Pacific front was in the Texas Panhandle, while the polar front had moved to Central Utah and Central Colorado. As Figure 13 shows, by 2100Z on 2 February, the Pacific front had dissipated, while the polar front had moved into the Texas Panhandle and northern New Mexico. The cirrus in advance of this front was sampled during the flight of 2 February. As shown in Figure 14 (a GOES visible satellite photo), an extensive area of low cloud was moving south with the polar front. Figure 15 (the corresponding infrared photo) shows the

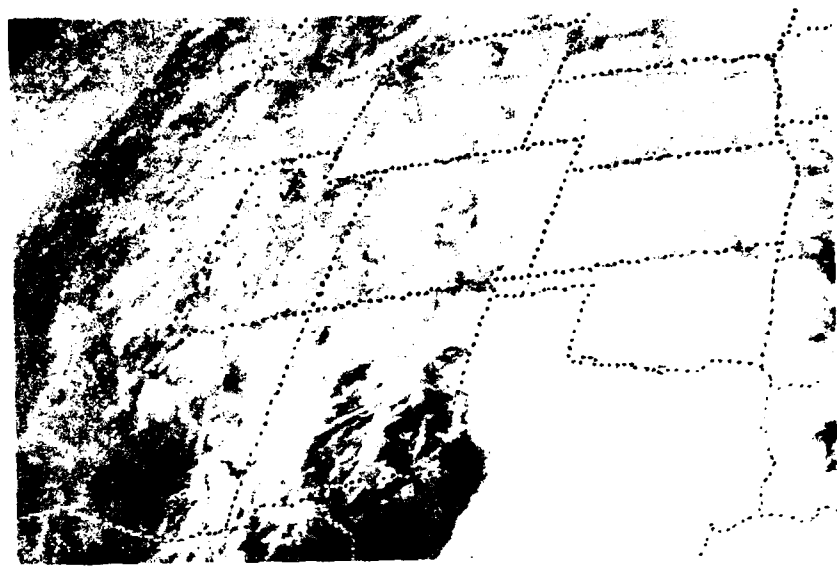


Figure 8. GOES-East Visible Photo of Cloud Conditions Over Southwest U.S. at 1901Z on 29 January 1979

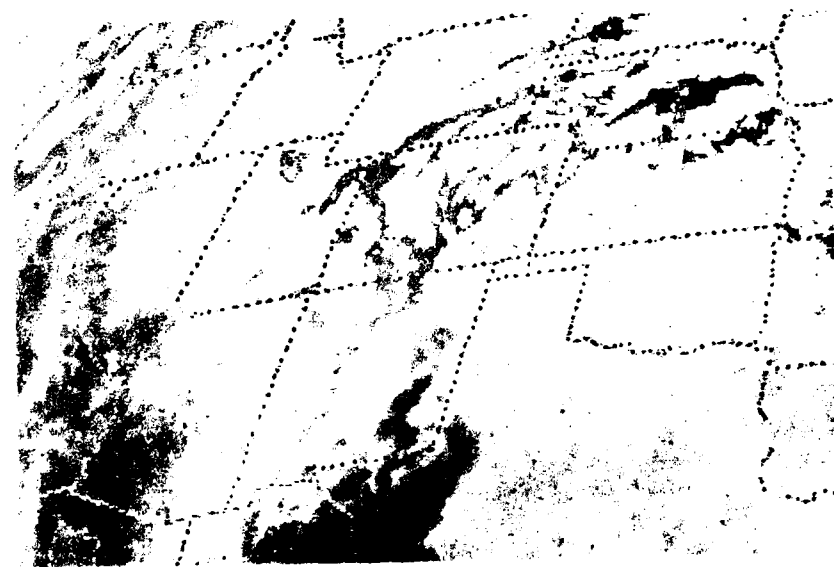


Figure 9. GOES-East Infrared Photo of Southwest U.S. at 1930Z on 29 January 1979

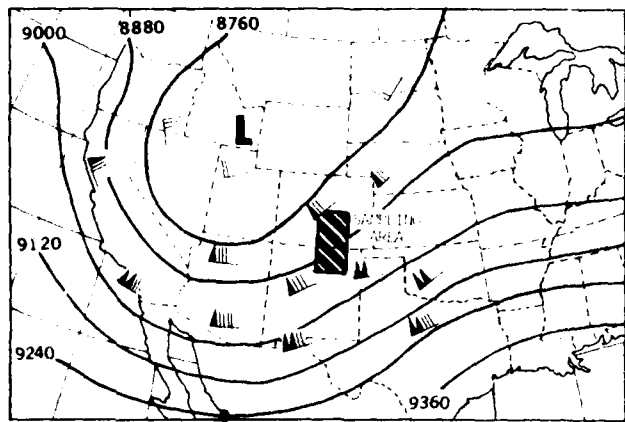


Figure 10. 300-mb Analysis 1200Z, 29 January 1979. Height in geopotential meters

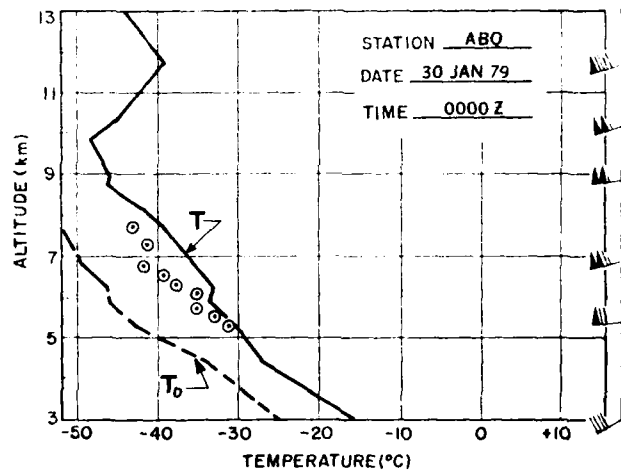


Figure 11. Albuquerque, N.M. Sounding 4 hr After 29 January 1979 Sampling. Circles are aircraft-measured temperatures along the flight track. Tropopause was at 9.8 km MSL

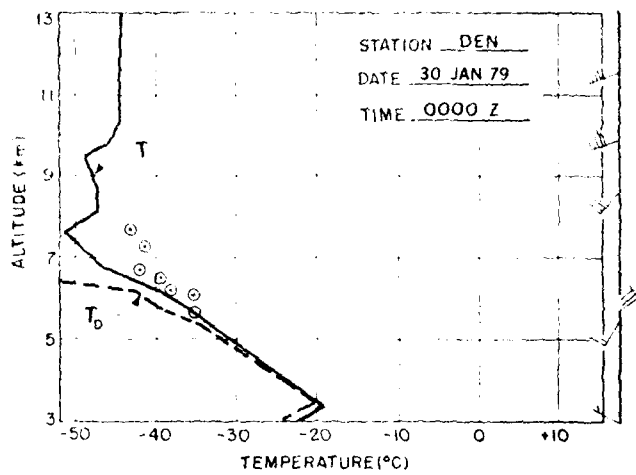


Figure 12. Denver, Colorado Sounding 4 hr After 29 January 1979 Sampling. Front is at 3 1/2 km. Circles are aircraft measured temperatures as on Albuquerque sounding. Tropopause was at 7.6 km MSL.

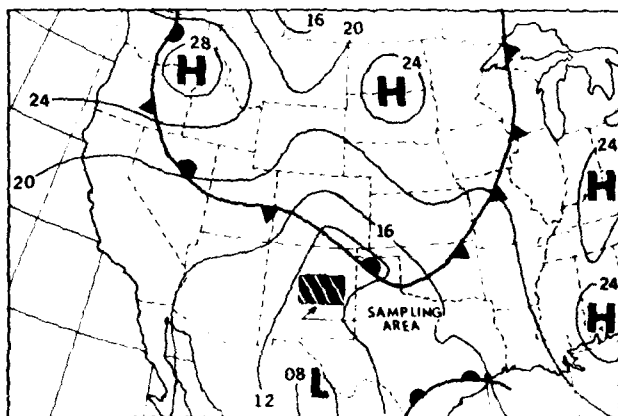


Figure 13. Surface Synoptic Chart at 2100Z, 2 February 1979. Add 1000 millibars to isobar values.

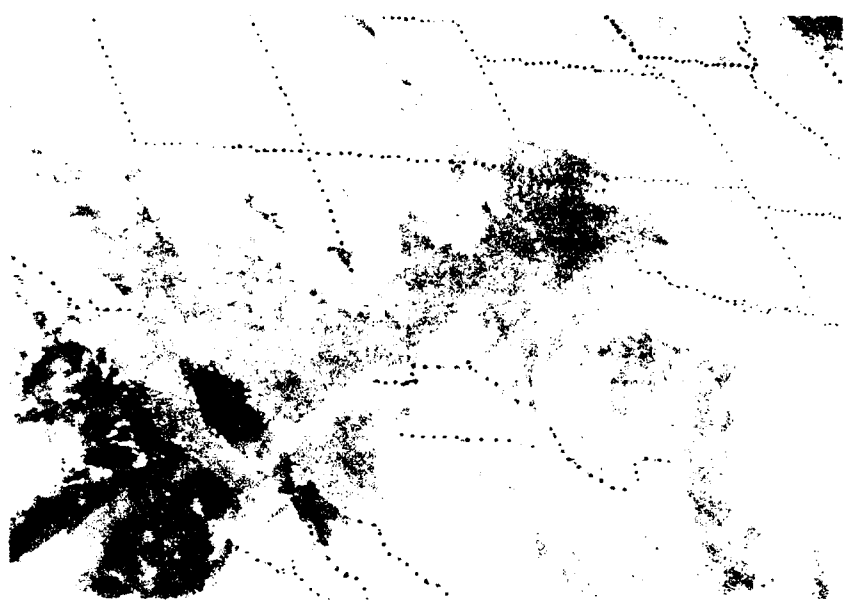


Figure 14. GOES-West Visible Photo Centered on North America at 2045Z, 2 February 1979.

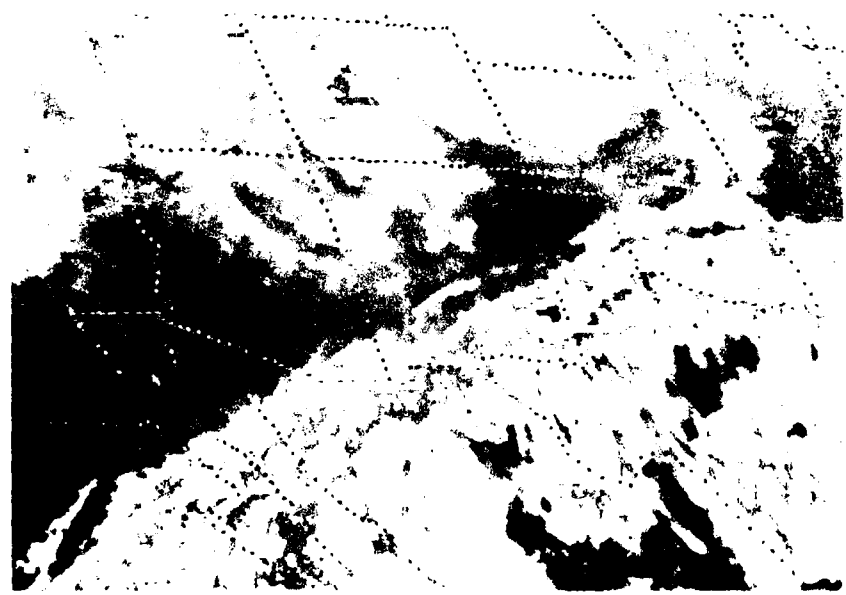


Figure 15. GOES Infrared Photo at 1945Z, 2 February 1979. This was last IR picture received before sampling 6 min later.

cirriform clouds associated with the weakening Pacific front in Oklahoma, Texas, and southeastern New Mexico. Much of this cirrus was so thin that it is almost invisible in Figure 15. Figure 16 shows the sharp 300-mb trough and strong jet stream with winds of 170 kt over central Arizona and New Mexico, which supported these systems. Figures 17 and 18 show the soundings at El Paso, Texas, and Albuquerque, New Mexico on the morning of 2 February. The Pacific front shows up clearly on the El Paso sounding at the 5-km level. The advancing cirrus shows up on the Albuquerque sounding as a thin moist layer at 7.5 km. During the day, the polar front became stationary while the Pacific front regenerated over eastern Texas. By 0000Z on 3 February, the polar front showed signs of weakening, but the cirrus over central New Mexico remained there through 1200Z. Thus a continuous, persistent shield of thin cirrus was present throughout the time of the third sampling flight. The synoptic situation on this flight was strikingly similar to that of an earlier flight,⁵ but on 2 February the upper air winds were somewhat stronger and the polar front somewhat weaker than on the earlier flight. Thus the resulting cirriform clouds seen on the previous occasion were more diffuse.

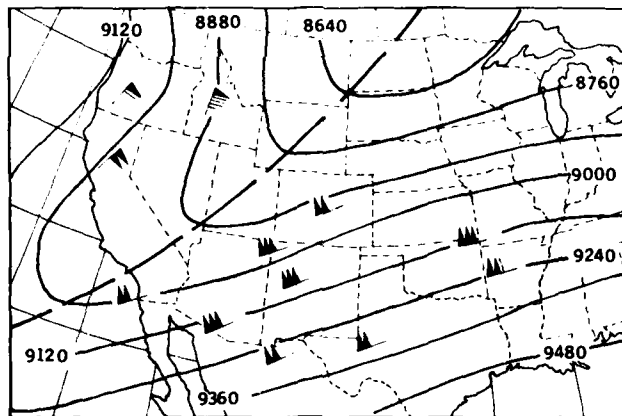


Figure 16. 300-mb Analysis at 0000Z, 3 February 1979. Heights shown in geopotential meters

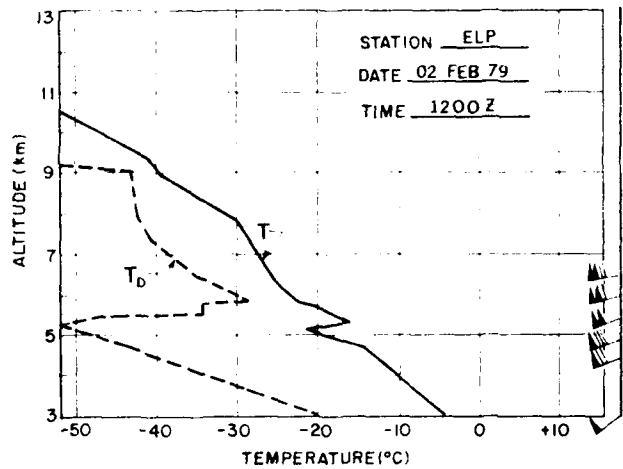


Figure 17. El Paso, Texas Sounding At 1200Z on 2 February 1979 Sampling Flight. Tropopause was at 11.8 km MSL. Winds were not measured above 6.6 km

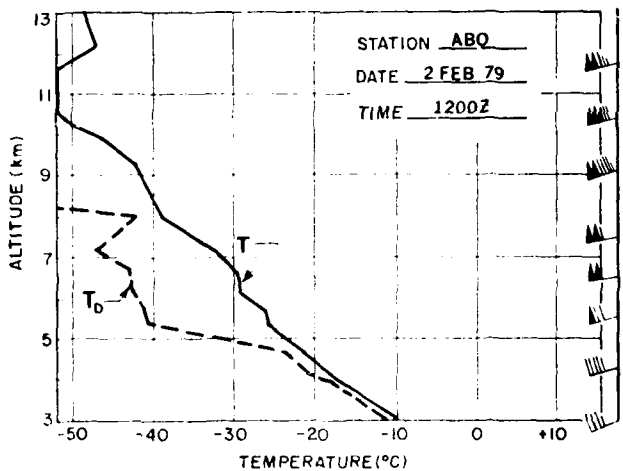


Figure 18. Albuquerque, N. M. Sounding At 1200Z on 2 February 1979 Sampling Flight. Tropopause was at 11.0 km MSL. Maximum wind was 181 ft at 16.5 km

4. 28 JANUARY 1979 FLIGHT AND DATA

The 28 January cirrus sampling began at Kirtland AFB, New Mexico, at 1924Z (1224 MST) and proceeded south, and then east. Most of the cirrus data were obtained over western Texas at altitudes between 7,5 and 9,5 km. The general flight track is shown in Figure 19.

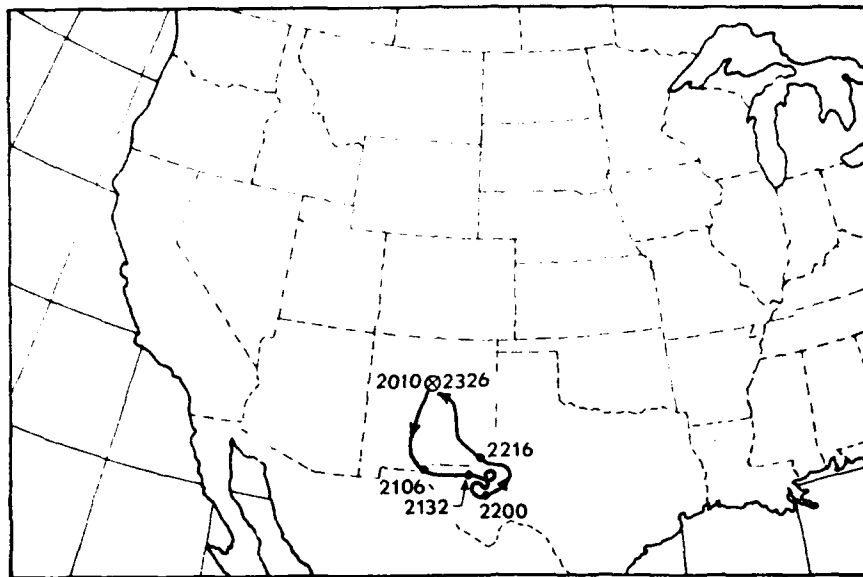


Figure 19. Path of C-130 Sampling Flight on 28 January 1979. Aircraft departed and landed at Kirtland AFB, Albuquerque, N. M. Numbers indicate times in UMT

4.1 Data Variations During the Flight

An over-all view of the variation of several parameters during part of the 28 January flight is shown in Figure 20. The top portion, for example, indicates, that the greatest altitude attained was near 9 km at about 2155Z. Outside air temperature during most of the flight at cirrus altitudes was between -30 and -36°C .

Part b of Figure 20 reflects mass determinations from the scatter probe (measuring particles from ~ 2 to $27 \mu\text{m}$), whereas Part c shows similar values for the combined cloud and precipitation probes (ranges of ~ 26 to $4700 \mu\text{m}$).

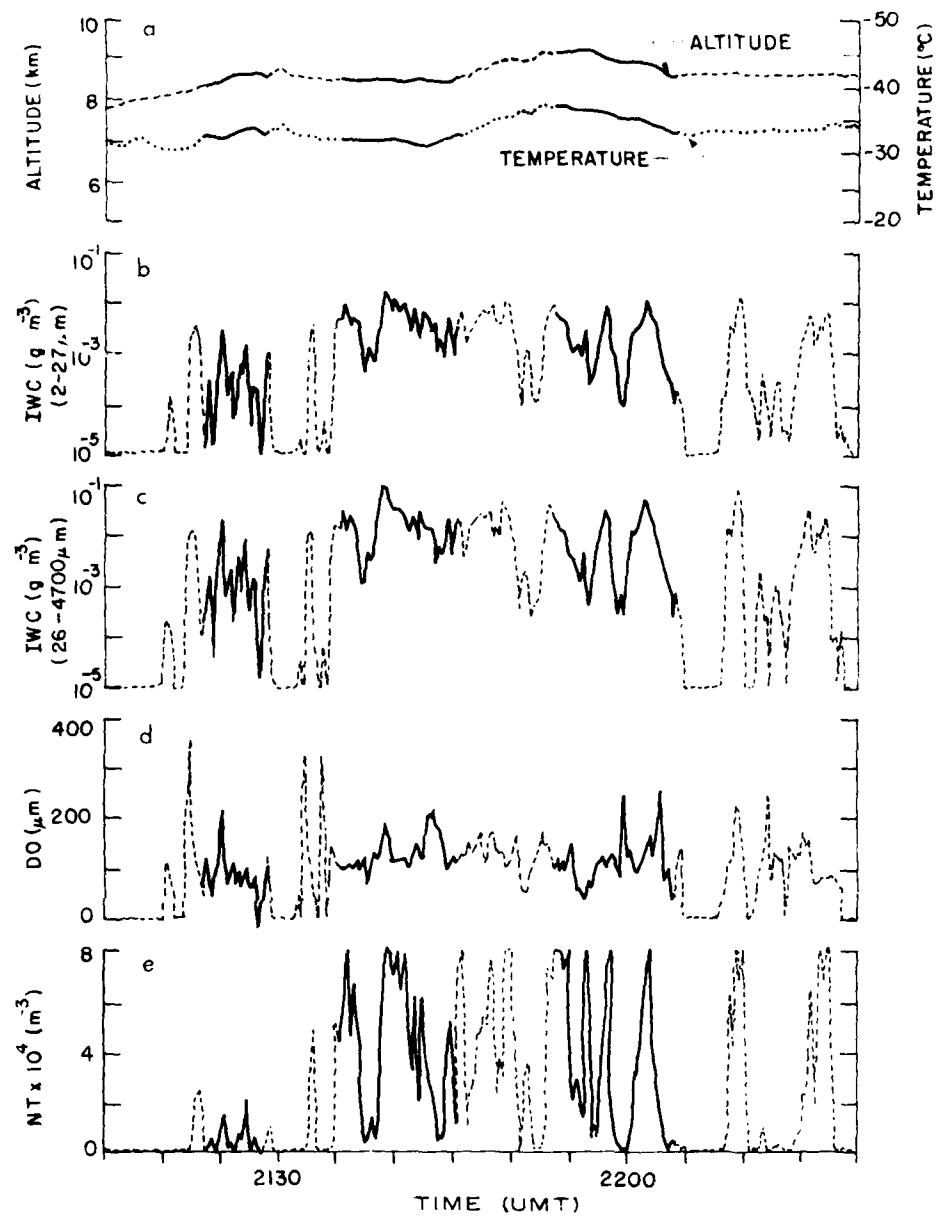


Figure 20. Variation With Time During 28 January Flight of (a) Aircraft Altitude and Temperature, (b) Ice Water Content from ASSP, (c) Ice Water Content from 1-D PMS Cloud and Precipitation Probes, (d) Median Volume Diameter of "Melted" Particles, and (e) Total Number of Particles Over 47-4700 μm Range. Based on values of consecutive 15 sec samples. Solid lines indicate data of the 3 passes described in Table 1.

Variations of mass, as calculated from the two sets of probes, are well correlated, although absolute values are different, as should be expected. The problems of determining the mass of ice crystal regimes through use of a scatter probe have been recognized for some time. Both Hobbs et al¹⁴ and Ryder¹⁵ have cautioned that the Axial Scattering Spectrometer Probe (ASSP) produces an overestimate of ice crystal concentration because of multiple pulsing from the many faceted scattering particles. Despite this problem concerning data from the ASSP, measurements have been included on Figure 20 and other data formats herein, in order to provide at least a relative record of the small-sized ice crystals present.

For the 28 January sampling, Part c of Figure 20 shows that the greatest calculated IWC for a 15-sec sample was nearly 0.09 g m^{-3} , occurring at $\sim 2139\text{Z}$. The second highest value of about 0.08 g m^{-3} was determined for data at 2210Z .

The variation during the flight of the particle median volume diameter, D_o , a calculated quantity based on particles in the 26 to $4700 \mu\text{m}$ -size range, is shown in Part d of Figure 20. The D_o is the "equivalent melted" particle diameter at the fiftieth percentile of the ice water content; that is, half of the ice water exists in smaller melted droplet sizes, and half in larger sizes. Typical D_o values during most of the cirrus sampling on this flight were between 75 and $200 \mu\text{m}$.

The variation of NT, the total number of particles in the 47- to $4700\text{-}\mu\text{m}$ range, is given in part f of Figure 20. This quantity varied considerably from very high to very low values as the aircraft passed through portions of heavier cirrus. Occasionally, values in excess of the $60,000 \text{ m}^{-3}$ upper limit of the figure were recorded. The greatest 15-sec NT was $142,000 \text{ m}^{-3}$, which occurred at 2153Z . Three other consecutive samples were greater than $120,000 \text{ m}^{-3}$ at about 2139Z .

A more comprehensive tabulation of the values on Figure 20 for each 15 sec sample is given in Appendix A. In addition, Appendix A lists L_{\max} , which is the mean physical size (in micrometers) of the largest spectrometer channel having $>1 \text{ particle m}^{-3} \text{ mm}^{-1}$. For many purposes, this can be considered the largest particle size contributing to a given number-size spectrum. The L_{\max} column in Appendix A shows the largest particles measured in most spectra, ranging from approximately 300 to $1300 \mu\text{m}$. Values of less than $1000 \mu\text{m}$ are usually indicative of a spectrum made up of a small number of small particles, and may be discounted ordinarily, except as an indicator of subvisible cloudiness.

14. Hobbs, P. V., Radke, L. F., and Atkinson, D. G. (1975) Airborne Measurements and Observations in Cirrus Clouds, AFCRL-TR-75-0249, AD A015 937, 117 pp.
15. Ryder, P. (1976) The measurement of cloud droplet spectra. Preprints of Internat. Conf. on Cloud Phys., Boulder, Colorado, Amer. Meteor. Soc., 775-780.

The form factor of each 15-sec sample is also given in Appendix A under the "FF" heading. The form factor is a mathematical value between 0. and 1.00, first described by Plank¹⁶ and Plank and Barnes.¹⁷ It has been found useful in characterizing the shape of given spectra.

The form factor is calculated as

$$FF = \frac{\sum_{i=1}^{i=n} (2i-1)^3 \sigma_i}{\left[\sum_{i=1}^{i=n} (2i-1)^3 \sigma_i \right]^{0.5}}$$

where i is the specific channel of data being considered (from 2 to 15 for the PMS cloud probe and from 4 to 15 for the precipitation probe) and σ_i is the ratio of the number of particles in channel i to the total number in all channels (for sizes from -47 to 4700 μ m).

Values of FF based on approximately 10 or fewer channels of particle data may be spurious and not meaningful. This is usually the case when FF is computed to be greater than 1.00 as often happens in the Appendices to this report. Plank¹⁸ has also warned that the form factor can be ambiguous in that two different spectra may have the same FF number. However, in a previous AFGL report,¹⁹ there was little difficulty in gaining useful intelligence from the form factor as long as the air temperature or altitude of a given sample was known. Figure 21, from that AFGL report, was developed from a study of particle spectra in both cirrus and lower clouds and shows the approximate FF values for four generalized spectra. The nearly straightline (on log-linear plots) exponential distributions are closely approximated by the factors in the 0.25 to 0.35 range.

The tabulations of data in the Appendices also include notes or comments made by the mission director during the course of the flights. He sat in the

16. Plank, V.G. (1977) Hydrometeor Data and Analytical-Theoretical Investigations Pertaining to the SAMS Rain Erosion Program of the 1972-73 Season at Wallops Island, Virginia, AFGL-TR-77-0149, Environmental Research Papers 603, AD A051 192, 239 pp.
17. Plank, V.G., and Barnes, A.A., Jr. (1978) An improvement in obtaining real-time water content values from radar reflectivity, Preprints of 18th Conf. Radar Meteor., Atlanta, Amer. Meteor. Soc., 426-431.
18. Plank, V.G. (1979) Private Correspondence.
19. Varley, D.J. (1980) Microphysical Properties Of a Large Scale Cloud System 1-3 March 1978, AFGL-TR-80-0002, Environmental Research Papers 690, AD A083 140, 100 pp.

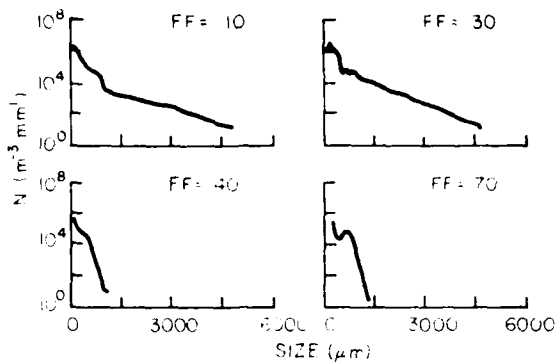


Figure 21. Typical Spectra and Representative Form Factor Values

aircraft cockpit and had a good vantage from which to see the type clouds being sampled.

4.2 Data for Particular Passes

After reviewing the mission director's notes, data tabulations, and the variation of data on Figure 20 we selected three periods during the flight for further studies. These are given in summary form in Table 1 and are also reflected on Figure 20 by the three intervals of solid lines across any given data plot. Brief order-of-magnitude (or larger) changes occurred in IWC and D_o during these periods, but generally cloud conditions were relatively homogeneous.

Table 1. Portions of 28 January 1979 Flight Examined in Figure 22

Pass	Period	Number of Samples	Average Temperature	Average Altitude (km)	Type
1	2123-2128Z	20	-33°C	8.5	Near Cs base
2	2135-2150Z	60	-33	8.6	In heavy Cs
3	2153-2203Z	40	-36	9.0	In heavy Cs

Data for five sets of variables for each of the three periods are shown in histogram form on Figure 22. The bottom row presents data for the 2123-2128Z period designated Pass 1, the middle row for 2135-2150Z Pass 2, and the top row for 2153-2203Z, Pass 3. The height of each histogram bar reflects the

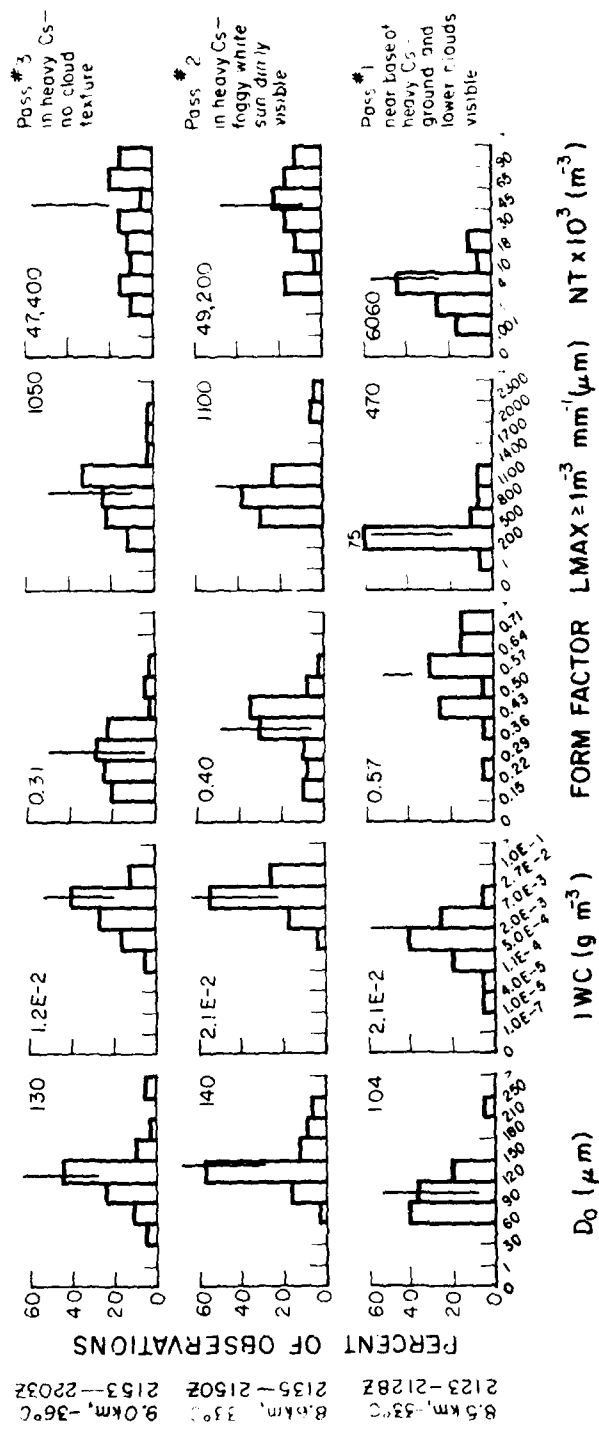


Figure 22. Percentage Frequency by Class of Five Measured or Calculated Variables. Based on total number of 15-sec mean values during 3 periods on 28 January 1979. Printed numbers and vertical lines are 50 percentile values. These do not consider data in cloud-free areas

percentage of sampling time that individual class values were measured or calculated. Each specific percentage was determined from the ratio of the number of 15-sec averages having a certain class value to the total number of 15-sec intervals in a sampling period, for example, the 5 min for the 2123-2128Z period had 20 samples.

The numerical value of the 50 percentile or median quantity of each variable is given with each Figure 22 histogram. A vertical line on each also gives the location of the mean along the abscissa scale. The mean value is based only on 15-sec samples when cloud data were being recorded. Intervals when the aircraft was outside all cloud, or was not recording ice particles are excluded in calculations of mean values, although these periods are reflected in a "no data" class at the extreme left in each histogram.

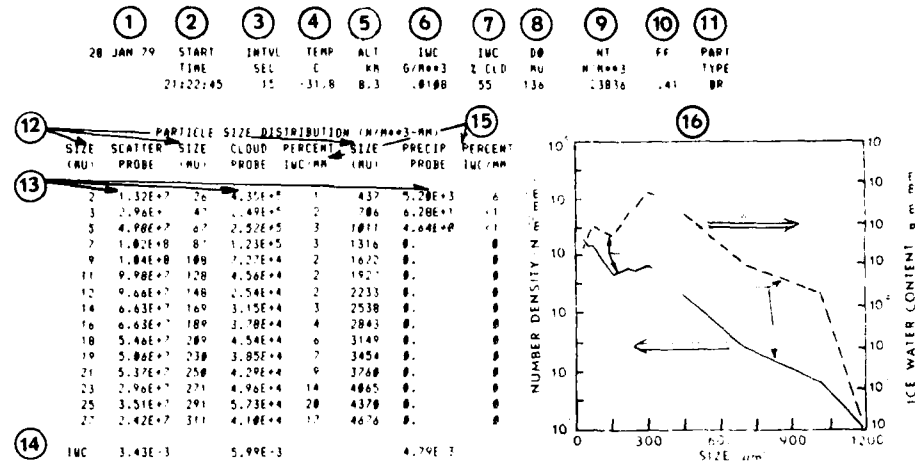
As an example of how Figure 22 may be read, it can be noted at the left side of the bottom row that the predominant (most frequently observed) D_o class was that having limits of 60 and 90 μm . It occurred in 40 percent of the 15 sec averages during the 2123 to 2128Z period. The mean value of D_o , however, was 104 μm . The location of the mean is indicated by a vertical line.

During the 2135 to 2150Z sampling period, the extreme left plot of the middle row of Figure 22 shows that nearly 60 percent of all D_o values were in the 120 to 150 μm class, and that the mean of 140 μm was also within those limits. The modal D_o class for Pass 3 was also that bounded by 120 and 150 μm , while the mean was 130 μm .

The five histograms of Pass 1 on the bottom row of Figure 22 are the result of a flight near or below the base of the visible portion of a heavy cirrostratus layer. The Pass 2 and 3 histograms show modal and mean values of various parameters in a heavier, more dense portion of the Cs. The IWC values in the latter two samples are nearly an order of magnitude greater than those acquired near the cloud base. Values of L_{max} , the largest particles recorded, were generally less than 500 μm in Pass 1, but were as large as 1100 μm during at least 20 percent of the sampling in heavy Cs. Another difference between Pass 1 and the other two was the larger mean number of particles, $47,000-49,000 \text{ m}^{-3}$, recorded in the middle of the Cs layer as opposed to a mean value of about $6,000 \text{ m}^{-3}$ at the base of it. These passes were not above one another but were consecutive along the flight path as may be seen in Figure 19.

Spectra representing typical cloud conditions during the three 28 January sampling periods will be presented on ensuing pages in the format shown in Figure 23. This format is similar to those given in previous parts of this series with certain additional information being added and explained in the figure.

One significant change in the data format is the addition of two columns of data presenting information on the percentage of the total ice water content



1. Date of sampling.
2. Beginning time of sample (Z time)
3. Sampling interval or duration in seconds over which data were averaged.
4. Average ambient temperature in °C during sample.
5. Average pressure altitude in km MSL of sample
6. Ice water content in g m⁻³ calculated from particles of ~26 - 4700 μm size.
7. Percent of IWC in 6, determined from cloud probe (26 to 311 μm) data.
8. Median diameter of "melted" particles (in μm).
9. Total number of particles m⁻³ in the ~47 to 4700 μm size range.
10. Form factor (see text).
11. Main recognizable particle type: Bullet rosettes.
12. Nominal particle sizes measured by each channel of the scatter (ASSP), cloud, and precipitation probes.
13. Number of particles m⁻³ mm⁻¹ in various size classes.
14. Ice water content (g m⁻³) calculated from data of each probe.
15. Percent of 6 above per mm sampling width (see text).
16. Particle number-size distribution in solid lines; ice water content shown in dashed lines.

Figure 23. Description of Data Format

(measured over the 26 to 4700-μm size range and indicated by [15] in Figure 23) that is contributed by each channel of the 1-D cloud and precipitation probes. Because these probes have different size measuring channels, it was necessary to normalize the IWC data to a common millimeter width just as the particle number distribution data have been done. This permits a direct comparison of data between the two probes as if they measured over the same channel widths.

Figure 23 shows that 3 channels of the precipitation probe centered at 437, 706 and 1011 μm contributed less than 8 percent of the total IWC (on a normalized channel size basis). However, because these three channels have a larger measuring area than the cloud probe channels they were actually responsible for 4.79×10^{-3} g m⁻³ (shown at bottom of "Precip Probe" column) of the actual total.

Whether the normalized or unnormalized values of IWC are more valuable will depend on the ultimate use of the data.

Particle spectra and other data from the 3 passes described in the Figure 8 histograms are shown in Figures 24, 25 and 26. They indicate averages of conditions over selected 15 second intervals within the overall 5 to 15 minute passes. The particular interval was chosen for display from the many given in Appendix A to show most of the characteristics indicated by the modal classes in Figure 22. Emphasis was placed more on the predominant classes than mean values for the overall sampling period because it was found that in some instances the mean values rarely occurred. For example, the L_{max} of the spectrum (not shown here) incorporating all the data of Pass 1 was near 1000 μm , while the pass data on Figure 22 showed that 60 percent of the samples during the 5 min Pass 1 period had values less than 500 μm , and the mean of the several samples was 470 μm . The average spectrum for the entire pass in this case reflected the presence of an anomalously large number of particles in some size ranges that were not recorded in most individual 15-sec samples.

Figure 24 presents representative tabulated and plotted data during Pass 1 when the aircraft was moving in and out of portions of the base of a Cs layer. The greatest particle size recorded was in the 437- μm channel of the precipitation probe. The most significant contribution to overall ice water content was from the five largest channels of the cloud probe each of which provided 12 to 13 percent of the total.

28 JAN 79	START	INTVL	TEMP	ALT	IWC	IUC	DO	HT	FF	PART
TIME	SEC		C	KM	G/M**3	% CLD	NU	N/M**3		TYPE
21:24:30	15	-32.0	8.4	.0011	99	107	4536	.60	BR	

PARTICLE SIZE DISTRIBUTION (N/M**3-MM)							
SIZE	SCATTER	SIZE	CLOUD	PERCENT	SIZE	PRECIP	PERCENT
(NU)	PROBE	(NU)	PROBE	IWC/MM	(NU)	PROBE	IUC/MM
2	1.59E+6	26	1.40E+5	2	437	1.42E+0	<1
3	1.59E+6	47	7.00E+4	3	706	0.	0
5	4.77E+6	67	1.83E+4	1	1011	0.	0
7	6.35E+6	87	1.64E+4	2	1316	0.	0
9	8.73E+6	108	7.39E+3	1	1622	0.	0
11	9.53E+6	128	1.37E+4	4	1927	0.	0
12	4.76E+6	148	1.94E+4	7	2233	0.	0
14	3.97E+6	169	1.24E+4	6	2538	0.	0
16	3.18E+6	189	9.61E+3	6	2843	0.	0
18	3.97E+6	209	6.29E+3	5	3149	0.	0
19	7.15E+6	230	1.15E+4	12	3454	0.	0
21	4.77E+6	250	1.07E+4	13	3760	0.	0
23	7.95E+5	271	8.09E+3	13	4065	0.	0
25	7.93E+5	291	6.36E+3	13	4370	0.	0
27	3.17E+6	311	5.01E+3	12	4676	0.	0

IWC 2.56E-4 1.09E-1 2.18E-1

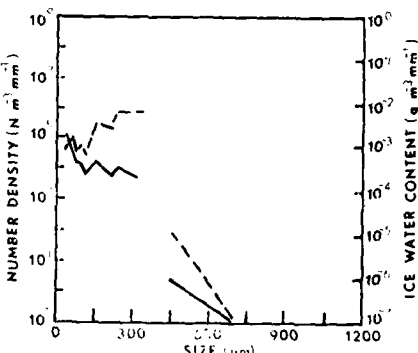


Figure 24. Representative Ice Crystal Spectrum for a 15-sec Interval During Pass 1 Through the Base of a Cirrostratus Layer on 28 January 1979

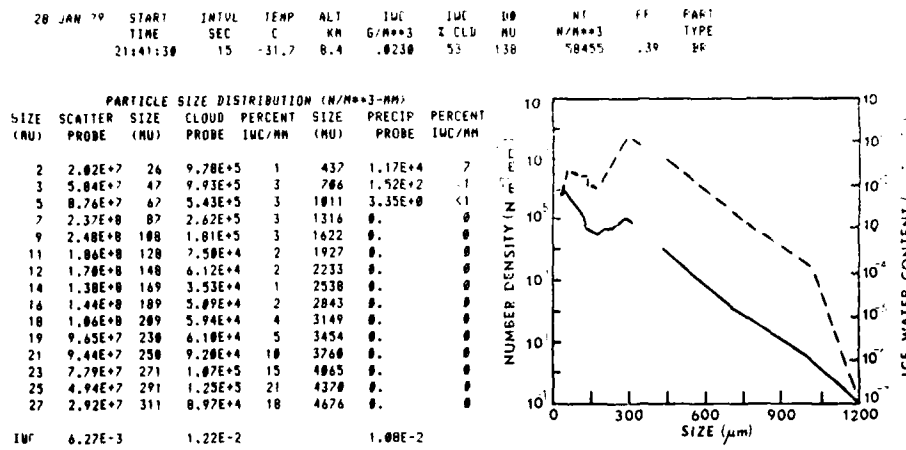


Figure 25. Representative Spectrum for a 15-sec Interval During Pass 2 Through Heavy Cs on 28 January 1979

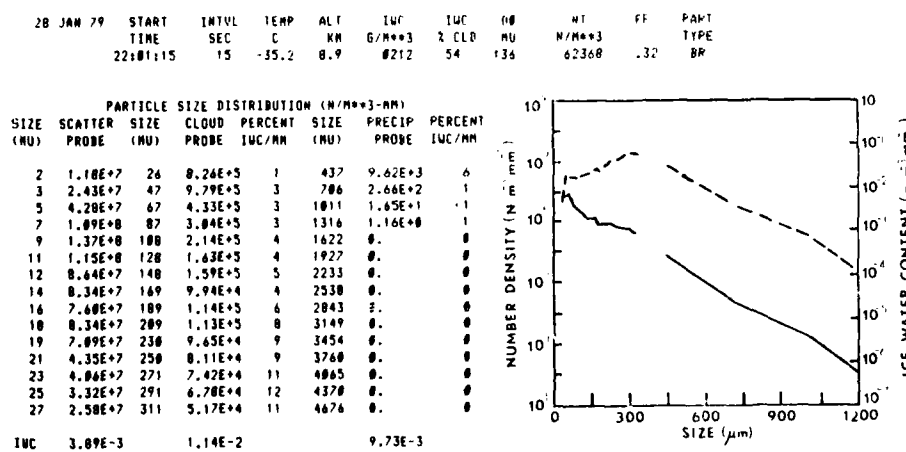


Figure 26. Representative Spectrum for a 15-sec Interval During Pass 3 Through Heavy Cs on 28 January 1979

The spectrum in Figure 25, representing the middle of a fairly heavy cirrostratus layer, exhibits a minimum in the distribution curve near the 170 μm particle size while there is a maximum in the curve at approximately 290 μm . Similar minima were observed in cirriform spectra described by Varley,¹⁰ They have also been pointed out by Heymsfield⁹ as being somewhat typical in cirrus uncinus heads. He thought the maximum at sizes near or below 500 μm might reflect an accumulation of crystals of that length in an updraft. Some 21 percent of the total Figure 25 IWC was due to particles recorded by the 291- μm channel size.

The distribution of Figure 26, in heavy fog-like Cs, has a nearly straight-line, exponential decrease of particle number with increasing size. As in the previous figure, the greatest contribution to over-all ice water mass was at the 291- μm channel size; but the IWC curve in Figure 26 is considerably smoother than those shown in Figures 24 and 25. The form factor of the Figure 26 spectrum is 0.32, which is in the 0.25 to 0.35 range previously identified and associated with exponential distributions.

Both Figures 25 and 26 spectra are from heavy cirrostratus clouds. While minimum and maximum points are evident at sizes less than 300 μm in the former, they are absent in the latter. Such valley-peak distributions may be evidence of an aggregation mechanism which occurs more frequently in the middle and lower portions of Cs. The Figure 26 spectrum represents data from an altitude of 8.9 km MSL, perhaps above the level that aggregation begins. At 8.4 km, the altitude of the Figure 25 spectrum, the aggregation process may have been better established.

5. 29 JANUARY 1979 FLIGHT AND DATA

The 29 January flight departed Kirtland AFB at 1647Z (0947 MST) and flew north and east into the Pueblo, Colorado area. Several sampling passes were made at lower levels east of the Rocky Mountains for another AFGL program, then sampling in the thin cirriform clouds above the surface storm began at about 1845Z. As the aircraft proceeded in a generally southerly direction back to Kirtland, the cloud tops decreased in height. The main portions of this day's flight track were as indicated on Figure 27.

5.1 Data Variations During the Flight

The variations of several measured or calculated variables during the 29 January sampling are plotted on Figure 28. Since the flight was made near the upper level low, the outside air temperature and cirrus tops were both lower

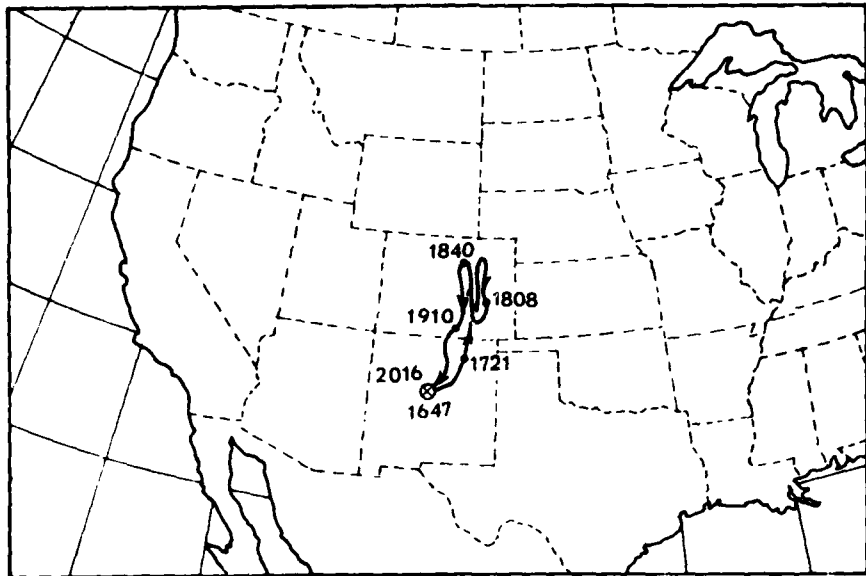


Figure 27. Flight Track of Sampling Aircraft on 29 January 1979.
Numbers indicate times in UMT

than those observed in most previous flights. As shown in the top of Figure 28, all sampling was accomplished at altitudes less than 8 km (26,000 ft) MSL. As the aircraft moved southward, the cirriform tops were found at progressively lower altitudes.

By 1945Z the C-130 was in the thin cloud tops over northern New Mexico at slightly above 5 km. There was some doubt at that time whether those clouds could be considered cirriform; however, they were definitely composed of ice particles and the temperature was -30°C or colder, which Mason,²⁰ among others, has indicated satisfies the criteria to be considered cirriform.

Parts (b) and (c) of Figure 28 show that the variations of IWC as determined from measurements of the scatter probe and the cloud plus precipitation probes were fairly well correlated. There was one extended period, however, beginning about 1905Z when the scatter probe recorded a small number of small particles when there were no measurements in the other probes. The largest calculated IWC of this sampling over the 26 to $4700 \mu\text{m}$ range was 0.06 g m^{-3} at about 1848Z. The radical high to low IWC changes occurring between 1920 and 1940Z are indicative of passage through numerous small cloud elements.

20. Mason, B.J. (1962) Clouds, Rain and Rainmaking, Cambridge University Press, 145 pp.

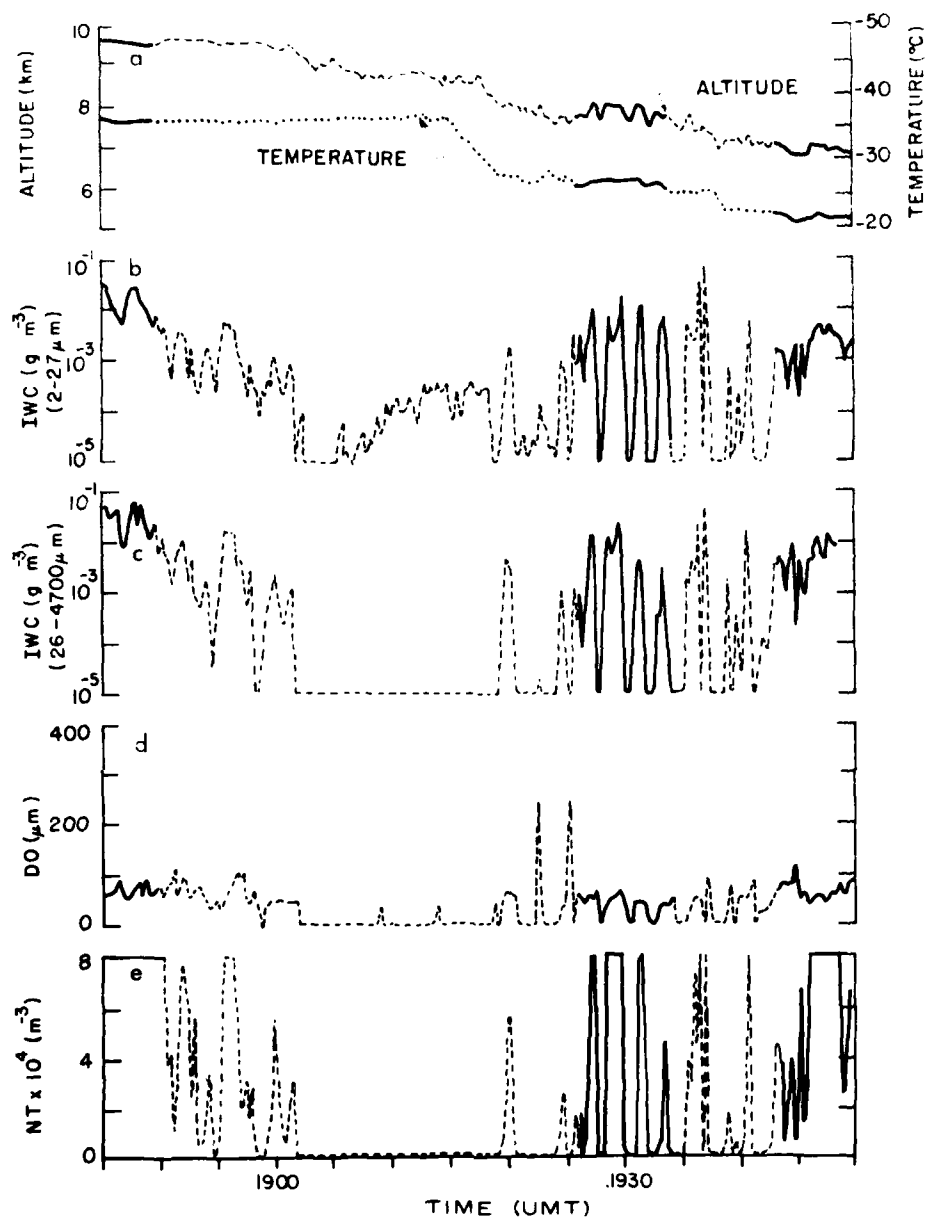


Figure 28. Variation With Time During 29 January 1979 Flight of (a) Aircraft Altitude and Temperature, (b) Ice Water Content from ASSP, (c) Ice Water Content from 1-D PMS Cloud and Precipitation Probes, (d) Median Volume Diameter of "Melted" Particles, (e) Total Number of Particles Over 47-4700 μ m Range. Based on values of consecutive 15-sec samples. Solid lines indicate data of the 3 passes described in Table 2

The median volume diameter of typical "melted" particles was quite small in this sampling. Values ranged from approximately 30 to 125 μm , with only a few higher than 150 μm . The variation of D_v during the flight is shown in Part (d) of Figure 28.

The total numbers of particles detected during most of the cloud penetrations on 29 January were high with respect to our previous experience. During the 1845 to 1850Z period, for example, the average number was $358,000 \text{ m}^{-3}$. This compares to an average of $25,000 \text{ m}^{-3}$ measured during a 9.0 km pass through thin cirrus over New Mexico on 1 March 1978 (Varley)¹⁹ and a mean of $49,000 \text{ m}^{-3}$ recorded during one pass in this report on 28 January 1979. The many changes of NT on Figure 28, Part (e) are again a reflection of the numerous entries into, and departures from, small cirriform cloud elements.

The Figures 29 and 30 photographs show the general type of cloud conditions sampled on 29 January. Figure 29 might be considered a "close up" view of the very thin cirrus filaments that fade with height above the main cloud mass into blue sky. Figure 30 shows the main layer of cirrostratus from a distance. An area of snow-covered ground is in the bottom left. The flight proceeded toward the very top of the clouds shown in Figure 30.

5.2 Data for Particular Passes

Three extended periods during the 29 January sampling were selected for further examination and given in Table 2. These were chosen because cloud conditions were fairly homogeneous; however, a few large changes in the microphysical variables did occur. In fact, during Pass 5 nearly 30 percent of the time the aircraft was above or between measurable cloud particles. Pass numbers were selected to be continuous from one day to the next, that is, "Pass 4" is the fourth pass considered in this report.

Table 2. Portions of 29 January 1979 Flight Examined in Figure 31

Pass	Period	Number of Samples	Average Temperature	Average Altitude (km)	Type
4	1845-1850Z	20	-48°C	7.7	In Cs near tops
5	1926-1934Z	32	-37	6.1	Skim. Cs/Cc tops
6	1943-1950Z	28	-31	5.2	Skim. Cs/Cc tops



Figure 29. Photo of Thin Cirrus Sampled Above Main Cs Cloud, 29 January at 1906Z. Dark blue sky at top. Near 37°47'N, 104°50'W

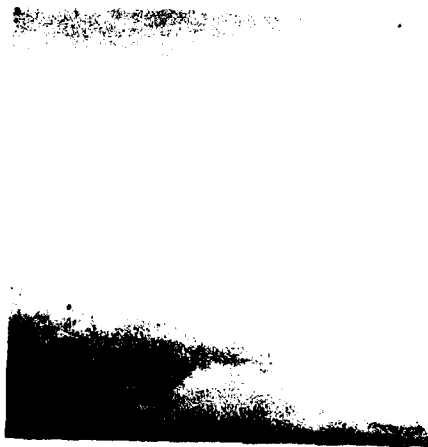


Figure 30. Photo of Main Cs Cloud 29 January at 1951Z. Sampling Proceeded Through Extreme Top of Cs Shown. Near 35°28'N, 105°29'W. Dark blue sky at top. Area of snow-covered ground at bottom left

During Pass 4, sampling took place in relatively dense clouds, the tops of the tops. A tail often appeared around the sun, since the sun was almost obscured by the higher portion of the Cs. There was some cloud penetration, so that the sunburst and blue sky could occasionally be seen. Up until 1845, the tops of the pass 4, the Cs had thinned considerably and much more blue sky could be seen than in the thin cirrus filaments above.

Sampling during both Pass 5 and Pass 6 was in the thin cirrus filaments above the main layer Cs and Cc. Occasionally one of the higher, denser stratiform clouds above the bulk of lower clouds was penetrated. These consisted of thin filaments which resembled fog overlaying a body of water, in addition to the Cs. The tops of these filaments faded into the blue sky at or slightly above the sampling altitude.

Of the three passes the largest values of IWC were calculated for particles during Pass 4, as shown on Figure 31. The average IWC was $1.1 \times 10^{-2} \text{ g m}^{-3}$ for Pass 4 and nearly an order of magnitude less for the other two passes.

As previously indicated, there was an extraordinarily high number of particles recorded in the Pass 4 Cs—more than $350,000 \text{ m}^{-3}$. The NT number class above $90,000 \text{ m}^{-3}$ was also the predominant one having most individual samples during the other passes, although the average figures in these cases were not as great— $78,000$ and $73,000 \text{ m}^{-3}$.

The L_{\max} histograms on Figure 31 show that the largest particles were recorded in Pass 4 going through Cs. About 15 percent of the particles were larger than $1100 \mu\text{m}$ and one 15 sec sample had an L_{\max} exceeding $2000 \mu\text{m}$. The predominant L_{\max} class for both the Pass 5 and 6 data was that bounded by 200 and $500 \mu\text{m}$.

The histograms showing median volume diameter, D_0 , on Figure 31 indicate a generally small range of occurrence. Most values of D_0 were less than $90 \mu\text{m}$, though one during Pass 6 was as great as $108 \mu\text{m}$. The averages of the three 29 January passes varied only from 46 through $67 \mu\text{m}$.

The differences in predominant form factor classes between the 3 passes indicate there were differences in typical number-size spectra. Some 50 percent of the form factors of the Pass 4 were less than 0.40, while about 40 percent of those during Pass 5 were equal to or greater than 0.71. Some of the differences are evident in the representative spectra for each of the passes shown in the following figures.

Figure 32 shows a particle spectrum representative of the predominant conditions recorded during the 1845 to 1850Z pass period on 29 January. Both this and the Figure 26 spectra were recorded in the upper parts of a Cs layer and both approximate an exponential decrease of particle number with increasing size. The median volume diameter of the Figure 32 data, however, is $32 \mu\text{m}$ while that

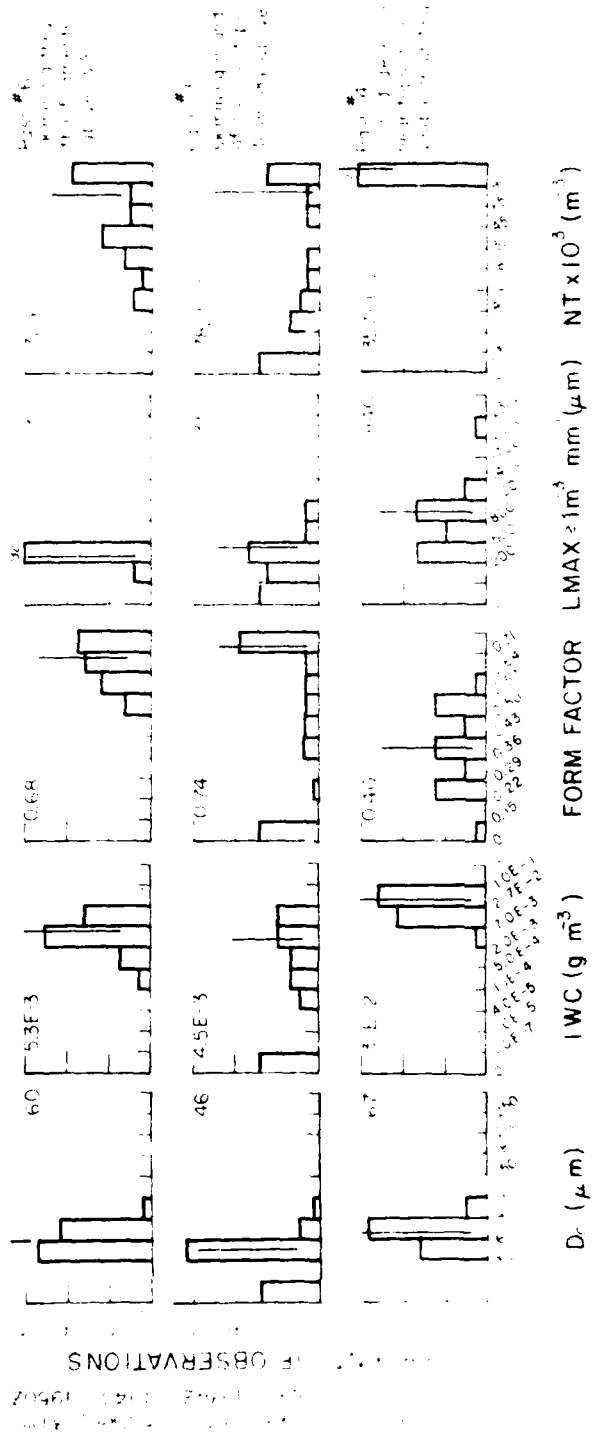


Fig. 1. Particle size frequency by class of five methods and by size. Note that total number of particles during 3 methods on 29 January 1970, permitted no further distinction between methods. Note also that no size data in cloud-free areas.

29 JAN 79 START INTVL TEMP ALT IWC IWC DO NT FF PART
TIME SEC C KM G/M³ % CLD MU N/M³ 310314 .38 BR

20:46:15 15 -47.7 6.7 .0405 67 8. 310314 .38 BR

PARTICLE SIZE DISTRIBUTION (N/M³·MM)
SIZE SCATTER SIZE CLOUD PERCENT SIZE PRECIP PERCENT
(MU) PROBE (MU) IWC/MM (MU) PROBE IWC/MM

2	3.71E+7	26	4.55E+6	4	437	0.	0.
3	5.32E+7	47	4.34E+6	5	706	3.78E+1	0.
5	9.91E+7	67	3.01E+6	1	1011	4.81E+0	0.
7	1.59E+8	87	2.42E+6	4	1316	0.	0.
9	2.15E+8	106	1.62E+6	6	1622	0.	0.
11	2.66E+8	126	1.24E+6	10	1927	0.	0.
12	2.05E+8	148	7.27E+5	9	2233	0.	0.
14	1.53E+8	169	4.76E+5	1	2538	0.	0.
16	1.97E+8	189	3.71E+5	7	2843	0.	0.
18	1.77E+8	209	3.09E+5	1	3149	0.	0.
19	1.79E+8	230	2.13E+5	6	3454	0.	0.
21	1.75E+8	250	1.56E+5	6	3760	0.	0.
23	1.77E+8	271	1.15E+5	6	4065	0.	0.
25	1.25E+8	291	8.52E+4	5	4370	0.	0.
27	1.20E+8	311	5.84E+4	4	4676	0.	0.

IWC 1.24E-2 3.55E-2 5.04E-3

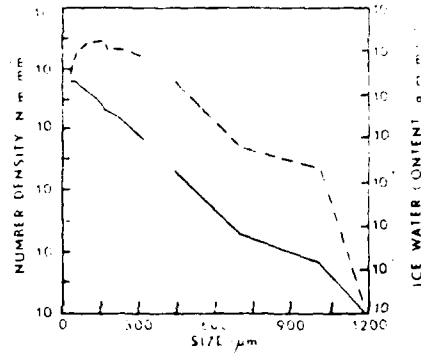


Figure 32. Representative Spectrum for a 15-sec Interval During Pass 4 Through Tops of Moderately Dense Cs on 29 January 1979

29 JAN 79 START INTVL TEMP ALT IWC IWC DO NT FF PART
TIME SEC C KM G/M³ % CLD MU N/M³ 05531 .75 BR

20:29:00 15 -38.0 6.2 .0049 100 51 05531 .75 BR

PARTICLE SIZE DISTRIBUTION (N/M³·MM)
SIZE SCATTER SIZE CLOUD PERCENT SIZE PRECIP PERCENT
(MU) PROBE (MU) IWC/MM (MU) PROBE IWC/MM

2	9.04E+5	26	1.35E+6	4	437	0.	0.
3	4.51E+6	47	1.44E+6	12	706	0.	0.
5	9.04E+6	67	1.23E+6	20	1011	0.	0.
7	1.36E+7	87	8.69E+5	24	1316	0.	0.
9	2.18E+7	106	3.42E+5	15	1622	0.	0.
11	2.44E+7	126	1.84E+5	11	1927	0.	0.
12	2.81E+7	148	6.15E+4	5	2233	0.	0.
14	2.27E+7	169	4.05E+4	4	2538	0.	0.
16	3.17E+7	189	1.89E+4	1	2843	0.	0.
18	1.99E+7	209	4.77E+3	1	3149	0.	0.
19	2.53E+7	230	1.31E+4	3	3454	0.	0.
21	3.26E+7	250	0.	0	3760	0.	0.
23	3.17E+7	271	0.	0	4065	0.	0.
25	2.81E+7	291	0.	0	4370	0.	0.
27	2.35E+7	311	0.	0	4676	0.	0.

IWC 2.15E-3 4.98E-3 0.

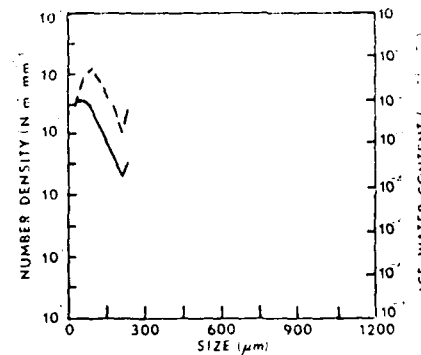


Figure 33. Representative Spectrum for a 15-sec Interval During Pass 5 While Skimming Cs/CC Tops on 29 January 1979

29 JAN 8 START TIME SEC TEMP C ALT KM IWC % ICP % NT N PROBE F1 F4K1
19:46:09 15 -31.0 5.2 0.0034 100 44 0.1300 1.10 0.00

PARTICLE SIZE DISTRIBUTION (IN MM)									
SIZE (MM)	SCATTER PROBE (MM)	SIZE CLOUD PROBE (MM)	PERCENT	SIZE (MM)	FREQUENCY PROBE	PERCENT	IWC	INC	3.91E-3
2	1.87E+6	26	2.67E+6	9	43	0			
3	1.57E+7	47	2.34E+6	24	706	0			
5	2.86E+7	67	1.31E+6	27	1011	0			
7	3.78E+7	87	5.98E+5	21	1316	0			
9	4.62E+7	108	1.68E+5	9	1622	0			
11	5.45E+7	128	4.88E+4	4	1927	0			
12	4.62E+7	148	2.02E+4	2	2233	0			
14	3.98E+7	169	6.32E+3	1	2538	0			
16	3.24E+7	189	1.12E+4	2	2843	0			
18	3.24E+7	209	2.49E+3	1	3149	0			
19	3.51E+7	230	0	0	3454	0			
21	4.34E+7	250	0	0	3760	0			
23	4.53E+7	271	5.57E+2	1	4065	0			
25	3.51E+7	291	1.11E+3	1	4370	0			
27	2.13E+7	311	2.23E+3	2	4676	0			
	IWC	2.78E-3			3.91E-3	0			

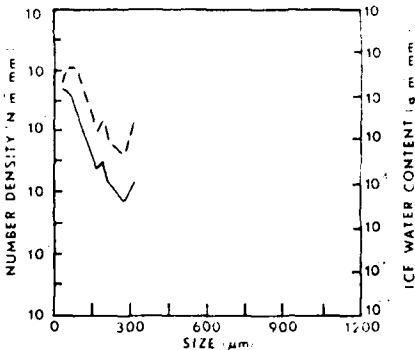


Figure 34. Representative Spectrum for a 15-sec Interval During Pass 6 Through Thin Filaments on Top of Cs/Ce Layer on 29 January 1979

for Figure 26 is 136 μm . Figures 33 and 34 show another difference between the two sets of data. The number density is about one-fourth of that detected lower in the Cs, but still a large figure in comparison to our other flight data. As mentioned above, these large NTs are probably associated with the proximity of the surface storm and the fact that particles were being generated profusely.

6. 2 FEBRUARY 1979 FLIGHT AND DATA

The cirriform clouds sampled on 2 February were primarily associated with a weak cold front and a band of strong winds aloft over the southwestern part of the United States. The aircraft recorded winds in excess of 150 kt. Most of the sampling was accomplished at altitudes between 9 and 10 km MSL over the eastern part of New Mexico as shown in Figure 35.

6.1 Data Variations During the Flight

As previously indicated, and as shown in the top part of Figure 36, most of the sampling on 2 February was conducted near the 9-km MSL level. Free air temperatures recorded by the C-130 were between -38 and -44°C .

The plots of Parts (b) and (c) on Figure 36 show that the variation of ice water mass determined from the scatter probe (in Part b) and the cloud and precipitation probes (in Part c) were generally well correlated. Several IWC values from

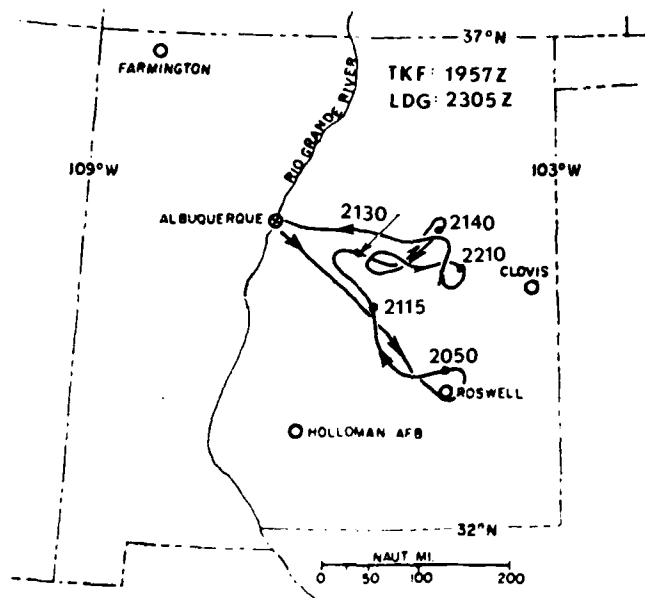


Figure 35. Flight Track of Sampling Aircraft on 2 February 1979. Numbers indicate times in UTC

the latter 2 probes reached as high as 0.005 g m^{-3} , while the peak values were 0.010 at 2108Z and 0.018 g m^{-3} at 2201Z. The relatively small amplitude swings in the IWC plot on Figure 29 indicate the cirriform clouds sampled on 2 February were more consistent and uniform over a given area than those examined on the other two days.

The median volume diameter, D_o , of individual 15-sec samples was generally less than $100 \mu\text{m}$ during most of this flight. As shown in Part d of Figure 29, none were as large as $150 \mu\text{m}$. There was more temporal variation in IWC value than in those of D_o , but this was to be anticipated since IWC varies with the third power of D_o .

There was extensive variation during the flight of the total number of particles detected in the 27 to $4700 \mu\text{m}$ range. Most values of NT were less than $60,000 \text{ m}^{-3}$, but there were two periods from 2107 to 2113Z and from 2201 to 2209Z when they were considerably greater. During the former period, the greatest single value was $156,000 \text{ m}^{-3}$ at 2108:45Z, and during the latter period the maximum was $255,000 \text{ m}^{-3}$ at 2201:15Z.

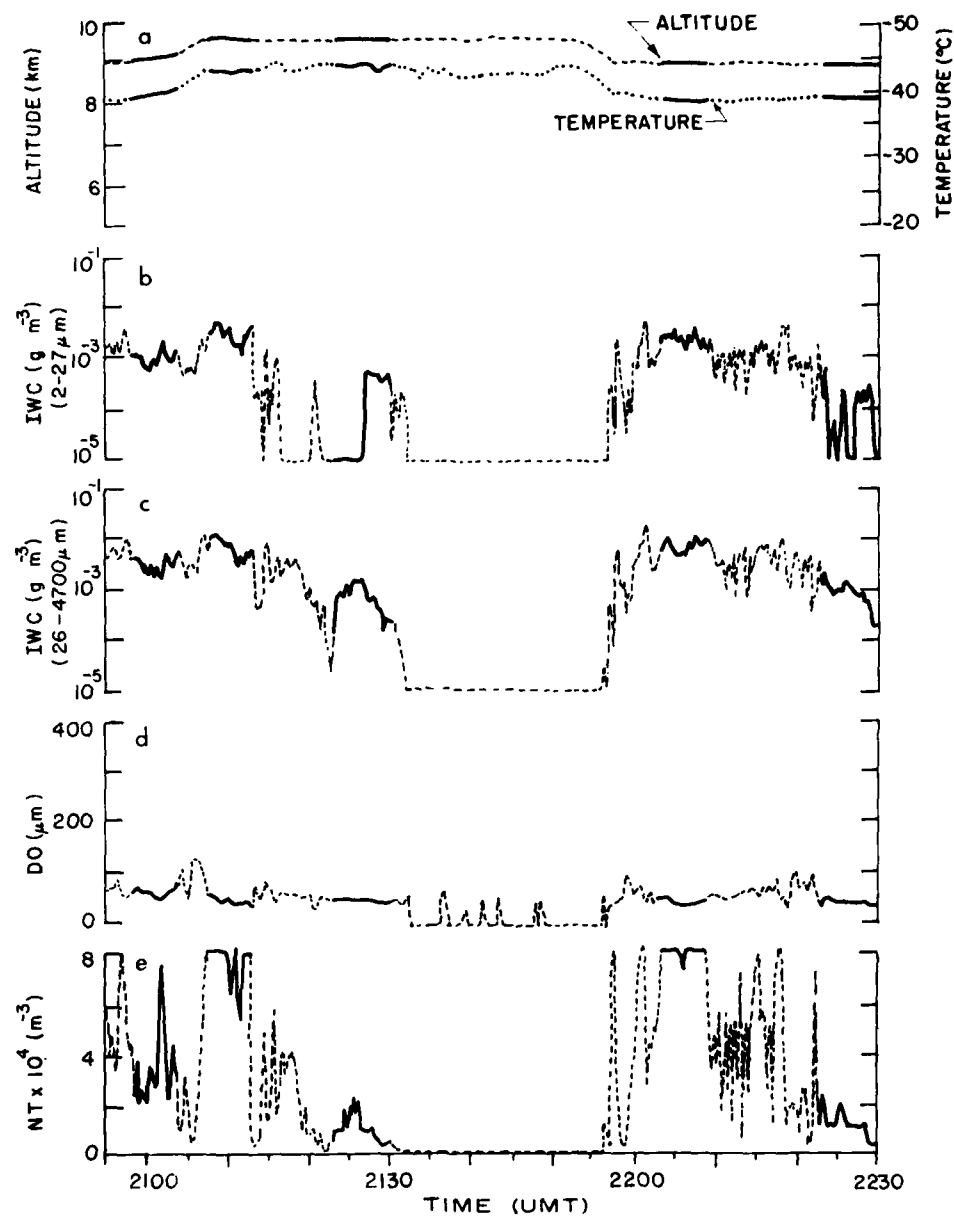


Figure 36. Variation With Time During 2 February 1979 Flight of (a) Aircraft Altitude and Temperature, (b) Ice Water Content from ASSP, (c) Ice Water Content from PMS Cloud, 1-D and Precipitation Probes, (d) Medium Volume Diameter of "Melted" Particles, (e) Total Number of Particles Over 47-4700 μm Range. Based on values of consecutive 15-sec samples. Solid lines indicate data of the 5 passes described in Table 3

6.2 Data for Particular Passes

Based on a review of the data variations on Figure 36 and of the tabulations in Appendix C, 5 periods of approximately 5 minutes or longer were selected for further examination. These were selected based on the relative homogeneity of the data. The period selected are as given in Table 3. The frequencies of particular class values within these periods are shown in the histograms of Figure 37.

Table 3. Portions of 2 February 1979 Flight Examined in Figure 37

Pass Number	Period	Number of Samples	Average Temperature	Average Altitude (km)	Type
7	2018-2104Z	26	-39°C	9.2	Moderate heavy Cs
8	2108-2113Z	21	-43	9.6	In tops of Cs
9	2123-2130Z	28	-44	9.6	Very thin Ci
10	2203-2209Z	24	-38	9.0	Heavy Cs
11	2223-2229Z	25	-39	8.9	Very thin Ci

During Pass 7 of this report (the first on 2 February), the aircraft was flying along and in a band of Cs of varying density. Most of the calculated values of ice water content were in the relatively narrow range of 2 to $7 \times 10^{-3} \text{ g m}^{-3}$ as shown on the bottom line of Figure 37. The $64 \mu\text{m}$ mean D_o value and the $340 \mu\text{m}$ mean L_{\max} value are the largest of those in the 5 passes examined here. The mean NT of $34,000 \text{ m}^{-3}$ is less than the corresponding values near $48,000 \text{ m}^{-3}$ detected in somewhat similar clouds in Passes 2 and 3 taken on 28 January 1979.

The data of Pass 8 were acquired while flying within about 1000 ft of the top of the Cs band. The sky was quite blue above and the ground was dimly visible, but horizontal visibility was greatly reduced. The mean D_o of $50 \mu\text{m}$ was the smallest of the five 2 February passes, but the mean particle count, NT, of $106,000 \text{ m}^{-3}$ was the largest.

Passes 9 and 11 were both made through very thin cirrus, and in both cases the mean number of particles detected was less than $13,000 \text{ m}^{-3}$, as indicated on Figure 37. Only Pass 1, when downward visibility was good, had a lower NT value. The greatest mean particle sizes, L_{\max} , were 170 and $215 \mu\text{m}$. These are the smallest of the 11 cases considered in this report. The calculated IWC values of $1 \times 10^{-3} \text{ g m}^{-3}$ or less are also the smallest ones in this report. While flying and acquiring data of Passes 9 and 11 the mission director noted that in the

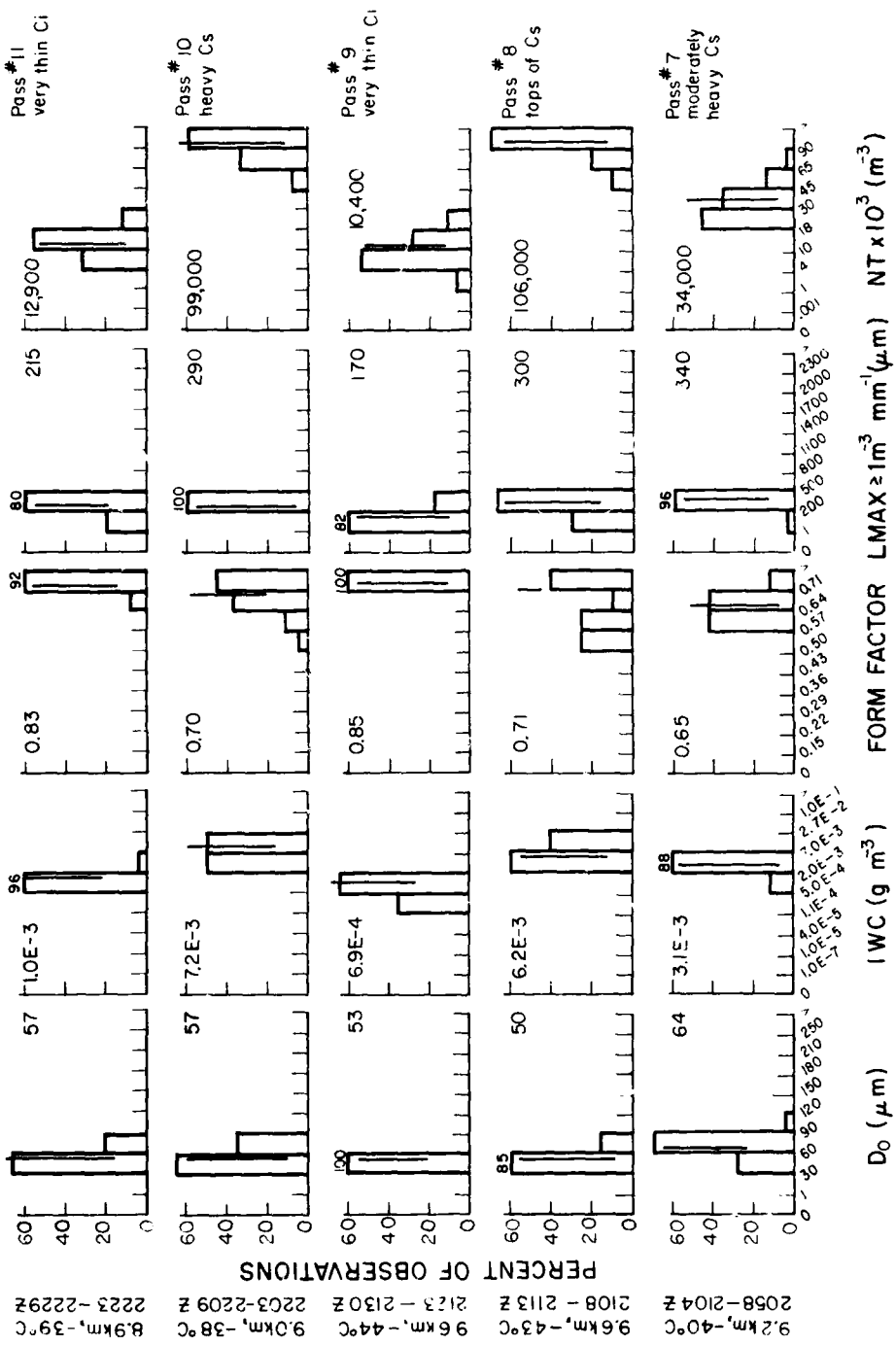


Figure 37. Percentage Frequency by Class of Five Measured or Calculated Variables. Based on total number of 1.5-sec mean values during 5 periods on 2 February 1979. Printed numbers and vertical lines are at 50 percentile values. These do not consider data in cloud-free areas

vicinity of the airplane there hardly seemed to be any cloud present at all. The data suggests that his observation might have been due to a lack of contrast with clouds all around.

The cloud sampled during Pass 10 was a relatively heavy cirrostratus that provided the highest mean IWC value of any of the five 2 February passes. The ground was only dimly visible and no blue sky could be seen, though the sun shone through the Cs. The number of particles detected in this case was $99,000 \text{ m}^{-3}$, only slightly less than that recorded during Pass 8.

Some representative particle data for the passes made on 2 February are given in the following figures. As in similar foregoing figures, the data have been averaged over a representative 15-sec segment of a particular pass period.

Data for the moderately heavy Cs samples on Pass 7 are shown in Figure 38. The largest particles detected were $437 \mu\text{m}$ in size, though there were very few of these. Particles in the 125 to $175 \mu\text{m}$ range made the greatest contribution to total calculated ice water content.

The spectrum given in Figure 39 has a maximum recorded particle size of $311 \mu\text{m}$, although the total particle count, NT, is in excess of $88,000 \text{ m}^{-3}$. There is a smooth decrease of particle counts as size increases, but without particles larger than $400 \mu\text{m}$, the form factor is a relatively high 0.70.

The greatest particle size recorded in the Figure 40 spectrum of very thin cirrus is $169 \mu\text{m}$. The bulk of the total IWC was contributed by particle sizes between 67 and $108 \mu\text{m}$. Since there are less than 10 channels of data in the cloud and precipitation probe ranges, the form factor computation is not necessarily meaningful. It does appear, however, that when few spectrometer channels have data, the form factor is quite high - above about 0.75.

There is considerable similarity between the spectra in Figures 39 and 41. In one case the NT is $88,000$ and in the other $100,000 \text{ m}^{-3}$. In both instances, the largest recorded particles were near $311 \mu\text{m}$, and in both the greatest contribution to IWC was made by particles in the approximate 50 - to $125\text{-}\mu\text{m}$ range.

Both of the thin cirrus spectra shown in Figures 40 and 42 exhibit maximum sized particles near $200 \mu\text{m}$ or smaller. They also have a relatively small number of particle counts in the ~ 47 - $4700\text{-}\mu\text{m}$ range, 8600 and $13,400 \text{ m}^{-3}$. Both also have high form factor values, though, as noted above these are based on a very small number of channels of data and hence are not very reliable.

02 FEB 79	START	INTVL	TEMP	ALT	IWC	IWC	DO	NT	FF	PART
TIME	SEC		C	KM	G/M ^{0.3}	Z CLO	NU	N/M ^{0.3}		
20:30:45	15	-38.9	9.1		.0032	99	74	25403	.63	BR

PARTICLE SIZE DISTRIBUTION (N/M ^{0.3} -MM)									
SIZE (MU)	SCATTER PROBE (MU)	SIZE PROBE (MU)	CLOUD PERCENT	SIZE IWC/MM	PRECIP PROBE (IWC/MM)	PERCENT	NT	FF	PART
2	4.05E+6	26	0	437	3.30E+0	0			
3	1.25E+7	47	2.83E+5	4	706	0			
5	1.14E+7	67	1.99E+5	5	1011	0			
7	3.93E+7	89	1.71E+5	7	1316	0			
9	3.87E+7	100	1.34E+5	9	1622	0			
11	2.78E+7	128	1.69E+5	16	1927	0			
12	2.29E+7	148	1.07E+5	13	2233	0			
14	1.09E+7	169	8.61E+4	14	2538	0			
16	1.81E+7	189	4.42E+4	9	2843	0			
18	8.66E+6	209	1.77E+4	5	3149	0			
19	1.82E+7	230	1.65E+4	6	3454	0			
21	6.56E+6	250	6.21E+3	3	3760	0			
23	1.25E+7	271	5.58E+3	3	4065	0			
25	1.51E+7	291	4.87E+3	3	4370	0			
27	7.61E+6	311	4.37E+3	4	4676	0			
IWC	1.01E-3		3.77E-3		5.78E-6				

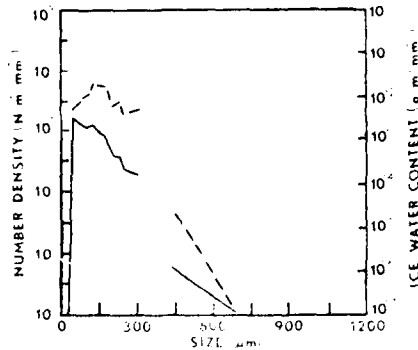


Figure 38. Representative Particle Spectrum for a 15-sec Interval During Pass 7 Through Moderately Heavy Cs on 2 February 1979

02 FEB 79	START	INTVL	TEMP	ALT	IWC	IWC	DO	NT	FF	PART
TIME	SEC		C	KM	G/M ^{0.3}	Z CLO	NU	N/M ^{0.3}		
21:11:00	15	-43.1	9.6		.0042	100	46	26329	.79	BR

PARTICLE SIZE DISTRIBUTION (N/M ^{0.3} -MM)									
SIZE (MU)	SCATTER PROBE (MU)	SIZE PROBE (MU)	CLOUD PERCENT	SIZE IWC/MM	PRECIP PROBE (IWC/MM)	PERCENT	NT	FF	PART
2	1.43E+6	26	3.13E+6	9	437	0	0	0	
3	9.27E+6	47	2.22E+6	21	706	0	0	0	
5	2.64E+7	67	1.19E+6	23	1011	0	0	0	
7	6.57E+7	87	5.09E+5	16	1316	0	0	0	
9	7.14E+7	100	2.33E+5	11	1622	0	0	0	
11	5.43E+7	128	8.88E+4	6	1927	0	0	0	
12	4.21E+7	148	4.47E+4	4	2233	0	0	0	
14	3.43E+7	169	1.44E+4	2	2538	0	0	0	
16	3.64E+7	189	1.04E+4	2	2843	0	0	0	
18	3.28E+7	209	9.43E+3	2	3149	0	0	0	
19	3.57E+7	230	6.22E+3	2	3454	0	0	0	
21	4.00E+7	250	2.31E+3	1	3760	0	0	0	
23	2.93E+7	271	1.41E+3	1	4065	0	0	0	
25	2.43E+7	291	8.65E+2	1	4370	0	0	0	
27	4.29E+6	311	5.38E+2	1	4676	0	0	0	
IWC	2.01E-3		4.25E-3		0				

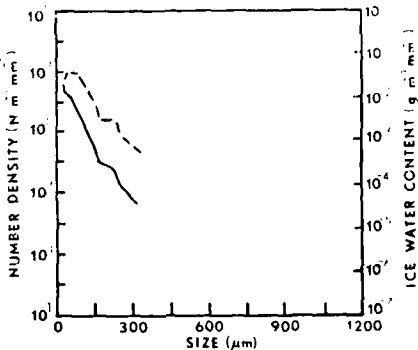


Figure 39. Representative Particle Spectrum for a 15-sec Interval During Pass 8 in Tops of Cs on 2 February 1979

#2 FEB 79											
TIME	START	INTVL	TEMP	ALT	INC	INC	DO	NT	FF	PART	
SEC			C	KM	G/M ³	Z CLD	MU	N/M ³		TYPE	
21:22:00		15	-44.0	9.0	.0006	100	55	8590	.85	BR	

PARTICLE SIZE DISTRIBUTION (N/M ³ -MM)											
SIZE (MU)	SCATTER PROBE	SIZE (MU)	CLOUD PROBE	PERCENT	SIZE INC/MM (MU)	PRECIP PROBE	PERCENT				
2	0.	26	1.37E+5	3	437	0.	0				
3	0.	47	1.08E+5	7	706	0.	0				
5	2.93E+5	67	8.43E+4	12	1011	0.	0				
7	1.18E+7	87	1.06E+5	25	1316	0.	0				
9	1.47E+7	108	7.97E+4	28	1622	0.	0				
11	1.83E+7	128	2.79E+4	14	1927	0.	0				
12	2.27E+7	148	1.58E+4	11	2233	0.	0				
14	1.47E+7	169	1.65E+3	1	2538	0.	0				
16	1.25E+7	189	0.	0	2843	0.	0				
18	8.88E+6	209	0.	0	3149	0.	0				
19	8.79E+6	230	0.	0	3454	0.	0				
21	6.59E+6	250	0.	0	3760	0.	0				
23	5.87E+6	271	0.	0	4065	0.	0				
25	6.59E+6	291	0.	0	4370	0.	0				
27	5.87E+6	311	0.	0	4676	0.	0				
INC		6.32E-4			5.92E-4						

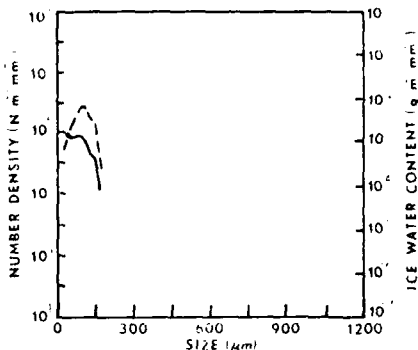


Figure 40. Representative Particle Spectrum for a 15-sec Interval During Pass 9 In Very Thin Ci on 2 February 1979

#2 FEB 79											
TIME	START	INTVL	TEMP	ALT	INC	INC	DO	NT	FF	PART	
SEC			C	KM	G/M ³	Z CLD	MU	N/M ³		TYPE	
22:07:00		15	-38.3	9.0	.0006	100	53	189551	.72	BR	

PARTICLE SIZE DISTRIBUTION (N/M ³ -MM)											
SIZE (MU)	SCATTER PROBE	SIZE (MU)	CLOUD PROBE	PERCENT	SIZE INC/MM (MU)	PRECIP PROBE	PERCENT				
2	0.	26	1.86E+6	4	437	0.	0				
3	1.33E+7	47	1.80E+6	12	706	0.	0				
5	1.40E+7	47	1.24E+6	17	1011	0.	0				
7	3.84E+7	87	9.28E+5	21	1316	0.	0				
9	3.55E+7	108	6.28E+5	22	1622	0.	0				
11	4.08E+7	128	2.07E+5	18	1927	0.	0				
12	3.10E+7	148	7.04E+4	5	2233	0.	0				
14	2.51E+7	169	2.16E+4	2	2538	0.	0				
16	2.34E+7	189	2.15E+4	2	2843	0.	0				
18	2.29E+7	209	1.56E+4	2	3149	0.	0				
19	2.14E+7	230	1.08E+4	2	3454	0.	0				
21	2.51E+7	250	2.38E+3	1	3760	0.	0				
23	2.81E+7	271	1.44E+3	1	4065	0.	0				
25	2.29E+7	291	0.93E+2	1	4370	0.	0				
27	1.55E+7	311	5.47E+2	1	4676	0.	0				
INC		1.82E-3			6.00E-3						

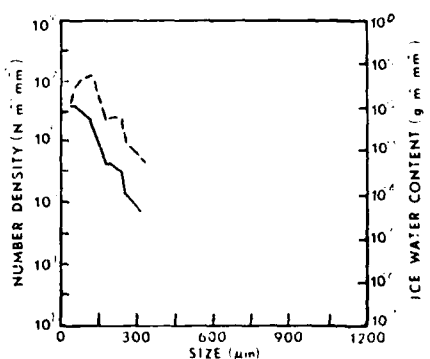


Figure 41. Representative Particle Spectrum for a 15-sec Interval During Pass 10 Through Heavy Cs on 2 February 1979

02 FEB '79	START	INTVL	TEMP	AL.	IWC	IWC	IR	NT	FF	PART
TIME	SEC	°C	°F	6.0E+3	1.0E+3	1.0E+3	4.0E+3	N/M+3	1.0E+3	TYPE
22:29:08	15	-38.7	0.9	.0006	100	47	11488	.82	96	

PARTICLE SIZE DISTRIBUTION (N/M+3-MM)										
SIZE (NU)	SCATTER PROBE (NU)	SIZE PROBE (NU)	CLOUD IWC/MM	PERCENT SIZE PROBE	PRECIP IWC/MM	PERCENT PRECIP IWC/MM	IR	NT N/M+3	FF	PART
2	2.94E+6	24	2.75E+5	6	437	0.	0	0	0	
3	2.21E+6	47	2.89E+5	19	706	0.	0	0	0	
5	5.15E+6	67	1.88E+5	25	1011	0.	0	0	0	
7	8.08E+6	87	1.36E+5	30	1316	0.	0	0	0	
9	8.09E+6	108	3.09E+4	10	1622	0.	0	0	0	
11	5.14E+6	128	1.27E+4	6	1927	0.	0	0	0	
12	4.41E+6	148	0.	0	2233	0.	0	0	0	
14	6.61E+6	169	1.65E+3	7	2538	0.	0	0	0	
16	5.88E+6	189	0.	0	2843	0.	0	0	0	
18	2.21E+6	209	1.94E+3	3	3149	0.	0	0	0	
19	5.88E+6	230	0.	0	3454	0.	0	0	0	
21	2.94E+6	250	0.	0	3760	0.	0	0	0	
23	6.62E+6	271	0.	0	4065	0.	0	0	0	
25	2.94E+6	291	0.	0	4370	0.	0	0	0	
27	0.	311	0.	0	4676	0.	0	0	0	
IWC			2.76E-4	6.14E-4			0.			

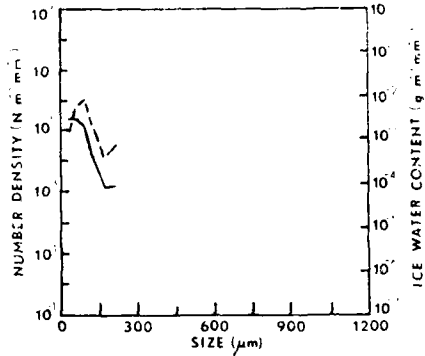


Figure 42. Representative Particle Spectrum for a 15-sec Interval During Pass 11 in Very Thin Ci on 2 February 1979

7. SUBVISIBLE CIRRUS

Barnes²¹ and Cohen and Barnes⁶ have observed two types of subvisible cirrus. The most frequent type is a continuous background of particles in the smallest channels of the ASSP (2 to 12 μm). This type of distribution has frequently been observed in extensive cloud-free areas sampled by the MC-130E during calibration flights or while en route to or from sampling locations. It was thought to be noise, but data-free periods, such as seen in Figure 36, have shown the data to be real. A second type of subvisible cirrus consists of isolated ice crystals, generally 100 μm or greater in diameter, occasionally exceeding 1000 μm . They have been detected on the PMS 1-D and 2-D probes and visually verified on the snow stick. Although generally observed while under cirrus clouds, they have also been found with no cloud above the airplane. They may form in moist layers high in the troposphere and fall to lower layers. In the Arctic region, they fall to the surface and are called "diamond dust." In warmer climates, they melt, evaporate, or are lost among other aerosols (fog, dust, sea spray, pollution, and so on) before reaching the surface.

Although the purpose of these flights was to obtain data in clouds, there were periods during which the airplane was in what appeared to be clear air. During

21. Barnes, A.A., Jr. (1980) Ice Particles in Clear Air. Communications a la VIII ème Conference Internationale sur la Physique des Nuages, Vol. I., Clermont-Ferrand, France, 15-19 July 1980, pp 189-190.

those times, there were occasions when particles were detected which indicated the presence of subvisible cirrus.

During three short periods on 28 January (2115:00 to 2121:45Z, 2129:15 to 2132:15Z, and 2205:00 to 2208:15Z), the airplane appeared to be in clear air, yet particles were detected. During the first and second, no small particles appeared on the ASSP, but a few larger particles (probably fallout from higher clouds) typical of the second type of subvisible cirrus were recorded. During the third period, the ASSP detected only a background of small particles typical of the first type of subvisible cirrus.

On 29 January, from 1901:45 to 1919:00Z, the ASSP showed results similar to those observed during the third period on 28 January but in addition, individual particles were also detected by the cloud and precipitation probes.

On 2 February (see Figure 36), from 2131:15 to 2157:00Z, no small particles were detected by the ASSP, but some subvisible cirrus particles greater than $50 \mu\text{m}$ in diameter were recorded by the cloud probe. The density of $50\text{-}\mu\text{m}$ particles was 21 m^{-3} . Particles greater than $100 \mu\text{m}$ had a density of 7 m^{-3} , which is considerably higher than the 0.12 m^{-3} found by Barnes²¹ in a cloud-free atmosphere at 5 km on 2 February 1980, using a modified 2-D precipitation probe. The larger number of subvisible cirrus particles may be due to additional moisture in the air due to the presence of visible clouds in the vicinity.

8. CONCLUDING COMMENTS

The three cirriform cloud sampling flights of 28 and 29 January and 2 February 1979 have added considerably to the small base of such data now available. The first and third flights were made in the vicinity of bands of cirriform clouds ahead of surface systems and close to jet stream winds. In the first case, the surface systems were intensifying, while in the third case, they were weak and dissipating. The second flight was made through the top portions of Cs and Cc clouds at the top of an active surface storm.

The 28 January flight encountered a variety of types of cirrostratus. The presence of larger particles at certain times during that flight indicate that aggregation of smaller particles into larger particles was probably occurring. We attribute this to the deepening of the low pressure areas to the south and west of the sampling area.

The 29 January flight through the top of the storm provided quite high particle counts, sometimes exceeding $300,000 \text{ m}^{-3}$. Even with this large number, however, the particle sizes were seldom greater than $1100 \mu\text{m}$, while typical ice water contents were near 0.03 g m^{-3} . Since the tropopause was relatively low on this day, we were able to acquire data at temperatures as low as -48°C . The large

number of particles detected may have been related both to their generation in or near the storm and also to the fact that we were able to sample at colder locations in the cloud than usually possible with the C-130.

The cirrostratus layers sampled on 28 January and 2 February were of different consistencies, although the in-flight meteorologist occasionally noted they were both heavy or moderately heavy cloud forms. On the first day, with a developing storm in the area, the largest particle sizes in two passes through or along the Cs were near $1400 \mu\text{m}$, while mean IWC values were 1 to $2 \times 10^{-2} \text{ g m}^{-3}$ and the median volume diameter was 130 to $140 \mu\text{m}$.

The Cs on 2 February with only weak, dissipating surface systems in the area, had maximum particle sizes near or less than $500 \mu\text{m}$ and a mean IWC of $7 \times 10^{-3} \text{ g m}^{-3}$ or less. Median volume diameters were also generally less than $90 \mu\text{m}$. Pass 10 on 2 February was considered by the mission director to be a sample of heavy Cs, while Passes 9 and 11 were through very thin cirriform clouds. It is interesting that the largest particles detected, L_{\max} , in each of these cases were not significantly different. The median volume diameters were also near $55 \mu\text{m}$ in each of the 3 cases. However, the number of particles, NT, was much greater, $99,000 \text{ m}^{-3}$, in the heavy Cs case, while the thinner cirrus examples had mean NT less than $13,000 \text{ m}^{-3}$. The larger particle count in the heavy Cs case also resulted in a greater ice mass than in the cases of the thinner cloud samples.

This is the first report in this series that has described and discussed total particle counts (NT), maximum particle size (L_{\max}) and form factor (FF). As described above, the NT and L_{\max} aid considerably in efforts to characterize particle data. The form factor has also been found useful in understanding the variation of particle spectra. Form factor values in the relatively low range of 0.20 to 0.45 are frequently associated with approximately exponential decreases of particle numbers out to sizes as large as 1000 to 2000 μm (in cirrus samples). Values of FF above approximately 0.70 are often related to spectra that extend only to particle sizes of $300 \mu\text{m}$ or less. Form factor calculations based on data from less than about 10 spectrometer channels are less reliable and meaningful, but a small number of cases indicates that, even here, high values of FF are associated with abbreviated spectra.

Two types of subvisible cirrus were detected during these flights. A continuous background of small particles was observed while in clear air during the first two flights. Occasional larger particles were observed in clear air on all three days.

Cirrus flights were conducted on the three days immediately following the 2 February flight. The results of these flights will be discussed in a future report.

References

1. Varley, D.J. (1978) Cirrus Particle Distribution Study, Part 1, AFGL-TR-78-0305, Air Force Surveys in Geophysics 394, AD A061 485, 71 pp.
2. Varley, D.J., and Brooks, D.M. (1978) Cirrus Particle Distribution Study, Part 2, AFGL-TR-78-0248, Air Force Surveys in Geophysics 399, AD A063 807, 108 pp.
3. Varley, D.J. (1978) Cirrus Particle Distribution Study, Part 3, AFGL-TR-78-0305, Air Force Surveys in Geophysics 404, AD A06 695, 67 pp.
4. Varley, D.J., and Barnes, A.A., Jr. (1979) Cirrus Particle Distribution Study, Part 4, AFGL-TR-79-0134, Air Force Surveys in Geophysics 413, AD A074 763, 91 pp.
5. Cohen, I.D. (1979) Cirrus Particles Distribution Study, Part 5, AFGL-TR-79-0155, Air Force Surveys in Geophysics 414, AD 077 361, 81 pp.
6. Cohen, I.D., and Barnes, A.A., Jr. (1980) Cirrus Particle Distribution Study, Part 6, AFGL-TR-80-0261, Air Force Surveys in Geophysics 430, (in press).
7. Heymsfield, A., and Knollenberg, R. (1972) Properties of cirrus generating cells, J. Atmos. Sci. 29:1358-1366.
8. Heymsfield, A. (1974) Ice crystal growth in deep cirrus systems. Preprints of Conf. on Cloud Phys., Tucson, 311-316.
9. Heymsfield, A. (1975) Cirrus uncinus generating cells and the evolution of cirriform clouds. Part I: Aircraft observations of the growth of the ice phase, J. Atmos. Sci. 32:799-808.
10. Knollenberg, R. (1975) The Response of Optical Array Spectrometers to Ice and Snow: A Study of Probe Size to Crystal Mass Relationships, AFGL-TR-75-0494, AD A020 276.
11. Knollenberg, R. (1976) Three new instruments for cloud physics measurements: the 2-D spectrometer, the forward scattering probe, and the active scattering spectrometer. Preprints of Intnl. Cld. Physics Conf., Boulder, Colorado, Amer. Meteor. Soc., 554-561.

12. Cunningham, R. (1978) Analysis of particle spectral data from optical array (PMS) 1-D and 2-D sensors. In Preprints of AMS Fourth Symposium on Meteorological Observations and Instrumentation, Denver, Colorado.
13. Hobbs, P. V., and Atkinson, D. G. (1976) The concentrations of ice particles in orographic clouds and cyclonic storms over the Cascade Mountains. J. Atmos. Sci., 33:1363-1374.
14. Hobbs, P. V., Radke, L. F., and Atkinson, D. G. (1975) Airborne Measurements and Observations in Cirrus Clouds, AFCRL-TR-75-0249, AD A015 937, 117 pp.
15. Ryder, P. (1976) The measurement of cloud droplet spectra. Preprints of Intnati. Conf. on Cloud Phys., Boulder, Colorado, Amer. Meteor. Soc., 576-580.
16. Plank, V. G. (1977) Hydrometeor Data and Analytical-Theoretical Investigations Pertaining to the SAMS Rain Erosion Program of the 1972-73 Season at Wallops Island, Virginia, AFGI-TR-77-0149, Environmental Research Papers 603, AD A051 182, 239 pp.
17. Plank, V. G., and Barnes, A. A., Jr. (1978) An improvement in obtaining real-time water content values from radar reflectivity. Preprints of 18th Conf. Radar Meteor., Atlanta, Amer. Meteor. Soc., 426-431.
18. Plank, V. G. (1979) Private Correspondence.
19. Varley, D. J. (1980) Microphysical Properties Of a Large Scale Cloud System 1-3 March 1978, AFGI-TR-80-0002, Environmental Research Papers 690, AD A083 140, 100 pp.
20. Mason, B. J. (1962) Clouds, Rain and Rainmaking, Cambridge University Press, 145 pp.
21. Barnes, A. A., Jr. (1980) Ice Particles in Clear Air. Communications à la VIII ème Conférence Internationale sur la Physique des Nuages, Vol. I., Clermont-Ferrand, France, 15-19 July 1980, pp 189-190.

Appendix A

28 January 1979 Data Tabulations

The example below explains the data format used in the tabulations that follow. The comments provided are from notes made during the flight by the mission director.

1 ↓ START TIME	2 ↓ ALT KM	3 ↓ TEMP °C	4 ↓ IWC-SC G/M ^{0.3}	5 ↓ IWC-CP G/M ^{0.3}	6 ↓ IWC %	7 ↓ 15 SECND CLD	8 ↓ AVERAGE DO [°]	9 ↓ NT N/M ^{0.3}	10 ↓ LMAX UM	11 ↓ FF	12 ↓ FF
20:55:00	9.1	-38.7	.0016	.0038	99	69	35385	437	.66		
20:55:15	9.1	-38.5	.0019	.0042	100	63	32414	311	.65		
20:55:30	9.1	-38.4	.0025	.0050	99	69	58656	437	.56		
20:55:45	9.1	-38.4	.0016	.0052	99	77	39564	437	.61		
20:56:00	9.1	-38.5	.0013	.0044	100	71	46072	311	.57		
20:56:15	9.1	-38.6	.0013	.0037	100	70	34446	311	.63		
20:56:30	9.1	-38.8	.0020	.0043	99	84	32615	437	.56		
20:56:45	9.1	-38.8	.0014	.0052	99	72	45554	437	.63		
20:57:00	9.1	-38.9	.0028	.0085	99	61	91805	437	.59		

1. Start time of sample. End was 14 sec later. Time in UMT.
2. Mean altitude of sample (km).
3. Mean temperature of sample (°C).
4. Date of sampling.
5. Ice water content in g/m³ calculated over 2 to 27-μm range of scatter probe.

6. Ice water content in g/m^3 calculated over 26 to 4700- μm range of cloud and precip probes.
7. Duration of each sample (sec).
8. Percent of total ice water content of 6 determined from cloud probe only.
9. Median volume diameter of equivalently melted particles. (D_0 in the text)
10. Particle number total $/\text{m}^3$ over 47 to 4700 μm size range. (The first channel of the cloud probe is not used to compute this value.)
11. Greatest size having ≥ 1 particle $\text{m}^{-3} \text{ mm}^{-1}$ (in μm).
12. Form Factor (see text).

START ALT TIME	15 SECOND AVERAGE			LMAX UN	FF
	TEMP KHN	TUC-SC 6/H**3	TUC-CP 6/H**3 x CLD		
21:15:00	7.8	-31.4	0.0000	0.0000	0 0.00
21:15:15	7.8	-31.2	0.0000	0.0000	0 0.00
21:15:30	7.8	-31.0	0.0000	0.0000	0 0.00
21:15:45	7.8	-30.9	0.0000	0.0000	0 0.00
21:16:00	7.8	-31.0	0.0000	0.0000	0 0.00
21:16:15	7.8	-31.2	0.0000	0.0000	0 0.00
21:16:30	7.9	-31.2	0.0000	0.0000	0 0.00
21:16:45	7.9	-31.5	0.0000	0.0000	0 0.00
21:17:00	7.9	-31.7	0.0000	0.0000	0 0.00
21:17:15	7.9	-31.8	0.0000	0.0000	0 0.00
21:17:30	7.9	-31.8	0.0000	0.0000	0 0.00
21:17:45	8.0	-31.9	0.0000	0.0000	0 0.00
21:18:00	8.0	-32.0	0.0000	0.0000	0 0.00
21:18:15	8.0	-31.9	0.0000	0.0000	0 0.00
21:18:30	8.0	-30.9	0.0000	0.0000	0 0.00
21:18:45	8.0	-30.6	0.0000	0.0000	0 0.00
21:19:00	8.0	-30.7	0.0000	0.0000	0 0.00
21:19:15	8.0	-30.7	0.0000	0.0000	0 0.00
21:19:30	8.0	-30.7	0.0000	0.0000	0 0.00
21:19:45	8.1	-30.5	0.0000	0.0000	0 0.00
21:20:00	8.1	-30.2	0.0000	0.0000	0 0.00
21:20:15	8.1	-30.4	0.0000	0.0002	92 437 -38
21:20:30	8.1	-30.5	0.0001	0.0002	94 104 544 437 -64
21:20:45	8.1	-30.4	0.0000	0.0001	100 69 1281 169 -77
21:21:00	8.2	-30.4	0.0000	0.0000	0 0.00
21:21:15	8.2	-30.1	0.0000	0.0000	0 0.00
21:21:30	8.2	-30.6	0.0000	0.0000	0 0.00
21:21:45	8.2	-30.7	0.0000	0.0000	0 0.00
21:22:00	8.2	-30.8	0.0000	0.0007	9 248 395 1316 -31
21:22:15	8.2	-31.0	0.0021	0.0112	6 368 8519 2233 -14
21:22:30	8.3	-31.4	0.0024	0.0117	24 198 20166 1622 -21
21:22:45	8.3	-31.8	0.0034	0.0108	55 136 23836 1011 -41
21:23:00	8.4	-32.3	0.0014	0.0065	82 113 23384 706 -48
21:23:15	8.4	-32.4	0.0001	0.0001	90 1227 437 -44
21:23:30	8.4	-32.2	0.0000	0.0001	100 64 133 473 311 -43
21:23:45	8.4	-31.9	0.0002	0.0005	100 89 3195 311 -61
21:24:00	8.4	-32.0	0.0002	0.0009	100 87 4684 311 -65
21:24:15	8.4	-32.2	0.0000	0.0000	100 63 469 169 -74
21:24:30	8.4	-32.0	0.0003	0.0011	99 107 4537 437 -60
21:24:45	8.4	-32.1	0.0006	0.0002	65 123 8934 1011 -43
21:25:00	8.5	-32.0	0.0025	0.0143	19 227 16255 1116 -26
21:25:15	8.5	-32.3	0.0005	0.0021	65 125 5882 706 -43
21:25:30	8.6	-32.6	0.0002	0.0005	99 92 2435 437 -63
21:25:45	8.6	-32.2	0.0004	0.0011	99 100 4074 437 -67
21:26:00	8.6	-32.9	0.0000	0.0002	100 124 877 311 -49
21:26:15	8.6	-33.2	0.0001	0.0003	100 94 1536 311 -59
21:26:30	8.6	-33.1	0.0006	0.0023	99 111 7746 437 -64
21:26:45	8.6	-33.3	0.0003	0.0008	100 79 5258 250 -73
21:27:00	8.6	-33.5	0.0011	0.0044	98 108 1917 437 -57
21:27:15	8.6	-33.5	0.0003	0.0011	97 89 4751 437 -66
21:27:30	8.7	-33.4	0.0000	0.0002	100 83 1173 250 -73
21:27:45	8.7	-33.5	0.0001	0.0008	100 76 5177 311 -57
21:28:00	8.7	-33.4	0.0002	0.0007	100 85 3401 311 -69
21:28:15	8.6	-33.3	0.0000	0.0000	0 0 0 0 0 0
21:28:30	8.6	-33.0	0.0000	0.0000	100 56 140 108 1.58
21:28:45	8.6	-33.2	0.0010	0.0004	83 84 7556 706 -.36

28 JAN 79 Heading 090° (East); 31°48'N, 105°32'W, TWS 220 kt; GS 320 kt. Cirrus layer above.

21:18:00 8.0 -32.0 0.0000 0.0000 0 0.00 Breaks in the cirrostratus above. Blue sky occasionally, visible

At 31°47'N, 105°09'W.

21:18:15 8.0 -31.9 0.0000 0.0000 0 0.00 Within 2-3,000 ft of cirrus above, but no particle counts yet.

21:18:30 8.0 -30.9 0.0000 0.0000 0 0.00

21:18:45 8.1 -30.5 0.0000 0.0000 0 0.00

21:19:00 8.1 -30.2 0.0000 0.0000 0 0.00

21:19:15 8.1 -30.7 0.0000 0.0000 0 0.00

21:19:30 8.0 -30.7 0.0000 0.0000 0 0.00

21:19:45 8.1 -30.5 0.0000 0.0000 0 0.00

21:20:00 8.1 -30.2 0.0000 0.0000 0 0.00

21:20:15 8.1 -30.4 0.0000 0.0000 0 0.00

21:20:30 8.1 -30.5 0.0001 0.0002 94 104 544 437 -64

21:20:45 8.1 -30.4 0.0000 0.0001 100 69 1281 169 -77

Getting very near cirriform cloud base.

21:21:00 8.2 -30.4 0.0000 0.0000 0 0.00

21:21:15 8.2 -30.1 0.0000 0.0000 0 0.00

21:21:30 8.2 -30.6 0.0000 0.0000 0 0.00

21:21:45 8.2 -30.7 0.0000 0.0000 0 0.00

21:22:00 8.2 -30.8 0.0000 0.0007 9 248 395 1316 -31

About to pass through a jagged piece of the Cs base.

21:22:15 8.2 -31.0 0.0021 0.0112 6 368 8519 2233 -14

At 31°46'N, 104°45'W. Ground and horizon are dimly visible through cirrostratus base that is nearly without texture. Not possible to estimate tops.

21:22:30 8.3 -31.4 0.0024 0.0117 24 198 20166 1622 -21

21:22:45 8.3 -31.8 0.0034 0.0108 55 136 23836 1011 -41

21:23:00 8.4 -32.3 0.0014 0.0065 82 113 23384 706 -48

Moved out of thicker cloud, but more is coming.

21:23:15 8.4 -32.4 0.0001 0.0001 90 1227 437 -44

21:23:30 8.4 -32.2 0.0000 0.0001 100 64 133 473 311 -43

21:23:45 8.4 -31.9 0.0002 0.0005 100 89 3195 311 -61

21:24:00 8.4 -32.0 0.0002 0.0009 100 87 4684 311 -65

21:24:15 8.4 -32.2 0.0000 0.0000 100 63 469 169 -74

21:24:30 8.4 -32.0 0.0003 0.0011 99 107 4537 437 -60

21:24:45 8.4 -32.1 0.0006 0.0002 100 123 8934 1011 -43

21:25:00 8.5 -32.0 0.0025 0.0143 19 227 16255 1116 -26

In milky textured cloud now.

21:25:15 8.5 -32.3 0.0005 0.0021 65 125 5882 706 -43

21:25:30 8.6 -32.6 0.0002 0.0005 99 92 2435 437 -63

21:25:45 8.6 -32.2 0.0004 0.0011 99 100 4074 437 -67

Apparently getting larger counts now. Climbing.

21:26:00 8.6 -32.9 0.0000 0.0002 100 124 877 311 -49

21:26:15 8.6 -33.2 0.0001 0.0003 100 94 1536 311 -59

21:26:30 8.6 -33.1 0.0006 0.0023 99 111 7746 437 -64

21:26:45 8.6 -33.3 0.0003 0.0008 100 79 5258 250 -73

Breaks of blue sky through relatively light cirriform clouds above.

21:27:00 8.6 -33.5 0.0011 0.0044 98 108 1917 437 -57

21:27:15 8.6 -33.5 0.0003 0.0011 97 89 4751 437 -66

21:27:30 8.7 -33.4 0.0000 0.0002 100 83 1173 250 -73

21:27:45 8.7 -33.5 0.0001 0.0008 100 76 5177 311 -57

21:28:00 8.7 -33.4 0.0002 0.0007 100 85 3401 311 -69

At 31°51'N, 104°06'W. Wind measured to be 242/141 kt.

21:28:15 8.6 -33.3 0.0000 0.0000 0 0 0 0 0 0

21:28:30 8.6 -33.0 0.0000 0.0000 100 56 140 108 1.58

A layer of altocumulus is several thousand feet below. Base of visible Cs is about 10000 ft above the aircraft.

START TIME	ALT MM	15 SECOND AVERAGE										FF
		TEMP INC-CP	INC-SC	INC	DO	NT	LNAX	UN	N/H=+3	UN	6/H=+3	
21:29:00	8.7	-33.6	.0009	.0040	60	129	11193	1011	.37			
21:29:15	8.7	-33.5	.0000	.0000	90	60	295	437	.44	At 31°51'N, 103°59'W. Visibility is good, but AC undercast obscures ground. A few patches of blue sky through CS above.		
21:29:30	8.7	-33.6	.0000	.0000	60	0	0	0	0.00			
21:29:45	8.7	-33.8	.0000	.0000	0	0	0	0	0.00			
21:30:00	8.7	-33.9	.0000	.0000	0	0	0	0	0.00			
21:30:15	8.7	-33.9	.0000	.0000	0	0	0	0	0.00			
21:30:30	8.7	-33.6	.0000	.0000	0	0	0	0	0.00			
21:30:45	8.6	-33.6	.0000	.0000	0	0	0	0	0.00			
21:31:00	8.6	-32.8	.0000	.0000	0	0	0	0	0.00			
21:31:15	8.6	-32.6	.0000	.0000	0	0	0	0	0.00			
21:31:30	8.6	-32.6	.0000	.0000	0	0	0	0	0.00			
21:31:45	8.6	-32.6	.0000	.0000	100	49	809	128	.80			
21:32:00	8.6	-32.6	.0000	.0000	0	0	0	0	0.00			
21:32:15	8.5	-32.4	.0000	.0000	15	316	38	706	.40	At 31°49'N, 103°38'W. Wind is 243°/138 kt. Very dark cloud ahead.		
21:32:30	8.5	-32.4	.0017	.0104	59	131	29134	1011	.38	Complete undercast below.		
21:32:45	8.5	-32.3	.0033	.0130	82	118	48676	706	.46			
21:33:00	8.5	-32.3	.0001	.0001	96	50	1075	437	.54			
21:33:15	8.5	-32.3	.0000	.0000	100	51	103	87	1.00			
21:33:30	8.5	-32.1	.0000	.0000	0	0	0	0	0.00			
21:33:45	8.5	-32.0	.0000	.0000	0	0	0	0	0.00			
21:34:00	8.5	-32.0	.0000	.0000	0	0	0	0	0.00			
21:34:15	8.5	-32.2	.0000	.0000	0	0	0	0	0.00			
21:34:30	8.5	-32.1	.0003	.0017	50	140	4372	1011	.41	Momentarily between layers. Nearing dark cloud ahead.		
21:34:45	8.5	-32.0	.0044	.0175	63	128	50424	1011	.41			
21:35:00	8.5	-32.1	.0039	.0163	72	124	43049	706	.48	Can't see ground through undercast.		
21:35:15	8.5	-32.1	.0036	.0158	80	113	50218	706	.49	Visibility approximately 1 mi, but nothing to gauge against.		
21:35:30	8.5	-32.0	.0080	.0105	74	122	68315	1011	.47			
21:35:45	8.5	-32.0	.0052	.0210	81	115	70952	706	.49	Milky white in all directions.		
21:36:00	8.5	-32.1	.0032	.0140	76	115	47303	1011	.45			
21:36:15	8.5	-32.1	.0049	.0255	65	126	66775	1011	.44	Still very foggy, only a hint of blue sky above.		
21:36:30	8.5	-32.1	.0043	.0168	77	121	47372	1316	.45			
21:36:45	8.5	-32.0	.0036	.0143	81	117	43061	706	.49	Beginning a left turn at 31°43'N, 103°37'W. Wind 243°/142 kt		
21:37:00	8.4	-31.9	.0010	.0025	74	121	8414	706	.44			
21:37:15	8.5	-31.9	.0004	.0012	66	130	4319	202	.40			
21:37:30	8.5	-32.0	.0006	.0014	86	65	6220	706	.43			
21:37:45	8.5	-32.0	.0011	.0047	72	119	13872	706	.46			
21:38:00	8.5	-32.0	.0006	.0033	55	136	5303	1011	.49			
21:38:15	8.5	-32.1	.0007	.0042	52	138	7473	1011	.43			
21:38:30	8.5	-32.0	.0031	.0167	56	134	46197	1011	.36	Visibility very low. No breaks of blue above.		
21:38:45	8.5	-31.8	.0079	.0340	46	148	66408	1011	.37			
21:39:00	8.5	-31.5	.0135	.0862	27	202	132399	2538	.15	Foggy white in all directions, but can see texture of AC below.		
21:39:15	8.5	-31.7	.0132	.0765	32	184	138669	2233	.17			
21:39:30	8.5	-31.6	.0107	.0593	34	181	123978	2233	.20			
21:39:45	8.5	-31.9	.0068	.0356	51	139	71952	1316	.38			
21:40:00	8.5	-31.8	.0023	.0151	59	130	91211	1316	.39			
21:40:15	8.5	-32.0	.0063	.0301	50	140	63290	1011	.39			
21:40:30	8.5	-31.8	.0073	.0345	57	133	85994	1316	.39			
21:40:45	8.5	-31.9	.0072	.0300	66	129	75600	1011	.45			
21:41:00	8.4	-31.8	.0047	.0187	84	116	58169	706	.53			
21:41:15	8.4	-31.8	.0023	.0122	75	122	32900	706	.50			
21:41:30	8.4	-31.7	.0063	.0230	53	138	58456	1011	.39			
21:41:45	8.4	-31.6	.0053	.0198	39	142	41675	1011	.34			
21:42:00	8.4	-31.7	.0017	.0087	52	138	18664	1316	.37			
21:42:15	8.4	-31.6	.0060	.0291	53	137	60939	1316	.41			
21:42:30	8.4	-31.7	.0048	.0198	34	174	33933	1011	.33			
21:42:45	8.4	-31.7	.0054	.0134	24	213	29575	1316	.22			

START	ALT	15 SECOND AVERAGE										
		TEMP	WFC-SC	WFC-CP	INC	DO	NT	LMAX	FF			
TIME												
21:43:00	8.4	-31.8	.0030	.0135	19	214	26168	1316	.23	Heading 200°, TAS 235 kt. Climbing, sun 103°17'W, wind 103°17'2 kt.		
21:43:15	8.4	-31.7	.0035	.0137	13	230	18725	2233	.18			
21:43:30	8.4	-32.1	.0010	.0021	24	195	4641	1316	.22			
21:43:45	8.4	-32.0	.0015	.0059	23	194	6849	1316	.30			
21:44:00	8.4	-31.9	.0012	.0038	34	171	5570	1011	.37			
21:44:15	8.4	-32.1	.0007	.0057	56	136	7905	1011	.54			
21:44:30	8.5	-32.4	.0038	.0200	83	116	48450	706	.58			
21:44:45	8.5	-32.8	.0030	.0158	76	120	34222	706	.56			
21:45:00	8.5	-32.8	.0009	.0039	54	137	9636	1011	.39			
21:45:15	8.6	-32.8	.0036	.0174	63	126	21954	1011	.33			
21:45:30	8.6	-32.8	.0059	.0252	72	112	101685	706	.39			
21:45:45	8.6	-33.0	.0048	.0148	70	122	39268	1011	.46			
21:46:00	8.6	-33.1	.0013	.0039	69	125	10819	706	.45	Still dense Cs, no breaks. No accumulation of particles on snow stick.		
21:46:15	8.6	-33.1	.0023	.0121	68	126	24017	1011	.52			
21:46:30	8.7	-33.5	.0031	.0176	45	151	28160	1011	.43			
21:46:45	8.7	-34.1	.0035	.0184	59	132	39885	1011	.44	At 31°45'N, 103°08'W, GS 86 kt. Climbing.		
21:47:00	8.7	-34.1	.0048	.0255	51	139	47705	1316	.43			
21:47:15	8.8	-34.2	.0058	.0265	48	144	47046	1316	.42	Still heavy Cs. No breaks.		
21:47:30	8.8	-34.8	.0061	.0272	39	162	52506	1316	.35			
21:47:45	8.8	-34.6	.0053	.0219	70	128	50443	706	.50			
21:48:00	8.9	-34.8	.0053	.0237	78	110	25982	706	.48			
21:48:15	8.9	-34.7	.0081	.0272	40	161	66294	1316	.44			
21:48:30	8.9	-35.1	.0043	.0096	51	177	22555	1011	.29	Heading 251°, GS 105 kt, at 31°45'N, 103°12'W.		
21:48:45	8.9	-35.2	.0035	.0180	61	132	37942	1011	.47			
21:48:59	8.9	-35.3	.0037	.0113	63	128	30874	706	.42	Still dense cloud, no texture.		
21:49:15	9.0	-35.2	.0103	.0458	59	131	94240	238	.25			
21:49:30	8.9	-35.3	.0089	.0048	70	123	10227	1011	.48			
21:49:45	9.0	-35.6	.0069	.0262	81	103	110194	706	.45			
21:50:00	9.0	-35.4	.0026	.0104	73	117	10104	1011	.29			
21:50:15	8.9	-35.6	.0019	.0070	62	127	20382	1011	.40	Interior of Cs slightly brighter now. At 31°45'N, 103°17'W. Cloud tops about 2-3000 ft above aircraft.		
21:50:30	9.0	-35.7	.0007	.0023	39	161	2680	1011	.46			
21:50:45	9.0	-35.7	.0001	.0004	89	106	1619	437	.50			
21:50:59	9.0	-36.0	.0001	.0003	56	134	351	706	.45	Can see texture of Ac below. Turning to left.		
21:51:15	9.0	-36.1	.0010	.0018	99	52	32210	437	.78			
21:51:30	9.0	-36.1	.0010	.0020	100	51	34776	230	.74			
21:51:45	9.1	-36.8	.0012	.0053	36	170	9473	1316	.30			
21:51:59	9.1	-35.9	.0005	.0003	96	100	1440	437	.50			
21:52:14	9.1	-36.2	.0001	.0003	46	149	22813	1316	.25	Visibility good to north. Can see Ac below, as above. Approaching more dense cloud.		
21:52:29	9.1	-36.7	.0001	.0004	89	106	127	124760	1316	.34		
21:52:45	9.1	-37.5	.0001	.0064	92	130	1730	437	.49			
21:52:59	9.1	-37.2	.0003	.0008	55	133	2095	706	.37			
21:53:14	9.2	-37.2	.0003	.0146	53	134	79010	1316	.23			
21:53:29	9.2	-37.1	.0039	.0219	49	143	29981	1316	.24			
21:53:44	9.2	-37.2	.0036	.0118	54	126	22668	1316	.17			
21:53:59	9.2	-36.8	.0064	.0343	46	149	16220	1316	.34			
21:54:14	9.2	-36.7	.0080	.0388	60	127	124760	1316	.34			
21:54:29	9.2	-37.0	.0015	.0051	54	131	28110	1011	.22			
21:55:15	9.2	-37.1	.0062	.0196	64	107	142307	1316	.21			
21:55:30	9.2	-37.1	.0050	.0192	53	134	2095	1011	.17			
21:55:45	9.2	-37.0	.0012	.0037	64	103	22191	1011	.21	At 31°37'N, 103°00'W. Headwind 165°. Sun fairly bright, but aircraft is not yet near Cs top. No accumulation on snow stick.		
21:56:00	9.2	-36.7	.0008	.0013	93	67	25957	706	.33			
21:56:15	9.2	-36.6	.0030	.0053	99	57	15458	437	.41			
21:56:30	9.2	-36.8	.0015	.0027	99	54	43935	706	.54			
21:56:45	9.2	-36.4	.0002	.0004	64	88	4211	706	.22			

START TIME	15 SECOND AVERAGE										LMAX UN	FF
	TEMP K	INC-SC C	INC-CP 6/M*3	INC-CP 2	DO CLD	DO UN	NT UN	NT UN	MAX UN	MAX UN		
21:55:00	9.2	-36.4	.0003	.0010	82	75	10164	706	.31			
21:57:15	9.2	-36.4	.0006	.0015	77	106	7327	706	.39			
21:57:30	9.1	-36.3	.0012	.0047	65	122	1478	1011	.39			
21:57:45	9.0	-36.4	.0025	.0114	57	131	38208	1011	.33			
21:58:00	9.0	-35.9	.0041	.0174	58	128	69663					
21:58:15	9.0	-35.8	.0074	.0280	42	114	141666					
21:58:30	8.9	-35.5	.0052	.0192	57	130	9519	1011	.24			
21:58:45	8.9	-35.5	.0012	.0032	58	129	8332	1011	.36			
21:59:00	8.9	-35.4	.0007	.0013	70	115	4305	706	.42			
21:59:15	8.9	-35.3	.0001	.0003	95	108	1641	437	.53			
21:59:30	8.9	-35.4	.0001	.0005	97	102	3471	437	.47			
21:59:45	8.9	-35.2	.0001	.0003	42	256	1007	706	.39			
22:00:00	8.9	-35.4	.0003	.0010	49	142	2128					
22:00:15	8.9	-35.5	.0023	.0059	50	141	17085	1316	.30			
22:00:30	8.9	-35.6	.0033	.0116	59	130	33157	1011	.37			
22:00:45	8.9	-35.5	.0025	.0096	68	123	32134	1011	.40			
22:01:00	8.9	-35.1	.0033	.0135	74	110	57282	706	.40			
22:01:15	8.9	-35.2	.0039	.0212	54	134	62368	1316	.32			
22:01:30	8.9	-35.4	.0084	.0355	46	149	123432	2233	.19			
22:01:45	8.9	-34.9	.0097	.0169	45	151	128091	1316	.26			
22:02:00	8.8	-34.4	.0049	.0245	32	175	41808	1316	.29			
22:02:15	8.8	-34.7	.0047	.0208	52	138	39878	1011	.42			
22:02:30	8.8	-34.4	.0029	.0099	26	198	19962	1316	.23			
22:02:45	8.7	-34.2	.0014	.0069	15	274	8492	1927	.18			
22:03:00	8.7	-33.9	.0005	.0040	20	321	1316					
22:03:15	8.6	-33.6	.0004	.0025	47	146	2216	706	.62			
22:03:30	8.6	-33.1	.0002	.0012	83	95	4924	706	.49			
22:03:45	8.6	-33.1	.0003	.0009	81	100	5184	706	.40			
22:04:00	8.6	-33.2	.0001	.0003	96	59	3197	706	.40			
22:04:15	8.6	-33.1	.0002	.0008	78	101	2895	706	.48			
22:04:30	8.6	-33.3	.0001	.0003	67	120	620	706	.50			
22:04:45	8.6	-33.5	.0001	.0002	55	134	304	706	.50			
22:05:00	8.6	-33.1	.0000	.0000	0	0	0	0	0			
22:05:15	8.6	-32.8	.0000	.0000	0	0	0	0	0			
22:05:30	8.6	-32.9	.0000	.0000	0	0	0	0	0			
22:05:45	8.6	-33.1	.0000	.0000	0	0	0	0	0			
22:06:00	8.6	-33.2	.0000	.0000	0	0	0	0	0			
22:06:15	8.6	-33.4	.0000	.0000	0	0	0	0	0			
22:06:30	8.6	-33.6	.0000	.0000	0	0	0	0	0			
22:06:45	8.6	-33.2	.0000	.0000	0	0	0	0	0			
22:07:00	8.6	-33.6	.0000	.0000	0	0	0	0	0			
22:07:15	8.6	-33.8	.0000	.0000	0	0	0	0	0			
22:07:30	8.6	-33.7	.0000	.0000	0	0	0	0	0			
22:07:45	8.6	-33.7	.0000	.0000	0	0	0	0	0			
22:08:00	8.6	-33.7	.0000	.0000	0	0	0	0	0			
22:08:15	8.6	-33.7	.0000	.0000	0	0	0	0	0			
22:08:30	8.6	-33.6	.0001	.0000	0	0	0	0	0			
22:08:45	8.6	-33.5	.0002	.0003	100	33	362	47	1.00			
22:09:00	8.6	-33.5	.0137	.0812	18	215	5003	437	.68			
22:09:15	8.6	-33.5	.0013	.0116	53	138	105148	2233	.19			
22:09:30	8.6	-33.5	.0002	.0000	78	79	24753	1011	.43			
22:09:45	8.6	-33.4	.0001	.0000	0	0	0	0	0			
22:10:00	8.6	-33.4	.0002	.0000	0	0	0	0	0			
22:10:15	8.6	-33.4	.0001	.0000	0	0	0	0	0			
22:10:30	8.6	-33.4	.0001	.0000	0	0	0	0	0			
22:10:45	8.6	-33.4	.0001	.0000	0	0	0	0	0			

START TIME	ALT KIN	TEMP 6/M**3	15 SECOND AVERAGE					LMAX UM	FF
			INC-SC	INC-CP	INC	INT	W/M**3		
22:11:00	8.6	-33.5	.0001	0.0000	0	0	0	.25	0.00
22:11:15	8.6	-33.7	.0000	0.0001	100	78	.684	.230	.82
22:11:30	8.6	-33.6	.0004	.0020	100	84	.9404	.311	.72
22:11:45	8.6	-33.4	.0001	.0002	100	116	.602	.311	.71
22:12:00	8.6	-33.7	.0001	.0003	100	115	.566	.311	.77
22:12:15	8.6	-33.9	.0000	.0000	0	242	1	.437	1.41
22:12:30	8.6	-33.8	.0001	.0002	95	76	1716	.796	.44
22:12:45	8.6	-33.7	.0002	.0007	95	130	2845	.437	.46
22:13:00	8.6	-33.7	.0003	.0012	72	125	2223	.706	.57
22:13:15	8.6	-33.5	.0000	.0003	94	117	718	.437	.63
22:13:30	8.6	-33.4	.0000	.0002	100	108	336	.311	.84
22:13:45	8.6	-33.4	.0000	.0000	0	0	0	.23	0.00
22:14:00	8.6	-33.7	.0000	.0002	98	132	.677	.437	.59
22:14:15	8.6	-33.8	.0001	.0007	89	110	2396	.437	.49
22:14:30	8.6	-33.8	.0004	.0015	88	120	4881	.437	.51
22:14:45	8.6	-33.5	.0010	.0042	74	124	9575	.706	.53
22:15:00	8.6	-33.7	.0019	.0084	64	127	23073	.1011	.42
22:15:15	8.6	-33.8	.0025	.0119	34	173	21807	.1011	.33
22:15:30	8.6	-33.8	.0049	.0271	46	149	43943	.1316	.40
22:15:45	8.6	-33.8	.0063	.0341	40	160	63770	.1927	.30
22:16:00	8.6	-33.8	.0013	.0051	59	122	17917	.1011	.29
22:16:15	8.6	-33.7	.0018	.0055	93	68	51101	.706	.46
22:16:30	8.6	-33.7	.0037	.0121	91	70	110598	.706	.42
22:16:45	8.6	-33.9	.0024	.0086	92	79	67451	.706	.45
22:17:00	8.6	-34.2	.0053	.0183	84	79	124795	.706	.39
22:17:15	8.6	-34.3	.0047	.0147	90	76	121908	.706	.42
22:17:30	8.6	-34.4	.0013	.0049	90	85	32331	.706	.45
22:17:45	8.6	-34.5	.0001	.0001	53	80	406	.706	.29
22:18:00	8.6	-34.5	.0000	.0001	79	79	836	.706	.29
22:18:15	8.6	-34.3	.0000	.0000	62	67	53	.437	.39
22:18:30	8.6	-34.0	.0000	.0001	100	62	998	.169	1.07
22:18:45	8.6	-34.3	.0000	.0000	0	0	0	.27	0.00
22:19:00	8.6	-34.3	.0000	.0000	0	0	0	0	0.00
22:19:15	8.6	-34.3	.0000	.0000	0	0	0	0	0.00
22:19:30	8.6	-34.2	.0000	.0000	0	0	0	0	0.00

At 31°59'N, 101°09'W. Wind is 245°/136 kt. Near base of Cs. Should be getting good particle counts.

Only a little Ac below aircraft to the north. Ground visible. Horizontal visibility about 1 mi. in hazy Cs. Reentering heavier Cs. Can see ice particles going by.

At 32°16', 101°22'. Wind 245°/140 kt. Beginning descent.

Appendix B

29 January 1979 Data Tabulations

Tabulations follow the format described in Appendix A.

29 JAN 79 15 SECOND AVERAGE												
START	ALT	TIME	TEMP	TWC-SC	TWC-CP	INC	D8	AVG	MAX	MIN	FF	
	MM	MM	C	0/Mes3	0/Mes3	z	CLD	UN	W/Hes3	UN	FF	
10:45:46	7.7	-47.3	-0.321	-0.499	0.84	84	725739	1011	.29			
10:45:51	7.7	-47.3	-0.322	-0.499	0.84	84	43244	1011	.33			
10:45:56	7.7	-47.3	-0.323	-0.499	0.84	84	692897	1011	.27			
10:45:59	7.7	-47.3	-0.323	-0.499	0.84	84	3466923	1316	.27			
10:46:04	7.7	-47.3	-0.324	-0.499	0.84	84	70	352219	.76	.49		
10:46:09	7.7	-47.3	-0.324	-0.499	0.84	84	6110	318314	1011	.38		
10:46:15	7.7	-47.3	-0.324	-0.499	0.84	84	286129	1011	.49			
10:46:30	7.7	-47.3	-0.324	-0.499	0.84	84	43	111332	.43	.56	In top of CS. Most cloud is below 15,000'. Blue sky above through thin cirriform	
10:46:45	7.7	-47.3	-0.324	-0.499	0.84	84	52	188147	311	.56	filaments near aircraft altitude.	
10:47:00	7.7	-47.4	-0.325	-0.499	0.84	84	36	297635	706	.39	In white, very hazy, heavy clouds overcast above, but sun is fairly bright above.	
10:47:15	7.7	-47.4	-0.325	-0.499	0.84	84	61	626795	1316	.25		
10:47:30	7.7	-47.4	-0.325	-0.499	0.84	84	71	670107	2233	.14		
10:47:45	7.7	-47.4	-0.325	-0.499	0.84	84	76	623553	1011	.25		
10:48:00	7.7	-47.4	-0.325	-0.499	0.84	84	55	327534	.706	.41		
10:48:15	7.7	-47.4	-0.325	-0.499	0.84	84	73	390364	1011	.27	Very small particles, sun snow streaks. Bounding 1011 at 20° 28' N, 104° 26' W.	
10:48:30	7.7	-47.4	-0.325	-0.499	0.84	84	67	315834	437	.53		
10:48:45	7.7	-47.4	-0.325	-0.499	0.84	84	69	105735	437	.53		
10:49:00	7.7	-47.4	-0.325	-0.499	0.84	84	83	37575	437	.54		
10:49:15	7.7	-47.4	-0.325	-0.499	0.84	84	99	172994	437	.53		
10:49:30	7.7	-47.5	-0.325	-0.499	0.84	84	99	159395	437	.56		
10:49:45	7.7	-47.5	-0.325	-0.499	0.84	84	99	70	199424	706	.46	
10:50:00	7.7	-47.5	-0.325	-0.499	0.84	84	99	56	189230	311	.58	CS has thinmed here in the top. Much haze, sun through thin filaments.
10:50:15	7.7	-47.5	-0.325	-0.499	0.84	84	99	69	105735	437	.58	Halo around sun.
10:50:30	7.7	-47.5	-0.325	-0.499	0.84	84	99	60	170107	2233	.14	
10:50:45	7.7	-47.5	-0.325	-0.499	0.84	84	99	49	626795	1316	.25	
10:51:00	7.7	-47.5	-0.325	-0.499	0.84	84	99	11679	311	.48		
10:51:15	7.7	-47.5	-0.325	-0.499	0.84	84	99	62	43644	311	.61	
10:51:30	7.7	-47.5	-0.325	-0.499	0.84	84	99	71	65311	437	.52	
10:51:45	7.7	-47.5	-0.325	-0.499	0.84	84	99	97	29926	437	.48	
10:52:00	7.7	-47.5	-0.325	-0.499	0.84	84	99	92	686112	437	.59	
10:52:15	7.7	-47.5	-0.325	-0.499	0.84	84	99	46	18123	311	.51	
10:52:30	7.7	-47.5	-0.325	-0.499	0.84	84	99	60	24286	311	.63	
10:52:45	7.7	-47.5	-0.325	-0.499	0.84	84	99	70	56429	311	.55	
10:53:00	7.7	-47.5	-0.325	-0.499	0.84	84	99	74	68645	311	.59	
10:53:15	7.7	-47.5	-0.325	-0.499	0.84	84	99	42	2746	311	.59	
10:53:30	7.7	-47.5	-0.325	-0.499	0.84	84	99	33	117337	128	.23	
10:53:45	7.7	-47.5	-0.325	-0.499	0.84	84	99	43	6742	230	.68	
10:54:00	7.7	-47.5	-0.325	-0.499	0.84	84	99	52	13829	230	.68	
10:54:15	7.7	-47.5	-0.325	-0.499	0.84	84	99	42	32230	311	.51	
10:54:30	7.7	-47.5	-0.325	-0.499	0.84	84	99	35	18646	169	.69	
10:54:45	7.7	-47.5	-0.325	-0.499	0.84	84	99	42	966	87	.91	
10:55:00	7.7	-47.5	-0.325	-0.499	0.84	84	99	44	28179	128	.83	
10:55:15	7.7	-47.5	-0.325	-0.499	0.84	84	99	51	2559	.148	.82	
10:55:30	7.7	-47.5	-0.325	-0.499	0.84	84	99	44	19217	.437	.53	
10:55:45	7.7	-47.5	-0.325	-0.499	0.84	84	99	65	164807	.437	.53	
10:56:00	7.7	-47.5	-0.325	-0.499	0.84	84	99	70	163465	.437	.55	
10:56:15	7.7	-47.5	-0.325	-0.499	0.84	84	99	87	86228	.437	.56	
10:56:30	7.7	-47.5	-0.325	-0.499	0.84	84	99	189	63842	.716	.54	
10:56:45	7.7	-47.5	-0.325	-0.499	0.84	84	99	44	15331	311	.56	
10:57:00	7.7	-47.5	-0.325	-0.499	0.84	84	99	65	28179	.437	.53	
10:57:15	7.7	-47.5	-0.325	-0.499	0.84	84	99	33	466	47	.69	
10:57:30	7.7	-47.5	-0.325	-0.499	0.84	84	99	0	0	21	.69	
10:57:45	7.7	-47.5	-0.325	-0.499	0.84	84	99	33	466	47	.69	

PRECEDING PAGE BLANK-NOT FILMED

START TIME	ALT WM	15 SECOND AVERAGE									
		TEMP C	INC-SC 6/Hee3	INC-CP 6/Hee3	IWC IWC	DO 6/Hee3	MT IWC	MAX UN	FF UN		
18:59:00	7.7	-47.4	.0002	.0002	.0002	.0002	.0002	.0039	.0039	1.11	
18:59:15	7.7	-47.3	.0003	.0003	.0003	.0003	.0003	.0040	.0040	.87	
18:59:30	7.4	-47.5	.0003	.0003	.0003	.0003	.0003	.0045	.0045	.84	
18:59:45	7.4	-46.9	.0013	.0013	.0013	.0013	.0013	.0045	.0045	.84	
19:00:00	7.6	-46.8	.0016	.0016	.0016	.0016	.0016	.0059	.0059	.76	
19:00:15	7.7	-46.8	.0006	.0006	.0006	.0006	.0006	.0059	.0059	.69	
19:00:30	7.7	-46.6	.0002	.0002	.0002	.0002	.0002	.0059	.0059	.69	
19:00:45	7.7	-46.6	.0003	.0003	.0003	.0003	.0003	.0059	.0059	.69	
19:01:00	7.7	-46.7	.0004	.0004	.0004	.0004	.0004	.0059	.0059	.69	
19:01:15	7.7	-47.0	.0003	.0003	.0003	.0003	.0003	.0059	.0059	.69	
19:01:30	7.7	-46.9	.0004	.0004	.0004	.0004	.0004	.0059	.0059	.69	
19:01:45	7.7	-46.1	.0009	.0009	.0009	.0009	.0009	.0059	.0059	.59	
19:02:00	7.7	-45.9	.0001	.0001	.0001	.0001	.0001	.0059	.0059	.59	
19:02:15	7.7	-45.5	.0001	.0001	.0001	.0001	.0001	.0059	.0059	.59	
19:02:30	7.7	-45.2	.0005	.0005	.0005	.0005	.0005	.0059	.0059	.59	
19:02:45	7.7	-45.8	0	0	0	0	0	0	0	0	
19:03:00	7.7	-44.5	.0009	.0009	.0009	.0009	.0009	.0059	.0059	.59	
19:03:15	7.7	-43.9	.0009	.0009	.0009	.0009	.0009	.0059	.0059	.59	
19:03:30	7.7	-43.7	.0009	.0009	.0009	.0009	.0009	.0059	.0059	.59	
19:03:45	7.7	-44.3	.0009	.0009	.0009	.0009	.0009	.0059	.0059	.59	
19:04:00	7.7	-44.5	.0009	.0009	.0009	.0009	.0009	.0059	.0059	.59	
19:04:15	7.7	-44.1	.0009	.0009	.0009	.0009	.0009	.0059	.0059	.59	
19:04:30	7.7	-44.3	.0009	.0009	.0009	.0009	.0009	.0059	.0059	.59	
19:04:45	7.7	-44.9	.0009	.0009	.0009	.0009	.0009	.0059	.0059	.59	
19:05:00	7.7	-45.8	.0009	.0009	.0009	.0009	.0009	.0059	.0059	.59	
19:05:15	7.7	-44.6	.0009	.0009	.0009	.0009	.0009	.0059	.0059	.59	
19:05:30	7.7	-44.3	.0009	.0009	.0009	.0009	.0009	.0059	.0059	.59	
19:05:45	7.7	-43.8	.0009	.0009	.0009	.0009	.0009	.0059	.0059	.59	
19:06:00	7.7	-43.4	.0009	.0009	.0009	.0009	.0009	.0059	.0059	.59	
19:06:15	7.7	-43.4	.0009	.0009	.0009	.0009	.0009	.0059	.0059	.59	
19:06:30	7.7	-43.4	.0009	.0009	.0009	.0009	.0009	.0059	.0059	.59	
19:06:45	7.7	-43.4	.0009	.0009	.0009	.0009	.0009	.0059	.0059	.59	
19:07:00	7.7	-43.4	.0009	.0009	.0009	.0009	.0009	.0059	.0059	.59	
19:07:15	7.7	-42.3	.0009	.0009	.0009	.0009	.0009	.0059	.0059	.59	
19:07:30	7.7	-42.2	.0009	.0009	.0009	.0009	.0009	.0059	.0059	.59	
19:07:45	7.7	-42.5	.0009	.0009	.0009	.0009	.0009	.0059	.0059	.59	
19:08:00	7.7	-42.7	.0009	.0009	.0009	.0009	.0009	.0059	.0059	.59	
19:08:15	7.7	-42.4	.0009	.0009	.0009	.0009	.0009	.0059	.0059	.59	
19:08:30	7.7	-42.3	.0009	.0009	.0009	.0009	.0009	.0059	.0059	.59	
19:08:45	7.7	-42.3	.0009	.0009	.0009	.0009	.0009	.0059	.0059	.59	
19:09:00	7.7	-42.6	.0001	.0001	.0001	.0001	.0001	.0059	.0059	.59	
19:09:15	7.7	-42.3	.0009	.0009	.0009	.0009	.0009	.0059	.0059	.59	
19:09:30	7.7	-42.4	.0001	.0001	.0001	.0001	.0001	.0059	.0059	.59	
19:09:45	7.7	-42.8	.0001	.0001	.0001	.0001	.0001	.0059	.0059	.59	
19:10:00	7.7	-41.9	.0001	.0001	.0001	.0001	.0001	.0059	.0059	.59	
19:10:15	7.7	-42.7	.0001	.0001	.0001	.0001	.0001	.0059	.0059	.59	
19:10:30	7.7	-42.9	.0002	.0002	.0002	.0002	.0002	.0059	.0059	.59	
19:10:45	7.7	-43.0	.0001	.0001	.0001	.0001	.0001	.0059	.0059	.59	
19:11:00	7.8	-42.9	.0001	.0001	.0001	.0001	.0001	.0059	.0059	.59	
19:11:15	7.8	-43.1	.0002	.0002	.0002	.0002	.0002	.0059	.0059	.59	
19:11:30	7.8	-43.0	.0003	.0003	.0003	.0003	.0003	.0059	.0059	.59	
19:11:45	7.8	-43.0	.0003	.0003	.0003	.0003	.0003	.0059	.0059	.59	
19:12:00	7.8	-43.0	.0003	.0003	.0003	.0003	.0003	.0059	.0059	.59	
19:12:15	7.8	-42.9	.0001	.0001	.0001	.0001	.0001	.0059	.0059	.59	
19:12:30	7.8	-43.1	.0002	.0002	.0002	.0002	.0002	.0059	.0059	.59	
19:12:45	7.8	-43.0	.0003	.0003	.0003	.0003	.0003	.0059	.0059	.59	

Ground has disappeared in the undercast.

Flying very near top of cirriform layer. Heavy Cs below, bright blue sky

29 JAN 79		15 SECOND AVERAGE							
START	ALT	TEMP	TWC-SC	TWC-CP	TWC	DO	NT	LMAX	FF
TIME	MN	C	6/N/e+3	6/N/e+3	2	CLD	UN	N/N/e+3	UN
19:13:00	7.7	-42.7	-42.3	.0003	0.0000	0	0	0	27 0.00
19:13:15	7.7	-42.7	.0002	0.0000	0	0	0	0	27 0.00
19:13:30	7.5	-42.2	.0002	0.0000	0	0	0	0	27 0.00
19:13:45	7.7	-42.4	.0003	0.0000	100	33	289	47 1.00	
19:14:00	7.7	-42.0	.0003	0.0000	0	0	0	0	27 0.00
19:14:15	7.7	-41.4	.0002	0.0000	0	0	0	0	27 0.00
19:14:30	7.7	-41.3	.0002	0.0000	0	0	0	0	27 0.00
19:14:45	7.7	-41.6	.0003	0.0000	0	0	0	0	27 0.00
19:15:00	7.1	-41.8	.0003	0.0000	0	0	0	0	27 0.00
19:15:15	7.5	-41.8	.0003	0.0000	0	0	0	0	23 0.00
19:15:30	7.5	-41.8	.0003	0.0000	0	0	0	0	23 0.00
19:15:45	7.0	-41.2	.0003	0.0000	0	0	0	0	27 0.00
19:16:00	7.0	-41.7	.0003	0.0000	0	0	0	0	27 0.00
19:16:15	6.9	-42.3	.0002	0.0000	0	0	0	0	27 0.00
19:16:30	6.9	-42.2	.0002	0.0000	0	0	0	0	23 0.00
19:16:45	6.8	-41.7	.0003	0.0000	0	0	0	0	27 0.00
19:17:00	6.6	-48.9	.0003	0.0000	0	0	0	0	27 0.00
19:17:15	6.6	-39.9	.0003	0.0000	0	0	0	0	27 0.00
19:17:30	6.6	-39.7	.0001	0.0000	0	0	0	0	23 0.00
19:17:45	6.4	-39.4	.0000	0.0000	0	0	0	0	27 0.00
19:17:50	6.7	-42.1	.0002	0.0000	0	0	0	0	27 0.00
19:18:05	6.8	-41.7	.0003	0.0000	0	0	0	0	27 0.00
19:18:20	6.6	-38.2	.0000	0.0000	0	0	0	0	27 0.00
19:18:35	6.3	-38.0	.0001	0.0000	0	0	0	0	27 0.00
19:18:50	6.3	-38.0	.0004	0.0000	0	0	0	0	27 0.00
19:19:05	6.3	-38.1	.0016	0.0000	0	0	0	0	27 0.00
19:19:20	6.3	-38.3	.0013	0.0000	0	0	0	0	27 0.00
19:19:35	6.3	-38.3	.0013	0.0000	0	0	0	0	27 0.00
19:19:50	6.3	-38.3	.0002	0.0000	0	0	0	0	27 0.00
19:20:05	6.3	-38.2	.0000	0.0000	0	0	0	0	27 0.00
19:20:20	6.3	-38.2	.0000	0.0000	0	0	0	0	27 0.00
19:20:35	6.3	-38.3	.0000	0.0000	0	0	0	0	27 0.00
19:20:50	6.3	-38.3	.0000	0.0000	0	0	0	0	27 0.00
19:21:05	6.2	-38.0	.0000	0.0000	0	0	0	0	27 0.00
19:21:20	6.2	-37.9	.0000	0.0000	0	0	0	0	27 0.00
19:21:35	6.2	-37.4	.0000	0.0000	0	0	0	0	27 0.00
19:21:50	6.2	-37.2	.0000	0.0000	0	0	0	0	27 0.00
19:22:05	6.1	-37.3	.0000	0.0000	0	0	0	0	27 0.00
19:22:20	6.1	-37.4	.0000	0.0000	0	0	0	0	27 0.00
19:22:35	6.1	-37.4	.0000	0.0000	0	0	0	0	27 0.00
19:22:50	6.1	-36.7	.0000	0.0000	0	0	0	0	27 0.00
19:23:05	6.1	-36.7	.0000	0.0000	0	0	0	0	27 0.00
19:23:20	6.1	-36.4	.0000	0.0000	0	0	0	0	27 0.00
19:23:35	6.1	-36.4	.0000	0.0000	0	0	0	0	27 0.00
19:23:50	6.1	-36.4	.0000	0.0000	0	0	0	0	27 0.00
19:24:05	6.1	-36.5	.0007	0.0000	100	33	7958	189 1.00	
19:24:20	6.1	-36.1	.0011	0.0000	100	34	26119	189 1.00	
19:24:35	6.2	-36.2	.0003	0.0000	100	69	217	289 1.21	
19:25:00	6.1	-36.2	.0000	0.0000	0	0	0	0	437 1.41
19:25:15	6.2	-35.5	.0000	0.0000	0	0	0	0	437 1.41
19:25:30	6.4	-35.9	.0000	0.0000	0	0	0	0	5 0.00
19:25:45	6.2	-35.5	.0000	0.0000	0	0	0	0	18 0.00
19:26:00	6.1	-36.4	.0030	0.0000	100	63	3434	259 .61	
19:26:15	6.1	-36.1	.0030	0.0000	100	48	18333	311 .54	
19:26:30	6.1	-36.2	.0000	0.0000	100	40	2512	168 .83	
19:26:45	6.1	-36.5	.0019	0.0000	99	57	12686	437 .52	

Skimming cloud tops through thin cirriform cloud.
 Beginning gradual descent to sample more cloud tops.
 Heading 177°, wind 21⁸/44 kt. Much blue sky above. At level of cloud tops.
 Blue sky above. Seems to be in clear air, though C₁ extends in all directions.
 Blue sky above. Leveling off at this altitude. Some cumuliform clouds in this area.
 Found dimly visible. Most clouds seem to be cumulonimbus (C₂) with relatively flat tops.

Blue sky above. Leveling off at this altitude. Some cumuliform clouds in this area.

START TIME	TEMP RH	15 SECOND AVERAGE									
		IND-SC	IND-CP	TWC	DB	WT	LMAX	FF	IND-SC	IND-CP	TWC
19:27:00	6.1	-36.7	.0042	.0031	99	54	48623	437	.48		
19:27:15	6.1	-37.5	.0092	.0111	94	53	18942	706	.39		
19:27:30	6.1	-38.0	.0036	.0071	96	66	92499	706	.48		
19:27:45	6.1	-37.3	.0000	.0000	0	0	0	0	.00		
19:28:00	6.1	-35.6	.0000	.0000	0	0	0	0	.00		
19:28:15	6.2	-37.6	.0001	.0001	100	33	2602	87	1.21		
19:28:30	6.2	-38.1	.0028	.0052	100	43	149818	169	.92		
19:28:45	6.2	-38.1	.0040	.0101	100	45	234497	269	.75		
19:29:00	6.2	-38.0	.0022	.0049	100	51	85531	239			
19:29:15	6.1	-38.2	.0023	.0074	100	58	181002	311	.71		
19:29:30	6.1	-38.2	.0037	.0114	99	63	126214	437	.65		
19:29:45	6.1	-37.9	.0174	.0265	95	51	439573	1011	.39		
19:30:00	6.1	-36.7	.0010	.0003	100	36	6116	87	1.24		
19:30:15	6.1	-36.0	.0000	.0000	0	0	0	0	.00		
19:30:30	6.1	-35.7	.0000	.0000	0	0	0	0	.00		
19:30:45	6.1	-35.7	.0000	.0000	0	0	0	0	.00		
19:31:00	6.1	-36.6	.0002	.0001	100	49	1318	148	1.18		
19:31:15	6.2	-37.8	.0071	.0033	100	36	81303	230	.88		
19:31:30	6.1	-37.8	.0121	.0047	100	35	101244	250	.89		
19:31:45	6.1	-37.3	.0068	.0097	100	36	23434	148	1.01		
19:32:00	6.0	-35.6	.0000	.0000	0	0	0	0	.00		
19:32:15	6.0	-34.7	.0000	.0000	0	0	0	0	.00		
19:32:30	6.0	-35.1	.0000	.0000	0	0	0	0	.00		
19:32:45	6.1	-36.2	.0000	.0000	0	0	0	0	.00		
19:33:00	6.1	-36.9	.0013	.0004	100	35	8679	189	.96		
19:33:15	6.1	-36.9	.0032	.0094	100	35	8346	189	.96		
19:33:30	6.1	-36.4	.0032	.0094	100	35	45936	1011	.27		
19:33:45	6.1	-36.2	.0073	.0097	100	41	101244	250	.89		
19:33:59	6.1	-36.7	.0013	.0003	100	31	6897	128	1.34		
19:34:00	5.9	-36.3	.0000	.0000	0	0	0	0	.00		
19:34:15	5.9	-35.5	.0000	.0000	0	0	0	0	.00		
19:34:30	5.8	-34.9	.0000	.0000	0	0	0	0	.00		
19:34:45	5.8	-35.0	.0000	.0000	0	0	0	0	.00		
19:35:00	5.8	-34.5	.0000	.0000	0	0	0	0	.00		
19:35:15	5.8	-34.8	.0000	.0000	0	0	0	0	.00		
19:35:30	5.9	-35.8	.0052	.0017	100	38	38295	189	1.33		
19:35:45	5.9	-36.5	.0027	.0016	99	43	31329	437	.56		
19:36:00	5.8	-36.9	.0023	.0048	95	52	72659	796	.43		
19:36:15	5.8	-34.4	.0022	.0025	99	49	44321	437	.54		
19:36:30	5.8	-34.6	.0285	.0183	98	47	36395	1011	.22		
19:36:45	5.9	-35.9	.0000	.0000	0	0	0	0	.00		
19:37:00	5.9	-35.5	.0000	.0000	0	0	0	0	.00		
19:37:15	5.9	-34.2	.0026	.0026	98	52	4994	437	.48		
19:37:30	5.9	-34.8	.0069	.0069	0	0	0	0	.00		
19:37:45	5.8	-33.7	.0000	.0000	0	0	0	0	.00		
19:38:00	5.8	-33.1	.0000	.0000	0	0	0	0	.00		
19:38:15	5.7	-31.6	.0000	.0000	0	0	0	0	.00		
19:38:30	5.5	-32.0	.0000	.0000	0	0	0	0	.00		
19:38:45	5.4	-32.4	.0000	.0000	0	0	0	0	.00		
19:39:00	5.4	-32.7	.0000	.0000	0	0	0	0	.00		
19:39:15	5.4	-32.9	.0000	.0000	0	0	0	0	.00		
19:39:30	5.4	-33.6	.0000	.0000	0	0	0	0	.00		
19:39:45	5.4	-32.9	.0000	.0000	0	0	0	0	.00		
19:40:00	5.4	-32.6	.0000	.0000	0	0	0	0	.00		
19:40:15	5.4	-32.4	.0000	.0000	0	0	0	0	.00		
19:40:30	5.4	-32.8	.0003	.0013	99	49	28826	437	.21		
19:40:45	5.5	-33.6	.0059	.0135	95	53	220463	706	.41		

START TIME	ALT WH	29 JAN 79			15 SEC AVERAGE			MAX WH	MIN WH	FF
		TEMP C	INC 6/Sec*3	INC 6/Sec*3 x CLD	D#	WT N/M*3	MAX WH			
19:41:00	5.4	-33.1	.0001	.0002	92	81	2675	.706	.28	
19:41:15	5.4	-32.4	.0000	.0000	0	0	0	0	0	
19:41:30	5.4	-32.4	.0000	.0000	100	23	0	26	0.99	
19:41:45	5.4	-32.1	.0000	.0000	100	23	0	26	0.99	
19:42:00	5.4	-32.4	.0000	.0000	100	23	0	26	0.99	
19:42:15	5.3	-32.4	.0000	.0000	100	25	949	47	2.88	
19:42:30	5.3	-32.0	.0001	.0001	100	41	1747	108	1.00	
19:42:45	5.3	-32.0	.0002	.0002	100	49	6326	230	.69	
19:43:00	5.3	-32.0	.0013	.0035	100	62	44686	311	.63	
19:43:15	5.3	-32.0	.0015	.0035	100	62	43025	311	.58	
19:43:30	5.3	-31.9	.0014	.0046	99	78	35979	437	.58	Continue flying in and out of white filament near cloud tops.
19:43:45	5.2	-31.3	.0014	.0039	99	73	37674	437	.53	
19:44:00	5.2	-31.3	.0003	.0003	100	72	5783	311	.68	
19:44:15	5.2	-31.1	.0000	.0000	99	77	22522	437	.55	
19:44:30	5.1	-30.3	.0012	.0044	100	77	37304	311	.58	
19:44:45	5.1	-30.2	.0015	.0070	99	108	25614	437	.66	
19:45:00	5.1	-30.4	.0002	.0002	100	45	4571	169	.76	
19:45:15	5.1	-30.3	.0010	.0043	100	57	66292	311	.69	
19:45:30	5.2	-30.7	.0003	.0010	100	58	15069	311	.52	
19:45:45	5.2	-30.8	.0011	.0010	100	38	31835	128	.94	At 36°37'N, 106°31'E, the aircraft is in the top of ice clouds.
19:46:00	5.2	-31.0	.0028	.0039	100	44	91381	311	.70	
19:46:15	5.3	-31.6	.0023	.0041	100	49	81552	250	.79	
19:46:30	5.3	-31.9	.0037	.0091	100	53	47348	311	.75	
19:46:45	5.3	-31.8	.0040	.0113	100	52	192681	311	.75	
19:47:00	5.3	-31.8	.0038	.0086	100	53	141241	311	.68	
19:47:15	5.3	-31.6	.0033	.0045	100	44	184983	289	.84	
19:47:30	5.2	-31.3	.0030	.0042	100	46	183025	289	.83	
19:47:45	5.2	-31.4	.0040	.0125	100	57	181325	311	.69	
19:48:00	5.2	-30.8	.0009	.0012	100	48	24230	230	.73	
19:48:15	5.2	-31.0	.0019	.0061	99	79	45129	437	.57	
19:48:30	5.2	-30.4	.0022	.0095	99	80	66228	437	.59	

Appendix C

2 February 1979 Data Tabulations

Tabulations follow the format described in Appendix A.

START TIME	02 FEB 79			15 SECOND AVERAGE			MAX UM	MIN UM	MAX UM	MIN UM
	REFP	IUC-CP	IUC-SC	IUC-CP	IUC	EQ				
20:55:00	9.1	-36.7	.0016	.0038	.99	.69	35385	437	.66	.65
20:55:15	9.1	-38.5	.0019	.0042	100	63	52414	511	.65	.65
20:55:30	9.1	-38.4	.0025	.0050	.99	.69	58635	437	.56	.56
20:55:45	9.1	-38.4	.0016	.0052	.99	.27	39564	437	.61	.61
20:56:00	9.1	-38.5	.0013	.0044	100	.71	46072	311	.57	.57
20:56:15	9.1	-38.6	.0013	.0037	100	.70	34446	311	.63	.63
20:56:30	9.1	-38.6	.0020	.0043	PP	.84	32615	437	.56	.56
20:56:45	9.1	-38.3	.0014	.0052	.99	.61	45554	437	.63	.63
20:57:00	9.1	-38.7	.0028	.0065	.99	.61	71805	437	.59	.59
20:57:15	9.1	-38.9	.0032	.0075	100	.58	109865	250	.71	.71
20:57:30	9.1	-38.8	.0042	.0081	100	.51	130812	311	.60	.60
20:57:45	9.1	-38.8	.0012	.0032	100	.62	48004	311	.62	.62
20:58:00	9.1	-38.8	.0012	.0032	100	.61	43705	311	.69	.69
20:58:15	9.1	-38.9	.0014	.0039	.99	.64	45731	437	.70	.70
20:58:30	9.1	-38.9	.0013	.0038	.99	.67	35629	437	.66	.66
20:58:45	9.1	-38.9	.0010	.0032	.99	.73	25404	437	.63	.63
20:59:00	9.1	-39.1	.0010	.0029	.99	.74	21202	437	.63	.63
20:59:15	9.1	-39.0	.0012	.0029	.99	.61	37282	437	.64	.64
20:59:30	9.1	-39.2	.0002	.0020	100	.62	20564	311	.58	.58
20:59:45	9.1	-39.4	.0008	.0020	100	.63	26615	311	.62	.62
21:00:00	9.2	-39.7	.0007	.0015	100	.63	23878	311	.61	.61
21:00:15	9.2	-39.5	.0007	.0019	100	.62	22698	250	.70	.70
21:00:30	9.2	-39.6	.0006	.0021	100	.64	20198	311	.55	.55
21:00:45	9.2	-39.6	.0007	.0015	100	.64	34251	311	.69	.69
21:01:00	9.2	-39.7	.0008	.0021	100	.56	30916	311	.65	.65
21:01:15	9.2	-39.7	.0007	.0015	100	.59	26137	189	.84	.84
21:01:30	9.2	-39.7	.0010	.0020	100	.53	33823	311	.61	.61
21:01:45	9.2	-39.9	.0013	.0030	100	.53	48964	230	.77	.77
21:02:00	9.2	-40.0	.0023	.0050	100	.55	74446	311	.65	.65
21:02:15	9.2	-40.0	.0014	.0024	.99	.56	50647	437	.72	.72
21:02:30	9.2	-40.1	.0012	.0032	100	.61	38680	311	.65	.65
21:02:45	9.2	-40.2	.0009	.0022	100	.62	25192	311	.70	.70
21:03:00	9.2	-40.2	.0009	.0024	100	.69	31116	311	.64	.64
21:03:15	9.2	-40.4	.0009	.0032	.99	.71	27937	437	.63	.63
21:03:30	9.2	-40.4	.0016	.0030	100	.75	38795	311	.62	.62
21:03:45	9.2	-40.5	.0015	.0042	.99	.82	42356	437	.59	.59
21:04:00	9.2	-40.6	.0009	.0041	100	.93	18827	311	.63	.63
21:04:15	9.2	-40.8	.0006	.0024	.98	.101	8932	437	.69	.69
21:04:30	9.3	-40.9	.0005	.0025	82	.111	8412	706	.50	.50
21:04:45	9.3	-41.1	.0008	.0014	.98	.64	15811	437	.55	.55
21:05:00	9.3	-41.3	.0009	.0026	.99	.60	31249	437	.56	.56
21:05:15	9.3	-41.5	.0015	.0049	.99	.97	1115	20399	.41	.41
21:05:30	9.4	-41.9	.0019	.0041	.99	.106	24996	437	.73	.73
21:05:45	9.4	-42.0	.0025	.0025	.67	.130	49397	311	.65	.65
21:06:00	9.4	-42.0	.0002	.0023	.71	.130	4310	706	.55	.55
21:06:15	9.4	-42.1	.0005	.0018	.75	.125	5010	256	.48	.48
21:06:30	9.4	-42.1	.0011	.0024	.75	.27	10472	706	.54	.54
21:06:45	9.4	-42.5	.0021	.0032	.97	.114	19145	437	.69	.69
21:07:00	9.4	-42.7	.0029	.0044	.100	.87	113042	437	.73	.73
21:07:15	9.4	-43.0	.0014	.0048	.100	.63	54647	311	.67	.67
21:07:30	9.4	-43.1	.0022	.0068	.100	.59	88458	311	.55	.55
21:07:45	9.4	-43.3	.0031	.0099	.99	.62	124084	437	.52	.52
21:08:00	9.4	-42.7	.0033	.0091	.22	.62	118485	437	.58	.58
21:08:15	9.4	-43.1	.0034	.0100	.99	.64	113042	437	.54	.54
21:08:30	9.4	-43.1	.0049	.0095	.100	.54	143578	311	.54	.54
21:08:45	9.4	-43.1	.0049	.0095	.99	.52	156377	437	.55	.55

PRECEDING PAGE BLANK-NOT FILMED

START TIME	HL1	TENF	TUC-SC	15 SECOND AVERAGE				FF
				IUC-CP	IUC	DO	NT	
21:10:00	9.5	-43.1	.0044	.0082	100	50	144858	311
21:10:10	9.5	-43.2	.0029	.0073	100	54	112004	311
21:10:15	9.5	-43.3	.0024	.0063	100	56	98668	311
21:10:25	9.5	-43.1	.0029	.0077	100	57	11837	311
21:10:35	9.5	-43.0	.0033	.0066	99	54	10676	437
21:10:45	9.5	-43.0	.0026	.0066	100	47	130857	311
21:10:50	9.5	-43.1	.0030	.0033	100	42	77347	230
21:10:55	9.5	-43.2	.0019	.0038	100	44	63888	189
21:11:00	9.5	-43.1	.0021	.0042	100	46	88330	311
21:11:10	9.5	-43.1	.0021	.0035	100	38	97216	189
21:11:15	9.5	-43.1	.0016	.0034	100	48	69152	189
21:11:20	9.5	-43.1	.0011	.0030	100	53	51433	230
21:11:25	9.5	-43.1	.0014	.0028	100	45	9874	189
21:11:30	9.5	-43.0	.0020	.0034	100	46	76121	169
21:11:35	9.5	-43.1	.0019	.0037	100	46	88330	169
21:11:40	9.5	-42.9	.0038	.0050	100	36	138202	169
21:11:45	9.5	-42.9	.0045	.0051	100	39	154226	169
21:11:50	9.5	-42.9	.0022	.0029	100	39	69726	209
21:11:55	9.5	-42.9	.0029	.0030	100	75	37339	311
21:12:00	9.5	-42.9	.0002	.0004	100	61	3163	230
21:12:05	9.5	-43.0	.0002	.0003	100	59	5082	189
21:12:10	9.5	-43.1	.0002	.0004	100	64	3491	230
21:12:15	9.5	-43.2	.0003	.0004	100	63	6853	250
21:12:20	9.5	-43.2	.0000	.0007	100	84	28982	311
21:12:25	9.5	-43.2	.0009	.0030	100	81	48448	311
21:12:30	9.5	-43.0	.0018	.0082	100	73	12238	311
21:12:35	9.5	-43.1	.0002	.0015	100	68	16880	230
21:12:40	9.5	-43.2	.0002	.0014	100	64	15457	250
21:12:45	9.5	-43.2	.0000	.0024	100	47	44302	250
21:12:50	9.5	-43.2	.0008	.0030	100	54	55348	250
21:12:55	9.5	-43.2	.0008	.0030	100	57	34394	230
21:13:00	9.5	-43.3	.0010	.0017	100	68	15193	250
21:13:05	9.5	-43.4	.0000	.0018	100	57	19164	311
21:13:10	9.5	-43.7	.0001	.0015	100	63	21188	250
21:13:15	9.5	-43.7	.0002	.0022	100	57	37276	250
21:13:20	9.5	-43.7	.0001	.0014	100	58	40466	250
21:13:25	9.5	-43.7	.0008	.0024	100	61	30430	250
21:13:30	9.5	-43.7	.0000	.0030	100	55	29778	269
21:13:35	9.5	-43.8	.0008	.0029	100	60	38891	250
21:13:40	9.5	-44.0	.0000	.0036	100	56	15238	81
21:13:45	9.5	-44.0	.0000	.0018	100	56	40331	250
21:13:50	9.5	-44.1	.0000	.0033	100	51	9316	148
21:13:55	9.5	-44.1	.0000	.0029	100	59	37276	148
21:14:00	9.5	-44.0	.0000	.0037	100	57	36744	230
21:14:05	9.5	-44.0	.0000	.0019	100	56	29778	269
21:14:10	9.5	-43.7	.0000	.0030	100	55	23279	209
21:14:15	9.5	-43.7	.0000	.0016	100	50	15425	85
21:14:20	9.5	-43.7	.0000	.0004	100	50	15238	81
21:14:25	9.5	-43.7	.0000	.0018	100	56	15238	81
21:14:30	9.5	-43.7	.0000	.0006	100	51	9316	148
21:14:35	9.5	-43.7	.0000	.0009	100	55	16703	189
21:14:40	9.5	-43.7	.0000	.0051	100	51	2681	148
21:14:45	9.5	-43.7	.0000	.0005	100	54	8012	189
21:14:50	9.5	-43.7	.0001	.0006	100	52	9585	189
21:14:55	9.5	-43.7	.0003	.0004	100	48	2741	128
21:15:00	9.5	-43.7	.0003	.0004	100	38	8363	148
21:15:05	9.5	-43.7	.0001	.0002	100	42	5193	128
21:15:10	9.5	-43.7	.0000	.0009	100	55	16703	148
21:15:15	9.5	-43.7	.0000	.0051	100	51	2681	148
21:15:20	9.5	-43.7	.0000	.0005	100	54	6366	148
21:15:25	9.5	-43.7	.0000	.0004	100	50	5459	148
21:15:30	9.5	-43.7	.0000	.0003	100	50	15425	85
21:15:35	9.5	-43.7	.0000	.0001	100	50	15238	81
21:15:40	9.5	-43.7	.0000	.0000	100	51	9316	148
21:15:45	9.5	-43.7	.0000	.0000	100	42	615	148
21:15:50	9.5	-43.7	.0000	.0000	100	49	86	148

START TIME	ALT M	15 SECOND AVERAGE										FF
		TEMP C	INC-SC 6/H**3	INC-CP 6/H**3	INC 2 CLD	DO UN	NT N/H**3	LMAX UN				
21:23:00	9.6	-44.0	0.0000	.0002	100	52	3581	108	.96			
21:23:15	9.6	-44.0	0.0000	.0005	100	53	7372	128	.89			
21:23:30	9.6	-44.1	0.0000	.0008	100	52	11132	169	.91			
21:23:45	9.6	-44.1	0.0000	.0006	100	55	7776	169	.92			
21:24:00	9.6	-43.9	0.0000	.0007	100	54	9776	169	.92			
21:24:15	9.6	-43.9	0.0000	.0006	100	55	7937	128	.91			
21:24:30	9.6	-43.7	0.0000	.0011	100	53	15405	169	.93			
21:24:45	9.6	-43.6	0.0000	.0007	100	57	8640	148	.92			
21:25:00	9.6	-43.6	0.0000	.0007	100	53	10525	128	.92			
21:25:15	9.6	-43.7	0.0000	.0013	100	55	17219	209	.92			
21:25:30	9.6	-43.7	0.0000	.0011	100	54	13853	189	.92			
21:25:45	9.6	-43.6	0.0000	.0015	100	54	22614	189	.84			
21:26:00	9.6	-43.6	0.0000	.0014	100	53	20339	209	.86			
21:26:15	9.6	-43.8	0.0000	.0011	100	57	17001	189	.78			
21:26:30	9.6	-43.9	0.0000	.0016	100	55	21051	209	.86			
21:26:45	9.6	-43.9	0.0003	.0008	100	58	10555	169	.86			
21:27:00	9.6	-44.0	0.0006	.0006	100	55	8590	169	.85			
21:27:15	9.6	-44.1	0.0006	.0005	100	54	7759	169	.83			
21:27:30	9.6	-44.1	0.0005	.0005	100	54	8864	230	.73			
21:27:45	9.6	-43.9	0.0005	.0005	100	53	8920	209	.79			
21:28:00	9.6	-43.6	0.0004	.0007	100	51	10938	189	.84			
21:28:15	9.6	-43.3	0.0005	.0004	100	51	2945	169	.76			
21:28:30	9.6	-43.1	0.0005	.0003	100	50	5938	148	.91			
21:28:45	9.6	-43.0	0.0004	.0003	100	47	6438	128	.96			
21:29:00	9.6	-43.3	0.0003	.0003	100	53	8920	209	.79			
21:29:15	9.6	-43.3	0.0003	.0003	100	53	5143	169	.75			
21:29:30	9.6	-43.5	0.0004	.0002	100	50	4513	169	.76			
21:29:45	9.6	-43.7	0.0004	.0002	100	51	3479	169	.81			
21:30:00	9.6	-43.7	0.0002	.0003	100	48	6403	148	.79			
21:30:15	9.6	-43.8	0.0008	.0002	100	56	2163	148	.88			
21:30:30	9.6	-43.7	0.0002	.0002	100	50	3637	128	.86			
21:30:45	9.6	-43.6	0.0002	.0002	100	50	2545	148	.96			
21:31:00	9.6	-43.2	0.0001	.0000	100	50	506	108	1.16			
21:31:15	9.6	-43.2	0.0002	.0000	100	44	1041	87	.97			
21:31:30	9.6	-43.6	0.0001	.0000	100	38	939	128	.72			
21:31:45	9.6	-44.0	0.0001	.0000	100	51	510	128	.73			
21:32:00	9.6	-44.1	0.0000	.0000	100	51	100	87	1.00			
21:32:15	9.6	-43.9	0.0000	.0000	100	0	0	0	0.00			
21:32:30	9.6	-43.0	0.0000	.0000	100	0	0	0	0.00			
21:32:45	9.6	-43.2	0.0000	.0000	100	0	0	0	0.00			
21:33:00	9.6	-43.6	0.0000	.0000	100	0	0	0	0.00			
21:33:15	9.6	-43.4	0.0000	.0000	100	0	0	0	0.00			
21:33:30	9.6	-42.9	0.0000	.0000	100	0	0	0	0.00			
21:33:45	9.6	-42.3	0.0000	.0000	100	0	0	0	0.00			
21:34:00	9.6	-42.1	0.0000	.0000	100	0	0	0	0.00			
21:34:15	9.6	-42.3	0.0000	.0000	100	0	0	0	0.00			
21:34:30	9.6	-42.8	0.0000	.0000	100	0	0	0	0.00			
21:34:45	9.6	-43.0	0.0000	.0000	100	0	0	0	0.00			
21:35:00	9.6	-43.1	0.0000	.0000	100	0	0	0	0.00			
21:35:15	9.6	-43.1	0.0000	.0000	100	0	0	0	0.00			
21:35:30	9.6	-43.0	0.0000	.0000	100	0	0	0	0.00			
21:35:45	9.6	-42.8	0.0000	.0000	100	0	0	0	0.00			
21:36:00	9.6	-42.7	0.0000	.0000	100	0	0	0	0.00			
21:36:15	9.6	-42.7	0.0000	.0000	100	62	144	128	.93			
21:36:30	9.6	-42.8	0.0000	.0000	100	65	48	128	1.00			
21:36:45	9.6	-43.3	0.0000	.0000	100	42	158	67	1.00			

Doesn't seem to be any cirrus here at all. There are some far below, but not an undercast.

Only getting very small particles now.

Getting small particles. Still turning to right.

Heading toward Cs band. At 34° 44' N, 105° 23' W. Very thin cirriform clouds.

Heading toward C_s band. At 34° 44' N, 105° 23' W. Very thin cirriform band is 5-10 miles ahead.

Blue sky is above it.

Will try to fly parallel to cirriform band.

Heading 147°, wind 2440/171 kt.

Definite cirriform layer off right wing. Bright blue sky above it.

Should be a good period for sampling thin Ci, but it must be farther than it looks. Heading 012°.

STATION	ALT	02 FEB '79									
		TEMP	WIND	15 SEC AVG							
1150100	9.0	-43.4	0.0000	0.0000	0	0	0	0	0	0	0.00
1150115	9.0	-43.4	0.0000	0.0000	0	0	0	0	0	0	0.00
1150130	9.0	-43.4	0.0000	0.0000	0	0	0	0	0	0	0.00
1150145	9.0	-43.5	0.0000	0.0000	0	0	0	0	0	0	0.00
1150160	9.0	-43.5	0.0000	0.0000	0	0	0	0	0	0	0.00
1150175	9.0	-43.5	0.0000	0.0000	0	0	0	0	0	0	0.00
1150190	9.0	-43.6	0.0000	0.0000	0	0	0	0	0	0	0.00
1150205	9.0	-43.6	0.0000	0.0000	0	0	0	0	0	0	0.00
1150220	9.0	-43.6	0.0000	0.0000	0	0	0	0	0	0	0.00
1150235	9.0	-43.6	0.0000	0.0000	0	0	0	0	0	0	0.00
1150250	9.0	-43.6	0.0000	0.0000	0	0	0	0	0	0	0.00
1150265	9.0	-43.6	0.0000	0.0000	0	0	0	0	0	0	0.00
1150280	9.0	-43.6	0.0000	0.0000	0	0	0	0	0	0	0.00
1150295	9.0	-43.6	0.0000	0.0000	0	0	0	0	0	0	0.00
1150310	9.0	-43.6	0.0000	0.0000	0	0	0	0	0	0	0.00
1150325	9.0	-43.6	0.0000	0.0000	0	0	0	0	0	0	0.00
1150340	9.0	-42.9	0.0000	0.0000	0	0	0	0	0	0	0.00
1150355	9.0	-42.8	0.0000	0.0000	0	0	0	0	0	0	0.00
1150370	9.0	-42.6	0.0000	0.0000	0	0	0	0	0	0	0.00
1150385	9.0	-42.5	0.0000	0.0000	0	0	0	0	0	0	0.00
1150400	9.0	-42.5	0.0000	0.0000	0	0	0	0	0	0	0.00
1150415	9.0	-42.5	0.0000	0.0000	0	0	0	0	0	0	0.00
1150430	9.0	-42.5	0.0000	0.0000	0	0	0	0	0	0	0.00
1150445	9.0	-42.5	0.0000	0.0000	0	0	0	0	0	0	0.00
1150460	9.0	-42.2	0.0000	0.0000	0	0	0	0	0	0	0.00
1150475	9.0	-42.0	0.0000	0.0000	0	0	0	0	0	0	0.00
1150490	9.0	-42.0	0.0000	0.0000	0	0	0	0	0	0	0.00
1150505	9.0	-42.0	0.0000	0.0000	0	0	0	0	0	0	0.00
1150520	9.0	-42.0	0.0000	0.0000	0	0	0	0	0	0	0.00
1150535	9.0	-42.0	0.0000	0.0000	0	0	0	0	0	0	0.00
1150550	9.0	-42.0	0.0000	0.0000	0	0	0	0	0	0	0.00
1150565	9.0	-42.0	0.0000	0.0000	0	0	0	0	0	0	0.00
1150580	9.0	-42.0	0.0000	0.0000	0	0	0	0	0	0	0.00
1150595	9.0	-39.3	0.0002	0.0004	100	38	10104	169	.96	.87	70% in very thin cirrus, thin cirrus, but can see through
1150610	9.0	-39.3	0.0003	0.0004	100	44	8263	189	.87	.75	70% in very thin cirrus, thin cirrus, but can see through
1150625	9.0	-39.3	0.0000	0.0000	0	0	180	138	.75	.60	70% in very thin cirrus, thin cirrus, but can see through
1150640	9.0	-39.3	0.0013	0.0033	100	45	7458	230	.80	.67	70% in very thin cirrus, thin cirrus, but can see through
1150655	9.0	-39.1	0.0026	0.0058	100	52	96536	230	.75	.67	70% in very thin cirrus, thin cirrus, but can see through
1150670	9.0	-39.3	0.0007	0.0012	100	42	31818	299	.77	.67	70% in very thin cirrus, thin cirrus, but can see through
1150685	9.0	-39.4	0.0002	0.0012	100	54	17881	189	.78	.67	70% in very thin cirrus, thin cirrus, but can see through
1150700	9.0	-39.5	0.0003	0.0003	100	75	8341	311	.67	.56	Good thin sampling conditions, visibility good, but can see thin cirrus, thin cirrus, but can see through
1150715	9.0	-39.5	0.0000	0.0003	100	98	1709	311	.56	.44	Good thin sampling conditions, visibility good, but can see thin cirrus, thin cirrus, but can see through
1150730	9.0	-39.3	0.0002	0.0002	100	92	3967	311	.60	.44	Good thin sampling conditions, visibility good, but can see thin cirrus, thin cirrus, but can see through
1150745	9.0	-39.0	0.0001	0.0005	100	81	2642	311	.69	.44	Good thin sampling conditions, visibility good, but can see thin cirrus, thin cirrus, but can see through
1150760	9.0	-39.0	0.0009	0.0022	100	69	23888	311	.68	.45	Approximately in middle of cirrus layer, 100% cirrus, 100% cirrus, can see thin cirrus, thin cirrus, but can see through
1150775	9.0	-39.5	0.0008	0.0030	100	63	34912	311	.65	.45	Approximately in middle of cirrus layer, 100% cirrus, 100% cirrus, can see thin cirrus, thin cirrus, but can see through
1150790	9.0	-39.4	0.0010	0.0049	100	72	32771	311	.58	.38	Can see thin cirrus, thin cirrus, but can see through
1150805	9.0	-39.5	0.0026	0.0058	100	57	188201	311	.73	.53	Can see thin cirrus, thin cirrus, but can see through
1150820	9.0	-39.4	0.0014	0.0044	100	52	83459	311	.71	.53	Can see thin cirrus, thin cirrus, but can see through
1150835	9.0	-39.4	0.0010	0.0026	100	66	25899	311	.73	.53	Can see thin cirrus, thin cirrus, but can see through
1150850	9.0	-39.4	0.0018	0.0036	100	64	26137	311	.65	.53	Can see thin cirrus, thin cirrus, but can see through
1150865	9.0	-39.6	0.0026	0.0083	100	61	41048	209	.83	.69	Can see thin cirrus, thin cirrus, but can see through
1150880	9.0	-39.7	0.0020	0.0020	100	49	40159	236	.80	.69	Can see thin cirrus, thin cirrus, but can see through
1150895	9.0	-39.1	0.0011	0.0032	100	55	49133	209	.80	.69	Can see thin cirrus, thin cirrus, but can see through
1150910	9.0	-39.2	0.0014	0.0044	100	64	48186	236	.74	.69	Can see thin cirrus, thin cirrus, but can see through
1150925	9.0	-39.7	0.0019	0.0069	100	67	56567	311	.71	.69	Can see thin cirrus, thin cirrus, but can see through
1150940	9.0	-39.7	0.0018	0.0036	100	64	26137	311	.65	.53	Can see thin cirrus, thin cirrus, but can see through
1150955	9.0	-39.6	0.0027	0.0095	100	60	122995	311	.64	.53	Can see thin cirrus, thin cirrus, but can see through
1150970	9.0	-39.5	0.0027	0.0093	100	66	91360	311	.61	.53	Can see thin cirrus, thin cirrus, but can see through
1150985	9.0	-39.5	0.0027	0.0061	100	58	83137	259	.71	.53	Can see thin cirrus, thin cirrus, but can see through
1151000	9.0	-39.4	0.0031	0.0056	100	49	11348	259	.71	.53	Can see thin cirrus, thin cirrus, but can see through

Start	02 Feb 79										15 Second Average											
	Temp	Inc-SC	Inc-TP	Inc	Do	NT	LMAX	FF	Inc-SC	Inc-TP	Inc	Do	NT	LMAX	FF	Inc-SC	Inc-TP	Inc	Do	NT	LMAX	
Alt	km	km	km	km	km	km	km	km	km	km	km	km	km	km	km	km	km	km	km	km	km	
Time																						
22:05:00	9.0	-38.4	-0.038	-0.043	100	47	85823	.72	9.0	-38.4	-0.023	-0.028	100	48	90452	.63	9.0	-38.4	-0.022	-0.027	100	47
22:05:15	8.9	-38.3	-0.022	-0.027	100	52	87356	.55	8.9	-38.3	-0.023	-0.028	100	52	88745	.61	8.9	-38.3	-0.023	-0.028	100	52
22:05:30	8.9	-38.3	-0.023	-0.028	100	52	88745	.55	8.9	-38.2	-0.023	-0.028	100	52	88720	.78	8.9	-38.2	-0.023	-0.028	100	52
22:05:45	8.9	-38.2	-0.023	-0.028	100	53	88720	.60	8.9	-38.2	-0.013	-0.018	100	52	71515	.20	8.9	-38.2	-0.013	-0.018	100	52
22:06:00	8.9	-38.2	-0.023	-0.028	100	53	88720	.78	8.9	-38.1	-0.013	-0.018	100	52	113918	.74	8.9	-38.1	-0.013	-0.018	100	52
22:06:15	8.9	-38.1	-0.013	-0.018	100	53	113918	.74	8.9	-38.1	-0.016	-0.021	100	53	11666	.75	8.9	-38.1	-0.016	-0.021	100	53
22:06:30	8.9	-38.1	-0.016	-0.021	100	53	11666	.75	8.9	-38.0	-0.018	-0.024	100	53	10552	.72	8.9	-38.0	-0.018	-0.024	100	53
22:06:45	8.9	-38.0	-0.022	-0.027	100	53	10552	.72	8.9	-38.0	-0.018	-0.024	100	53	105020	.72	8.9	-38.0	-0.018	-0.024	100	53
22:07:00	9.0	-38.0	-0.022	-0.027	100	64	119080	.70	9.0	-38.0	-0.016	-0.021	100	64	10382	.68	9.0	-38.0	-0.016	-0.021	100	64
22:07:15	9.0	-38.0	-0.022	-0.027	100	64	10382	.72	9.0	-38.0	-0.022	-0.027	100	64	14266	.71	9.0	-38.0	-0.022	-0.027	100	64
22:07:30	9.0	-38.0	-0.023	-0.028	100	64	14266	.72	9.0	-38.0	-0.022	-0.027	100	64	12834	.73	9.0	-38.0	-0.022	-0.027	100	64
22:07:45	9.0	-38.0	-0.023	-0.028	100	64	12834	.73	9.0	-38.0	-0.021	-0.026	100	64	92001	.78	9.0	-38.0	-0.021	-0.026	100	64
22:08:00	9.0	-38.0	-0.016	-0.021	100	64	92001	.78	9.0	-38.0	-0.016	-0.021	100	64	102085	.71	9.0	-38.0	-0.016	-0.021	100	64
22:08:15	9.0	-38.0	-0.016	-0.021	100	64	102085	.71	9.0	-38.0	-0.018	-0.024	100	64	132372	.68	9.0	-38.0	-0.018	-0.024	100	64
22:08:30	8.9	-38.0	-0.022	-0.027	100	64	132372	.68	8.9	-38.0	-0.011	-0.016	100	64	47157	.70	8.9	-38.0	-0.011	-0.016	100	64
22:08:45	8.9	-38.0	-0.022	-0.027	100	64	47157	.70	8.9	-38.0	-0.011	-0.016	100	64	31729	.70	8.9	-38.0	-0.011	-0.016	100	64
22:09:00	8.9	-38.0	-0.016	-0.021	100	64	31729	.70	8.9	-38.0	-0.016	-0.021	100	64	58469	.73	8.9	-38.0	-0.016	-0.021	100	64
22:09:15	8.9	-38.0	-0.016	-0.021	100	64	58469	.73	8.9	-38.0	-0.016	-0.021	100	64	35384	.70	8.9	-38.0	-0.016	-0.021	100	64
22:09:30	8.9	-38.0	-0.009	-0.014	100	64	35384	.70	8.9	-38.0	-0.010	-0.015	100	64	15877	.79	8.9	-38.0	-0.010	-0.015	100	64
22:09:45	9.0	-38.0	-0.009	-0.014	100	64	15877	.79	9.0	-38.0	-0.009	-0.014	100	64	38484	.75	9.0	-38.0	-0.009	-0.014	100	64
22:10:00	9.0	-38.5	-0.005	-0.011	100	64	38484	.75	9.0	-38.5	-0.005	-0.011	100	64	55464	.80	9.0	-38.5	-0.005	-0.011	100	64
22:10:15	9.0	-38.5	-0.005	-0.011	100	64	55464	.80	9.0	-38.5	-0.005	-0.011	100	64	24736	.80	9.0	-38.5	-0.005	-0.011	100	64
22:10:30	9.0	-38.5	-0.005	-0.011	100	64	24736	.80	9.0	-38.5	-0.005	-0.011	100	64	48925	.71	9.0	-38.5	-0.005	-0.011	100	64
22:10:45	9.0	-38.5	-0.005	-0.011	100	64	48925	.71	9.0	-38.5	-0.005	-0.011	100	64	11183	.82	9.0	-38.5	-0.005	-0.011	100	64
22:11:00	9.0	-38.5	-0.004	-0.011	100	64	11183	.82	9.0	-38.5	-0.004	-0.011	100	64	13739	.70	9.0	-38.5	-0.004	-0.011	100	64
22:11:15	9.0	-38.5	-0.004	-0.011	100	64	13739	.70	9.0	-38.5	-0.003	-0.011	100	64	58	.70	9.0	-38.5	-0.003	-0.011	100	64
22:11:30	9.0	-38.5	-0.004	-0.011	100	64	58	.70	9.0	-38.5	-0.002	-0.011	100	64	49884	.70	9.0	-38.5	-0.002	-0.011	100	64
22:11:45	9.0	-38.5	-0.004	-0.011	100	64	49884	.70	9.0	-38.5	-0.002	-0.011	100	64	28209	.69	9.0	-38.5	-0.002	-0.011	100	64
22:12:00	9.0	-38.5	-0.004	-0.011	100	64	28209	.69	9.0	-38.5	-0.002	-0.011	100	64	70661	.69	9.0	-38.5	-0.002	-0.011	100	64
22:12:15	9.0	-38.5	-0.004	-0.011	100	64	70661	.69	9.0	-38.5	-0.002	-0.011	100	64	6176	.70	9.0	-38.5	-0.002	-0.011	100	64
22:12:30	9.0	-38.5	-0.004	-0.011	100	64	6176	.70	9.0	-38.5	-0.002	-0.011	100	64	13739	.70	9.0	-38.5	-0.002	-0.011	100	64
22:12:45	9.0	-38.5	-0.004	-0.011	100	64	13739	.70	9.0	-38.5	-0.002	-0.011	100	64	52882	.68	9.0	-38.5	-0.002	-0.011	100	64
22:13:00	9.0	-38.5	-0.004	-0.011	100	64	52882	.68	9.0	-38.5	-0.002	-0.011	100	64	44984	.71	9.0	-38.5	-0.002	-0.011	100	64
22:13:15	9.0	-38.5	-0.004	-0.011	100	64	44984	.71	9.0	-38.5	-0.002	-0.011	100	64	23897	.68	9.0	-38.5	-0.002	-0.011	100	64
22:13:30	9.0	-38.5	-0.004	-0.011	100	64	23897	.68	9.0	-38.5	-0.002	-0.011	100	64	44671	.71	9.0	-38.5	-0.002	-0.011	100	64
22:13:45	9.0	-38.5	-0.004	-0.011	100	64	44671	.71	9.0	-38.5	-0.002	-0.011	100	64	53791	.70	9.0	-38.5	-0.002	-0.011	100	64
22:14:00	9.0	-38.5	-0.004	-0.011	100	64	53791	.70	9.0	-38.5	-0.002	-0.011	100	64	6176	.70	9.0	-38.5	-0.002	-0.011	100	64
22:14:15	9.0	-38.5	-0.004	-0.011	100	64	6176	.70	9.0	-38.5	-0.002	-0.011	100	64	95173	.69	9.0	-38.5	-0.002	-0.011	100	64
22:14:30	9.0	-38.5	-0.004	-0.011	100	64	95173	.69	9.0	-38.5	-0.002	-0.011	100	64	29900	.65	9.0	-38.5	-0.002	-0.011	100	64
22:14:45	9.0	-38.5	-0.004	-0.011	100	64	29900	.65	9.0	-38.5	-0.002	-0.011	100	64	51617	.69	9.0	-38.5	-0.002	-0.011	100	64
22:15:00	9.0	-38.5	-0.004	-0.011	100	64	51617	.69	9.0	-38.5	-0.002	-0.011	100	64	57212	.62	9.0	-38.5	-0.002	-0.011	100	64
22:15:15	9.0	-38.5	-0.004	-0.011	100	64	57212	.62	9.0	-38.5	-0.002	-0.011	100	64	49088	.69	9.0	-38.5	-0.002	-0.011	100	64
22:15:30	9.0	-38.5	-0.004	-0.011	100	64	49088	.69	9.0	-38.5	-0.002	-0.011	100	64	24831	.71	9.0	-38.5	-0.002	-0.011	100	64
22:15:45	9.0	-38.5	-0.004	-0.011	100	64	24831	.71	9.0	-38.5	-0.002	-0.011	100	64	41346	.68	9.0	-38.5	-0.002	-0.011	100	64
22:16:00	9.0	-38.5	-0.004	-0.011	100	64	41346	.68	9.0	-38.5	-0.002	-0.011	100	64	56924	.71	9.0	-38.5	-0.002	-0.011	100	64
22:16:15	9.0	-38.5	-0.004	-0.011	100	64	56924	.71	9.0	-38.5	-0.002	-0.011	100	64	12112	.70	9.0	-38.5	-0.002	-0.011	100	64
22:16:30	9.0	-38.5	-0.004	-0.011	100	64	12112	.70	9.0	-38.5	-0.002	-0.011	100	64	52743	.59	9.0	-38.5	-0.002	-0.011	100	64
22:16:45	9.0	-38.5	-0.004	-0.011	100	64	52743	.59	9.0	-38.5	-0.002	-0.011	100	64	113149	.70	9.0	-38.5	-0.002	-0.011	100	64
22:17:00	9.0	-38.5	-0.004	-0.011	100	64	113149	.70	9.0	-38.5	-0.002	-0.011	100	64	156712	.67	9.0	-38.5	-0.002	-0.011	100	64
22:17:15	9.0	-38.5	-0.004	-0.011	100	64	156712	.67	9.0	-38.5	-0.002	-0.011	100	64	66732	.70	9.0	-38.5	-0.002	-0.011	100	64
22:17:30	9.0	-38.5	-0.004	-0.011	100	64	66732	.70	9.0	-38.5	-0.002	-0.011	100	64	41839	.78	9.0	-38.5	-0.002	-0.011	100	64
22:17:45	9.0	-38.5	-0.004	-0.011	100	64	41839	.78	9.0	-38.5	-0.002	-0.011	100	64	113149	.70	9.0	-38.5	-0.002	-0.011	100	64
22:18:00	9.0	-38.5	-0.004	-0.011	100	64	113149	.70	9.0	-38.5	-0.002	-0.011	100	64	41346	.71	9.0	-38.5	-0.002	-0.011	100	64
22:18:15	9.0	-38.5	-0.004	-0.011	100	64	41346	.71	9.0	-38.5	-0.002	-0.011	100	64	56924	.71	9.0	-38.5	-0.002	-0.011	100	64
22:18:30	9.0	-38.5	-0.004	-0.011	100	64																

START TIME	ALT MM	15 SECOND AVERAGE										FF
		TEMP C	INC-SC B/H ^{4.3}	INC-CP B/H ^{4.3}	INC-T B/H ^{4.3}	DO B/H ^{4.3}	WT B/H ^{4.3}	LMAX B/H ^{4.3}	MT B/H ^{4.3}	DO B/H ^{4.3}	WT B/H ^{4.3}	
221900	9.0	-38.3	.0040	.0011	100	33	24468	250	.74			
221915	8.9	-38.4	.0006	.0010	100	92	9623	311	.45			
221930	9.0	-38.7	.0009	.0041	100	93	17653	311	.66			
221945	8.9	-38.8	.0011	.0046	100	97	18278	311	.67			
222000	9.0	-38.8	.0010	.0051	99	100	18414	437	.69	Just getting out of heaviest Cs. Visibility has improved to about 15 mi		
222015	9.0	-38.8	.0007	.0029	100	78	20262	311	.68	on slant downward. At 34° 31'N, 104° 26'W. Heading 333°.		
222030	9.0	-38.8	.0007	.0021	100	74	14850	250	.69			
222045	9.0	-38.7	.0003	.0009	100	88	6426	311	.56			
222100	9.0	-38.4	.0009	.0040	100	79	25582	311	.70			
222115	9.0	-38.8	.0024	.0024	100	72	20015	311	.65			
222130	9.0	-39.0	.0011	.0046	100	84	25618	311	.66			
222145	9.0	-39.1	.0008	.0035	100	88	14443	311	.67			
222200	9.0	-38.2	.0001	.0004	100	97	2311	311	.56			
222215	9.0	-38.8	.0001	.0009	100	69	8987	311	.65			
222230	9.0	-38.7	.0003	.0010	100	56	15489	209	.76			
222245	9.0	-38.8	.0032	.0018	100	46	70247	311	.67			
222300	9.0	-38.8	.0003	.0016	100	60	19464	209	.76			
222315	9.0	-38.7	.0002	.0010	100	43	9836	311	.67			
222330	9.0	-38.7	.0005	.0021	100	65	20629	311	.66	Good sampling area for thin ciriform filaments. Pretty much in clear.		
222345	8.9	-38.7	.0002	.0016	100	55	22644	209	.83	Will move over closer to the cloud band.		
222400	8.9	-38.8	0.0000	.0009	100	52	12734	148	.91			
222415	8.9	-38.8	0.0000	.0009	100	60	11466	189	.85			
222430	8.9	-38.8	0.0000	.0007	100	53	9447	169	.89			
222445	8.9	-38.8	0.0000	.0010	100	61	9797	209	.91			
222500	8.9	-38.7	0.0000	.0009	100	54	16985	209	.84			
222515	8.9	-38.6	0.0000	.0010	100	59	12492	209	.82			
222530	8.9	-38.4	0.0002	.0007	100	58	8653	209	.81			
222545	8.9	-38.7	.0001	.0014	100	59	15620	230	.82			
222600	8.9	-38.8	.0000	.0007	100	57	17747	230	.82			
222615	8.9	-38.8	.0000	.0015	100	59	16610	209	.85			
222630	8.9	-38.8	.0000	.0014	100	56	16679	230	.86			
222645	8.9	-38.8	.0000	.0011	100	58	11507	209	.90			
222700	8.9	-38.8	0.0000	.0011	100	54	12814	209	.88	Moving closer. Very few counts in ASSP.		
222715	8.9	-38.7	0.0000	.0008	100	58	6491	230	.87			
222730	8.9	-38.7	.0002	.0008	100	55	11513	230	.83			
222745	8.9	-38.7	.0001	.0007	100	56	9226	209	.84			
222800	8.9	-38.7	.0002	.0009	100	58	11011	209	.85			
222815	8.9	-38.7	.0001	.0008	100	60	9455	209	.84			
222830	8.9	-38.7	.0002	.0006	100	51	10615	169	.84			
222845	8.9	-38.7	.0002	.0005	100	53	6804	189	.77			
222900	8.9	-38.7	.0003	.0006	100	47	13400	209	.82	Nearly clear air. Cu below and to right. Blue sky above.		
222915	9.0	-38.8	.0000	.0003	100	55	3609	148	.94	At 34° 40'N, 104° 33'W. Thin Ci uncinus ahead, but may be too high to sample. Heading 232°.		
222930	8.9	-38.8	0.0000	.0002	100	55	2967	148	.87			

Appendix D

List of Abbreviations

Ac	- Altocumulus
AFB	- Air Force Base
AFGL	- Air Force Geophysics Laboratory
AFWL	- Air Force Weapons Laboratory
Alt	- Altitude (above mean sea level unless otherwise specified)
ART	- Airborne Radiation Technology
ASSP	- Axial Scattering Spectrometer Probe
C	- Cloud (or droplet) probe
°C	- Temperature in degrees Celsius
Cc	- Cirrocumulus
Ci	- Cirrus
Cs	- Cirrostratus
Do	- Medium volume diameter
FF	- Form factor
GOES	- Geostationary Operational Environmental Satellite
g-m ⁻³	- Grams per cubic meter
Hdg	- Aircraft heading
IAS	- Indicated airspeed
IWC	- Ice water content
km	- Kilometer
L _{max}	- Maximum particle diameter

mb	- Millibar
MSL	- Mean sea level
MST	- Mountain Standard Time
NT	- Particle Density
1-D	- One-dimensional particle measuring system
P	- Precipitation probe
T	- Temperature
TAS	- True air speed
2-D	- Two-dimensional particle measuring system
UMT or Z	- Universal (or Greenwich) Mean Time
Z	- Calculated radar reflectivity

